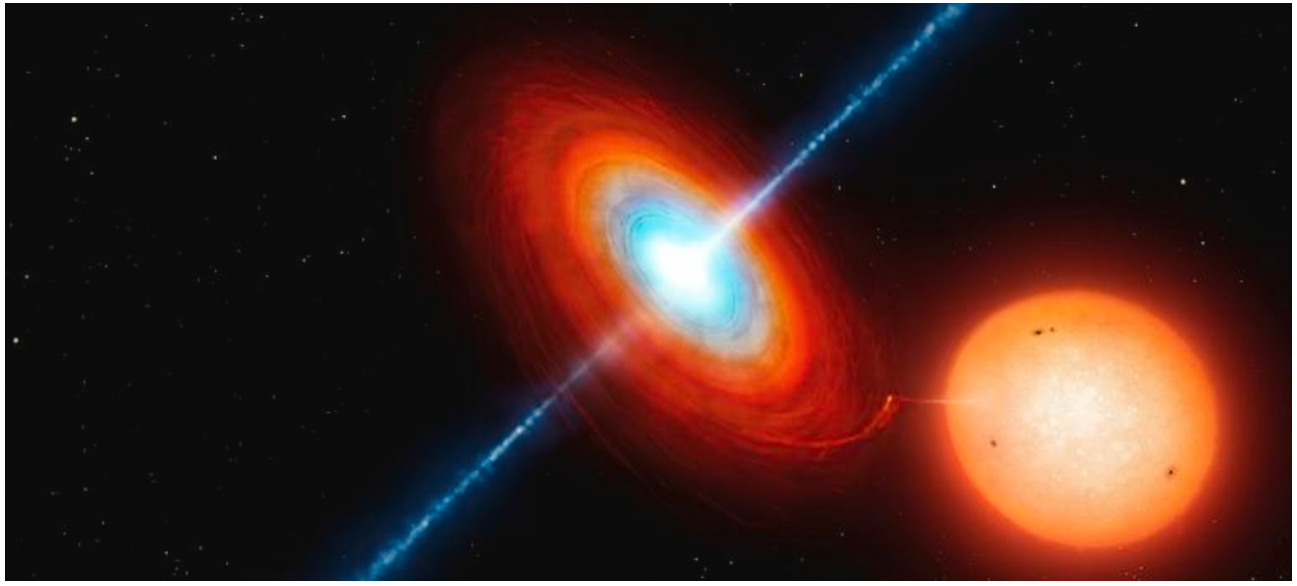

Gamma-Ray Emission from Microquasars

Dmitriy Khangulyan

January 14$^{\text{th}}$ 2026 (Gran Sasso Science Institute)

中國科學院高能物理研究所
Institute of High Energy Physics
Chinese Academy of Sciences

Outline

Outline

Very-High-Energy Telescopes

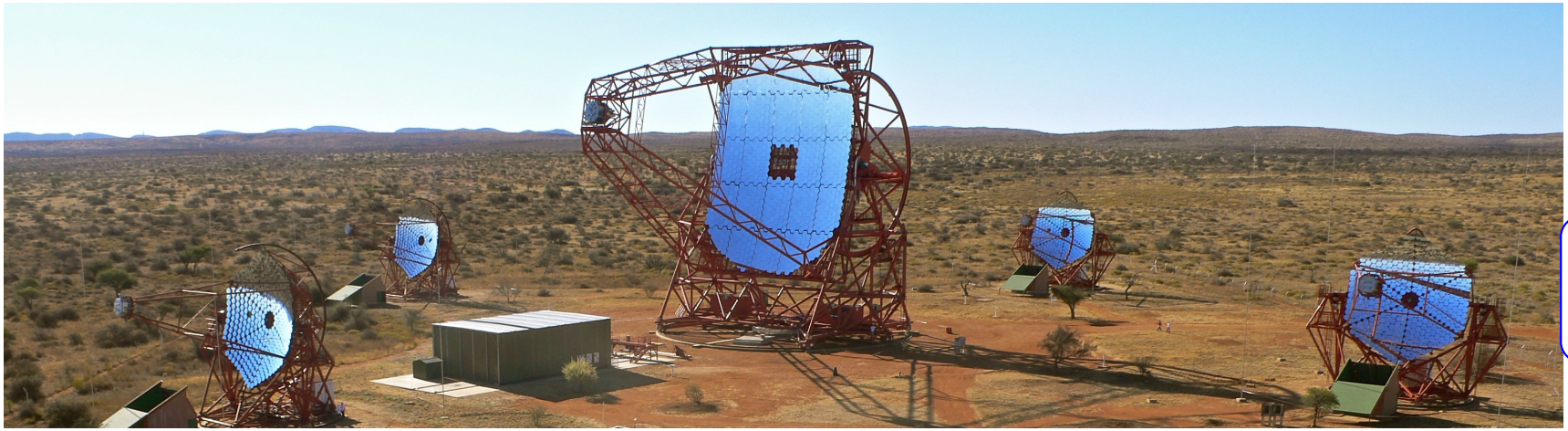

H.E.S.S.

MAGIC

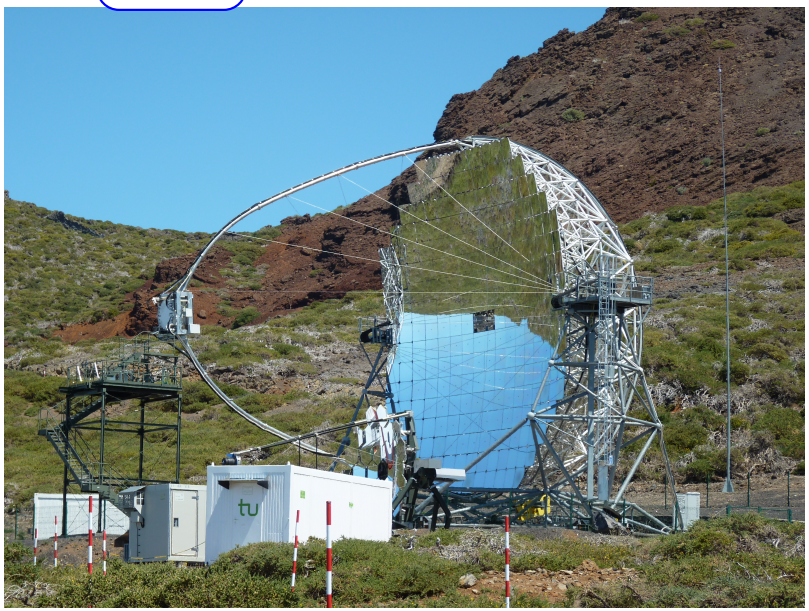

VERITAS

Very-High-Energy Telescopes

HAWC

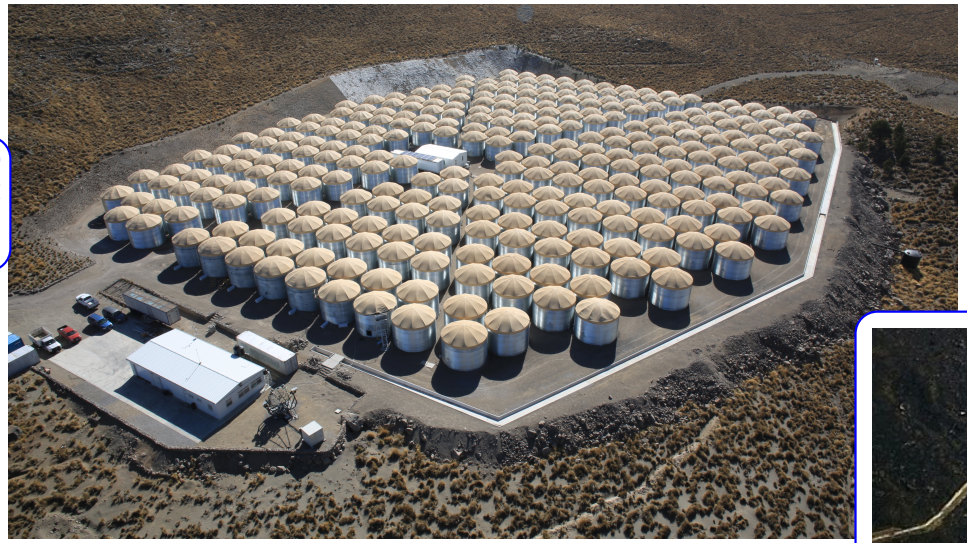

CGRO, 1991

Also viable information on gamma-ray binary systems is obtained at lower frequencies, in X-ray, optical, radio bands

AGILE

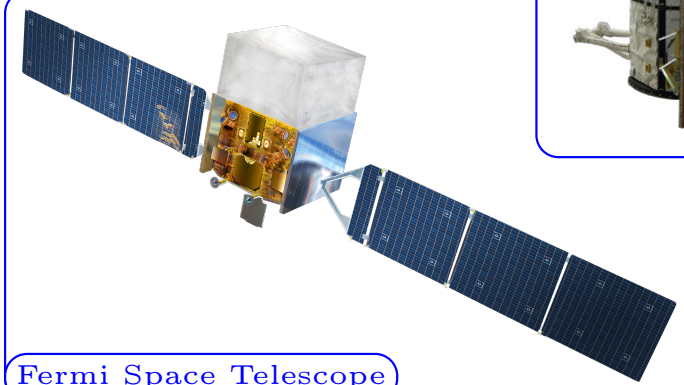

Fermi Space Telescope

LHAASO

Sensitivity of High-Energy Instruments

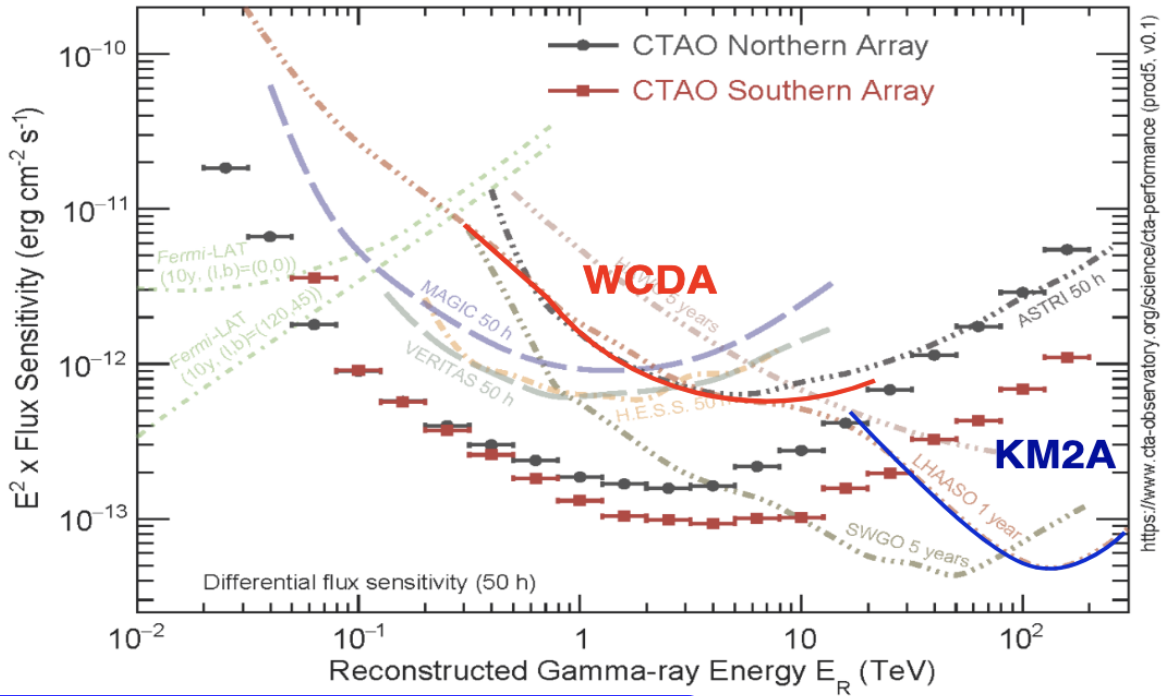

della Volpe, LHAASO Collaboration (2022)

Sensitivity of High-Energy Instruments

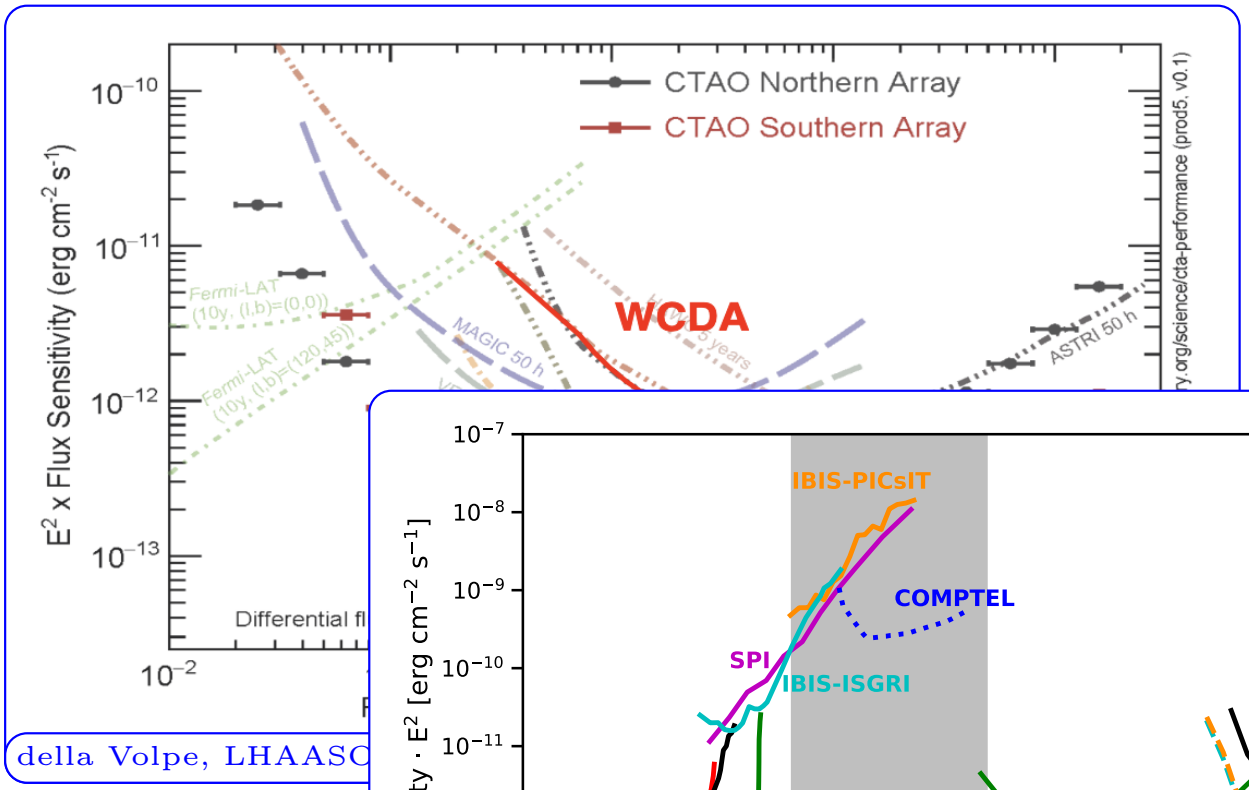

della Volpe, LHAASO

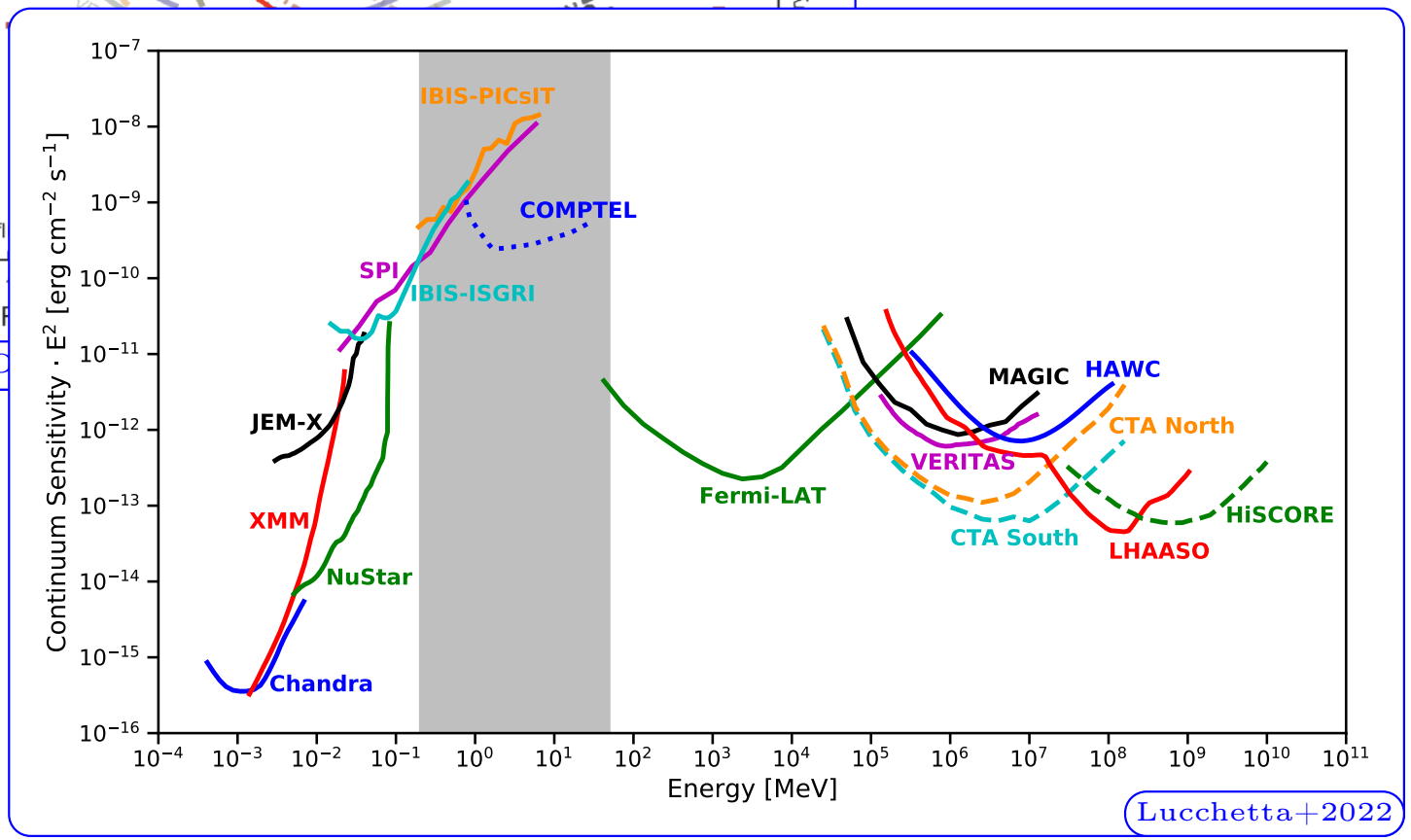

Lucchetta+2022

Binary systems detected in the VHE regime

LHAASO@29°N, zenith angle $< 55°$

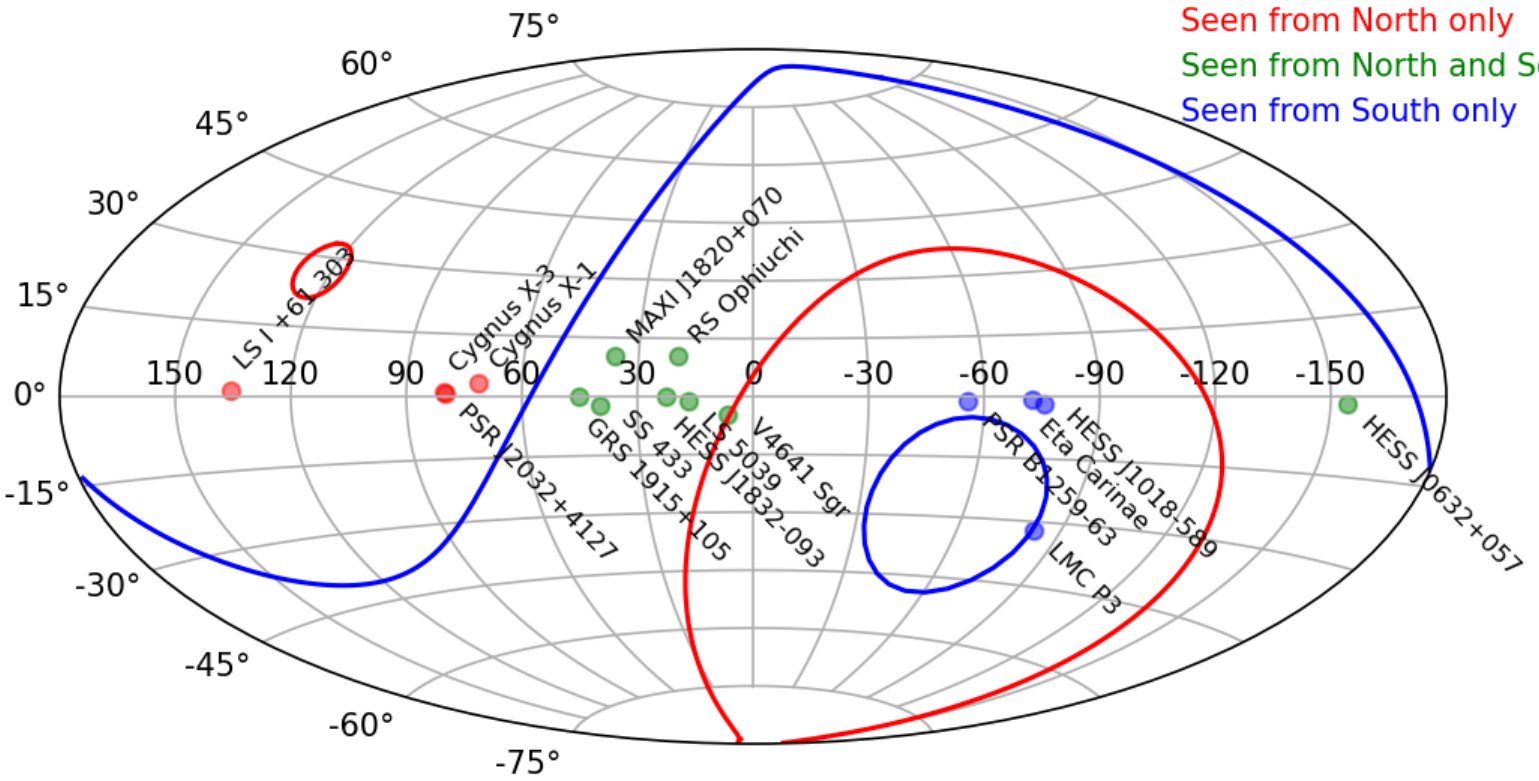

TeVCAT + Cygnus X-3

H.E.S.S. @23°S, zenith angle $< 45°$

Binary Systems@VHE γ rays

System	Star	Star*	P	VHE	HE	X-ray
PSR B1259-63/LS2883	psr	O/Be	1237d	periodic	variable	periodic
LS 5039	psr(?)	O	3.9d	periodic	periodic	periodic
LS I +61+303	psr(?)	Be	27d	variable	periodic	variable
HESS J0632+057	?	Be	320d	variable	steady(?)	variable
HESS J1832-093	?	Be(?)	86d(?)	variable(?)	periodic(?)	periodic
1FGL J1018.6-5856	?	O	17d	variable	periodic	variable
PSR J2032+4127	psr	Be	50yr	variable	variable	variable
LMC P3	?	O	10d	periodic	periodic	variable
Cyg X-1	bh	O	5.6d	flare	flare	—
Cyg X-3	bh(?)	WR	4.8h	flare	flare	—
SS433	bh	A	13d	steady	steady(?)	steady
V4641 Sgr	bh	B	2.8d	steady(?)	—	flare
MAXI J1820+070	bh	KG	0.7d	steady(?)	—	flare
GRS 1915+105	bh	RG	33.5d	steady(?)	steady(?)	flare
η Car	BG	O	5.5yr	variable(?)	variable	variable
RS Oph	WD	RG	1.2yr	flare	flare	flare

Binary Systems@VHE γ rays

System	Star	Star*	P	VHE	HE	X-ray
PSR B1259-63/LS2883	psr	O/Be	1237d	periodic	variable	periodic
LS 5039	psr(?)	O	3.9d	periodic	periodic	periodic
LS I +61+303	psr(?)	Be	27d	variable	periodic	variable
HESS J0632+057	?	Be	320d	variable	steady(?)	variable
HESS J1832-093	?	Be(?)	86d(?)	variable(?)	periodic(?)	periodic
1FGL J1018.6-5856	?	O	17d	variable	periodic	variable
PSR J2032+4127	psr	Be	50yr	variable	variable	variable
LMC P3	?	O	10d	periodic	periodic	variable
Cyg X-1	bh	O	5.6d	flare	flare	—
Cyg X-3	bh(?)	WR	4.8h	flare	flare	—
SS433	bh	A	13d	steady	steady(?)	steady
V4641 Sgr	bh	B	2.8d	steady(?)	—	flare
MAXI J1820+070	bh	KG	0.7d	steady(?)	—	flare
GRS 1915+105	bh	RG	33.5d	steady(?)	steady(?)	flare
η Car	BC	O	5.5yr	variable?	variable	variable
RS Oph	WD	RG	1.2yr	flare	flare	flare

Gamma-Ray Binaries

MicroQuasars

Gamma-Ray Emitting BS

Binary systems detected in the VHE regime

LHAASO@29°N, zenith angle $< 55°$

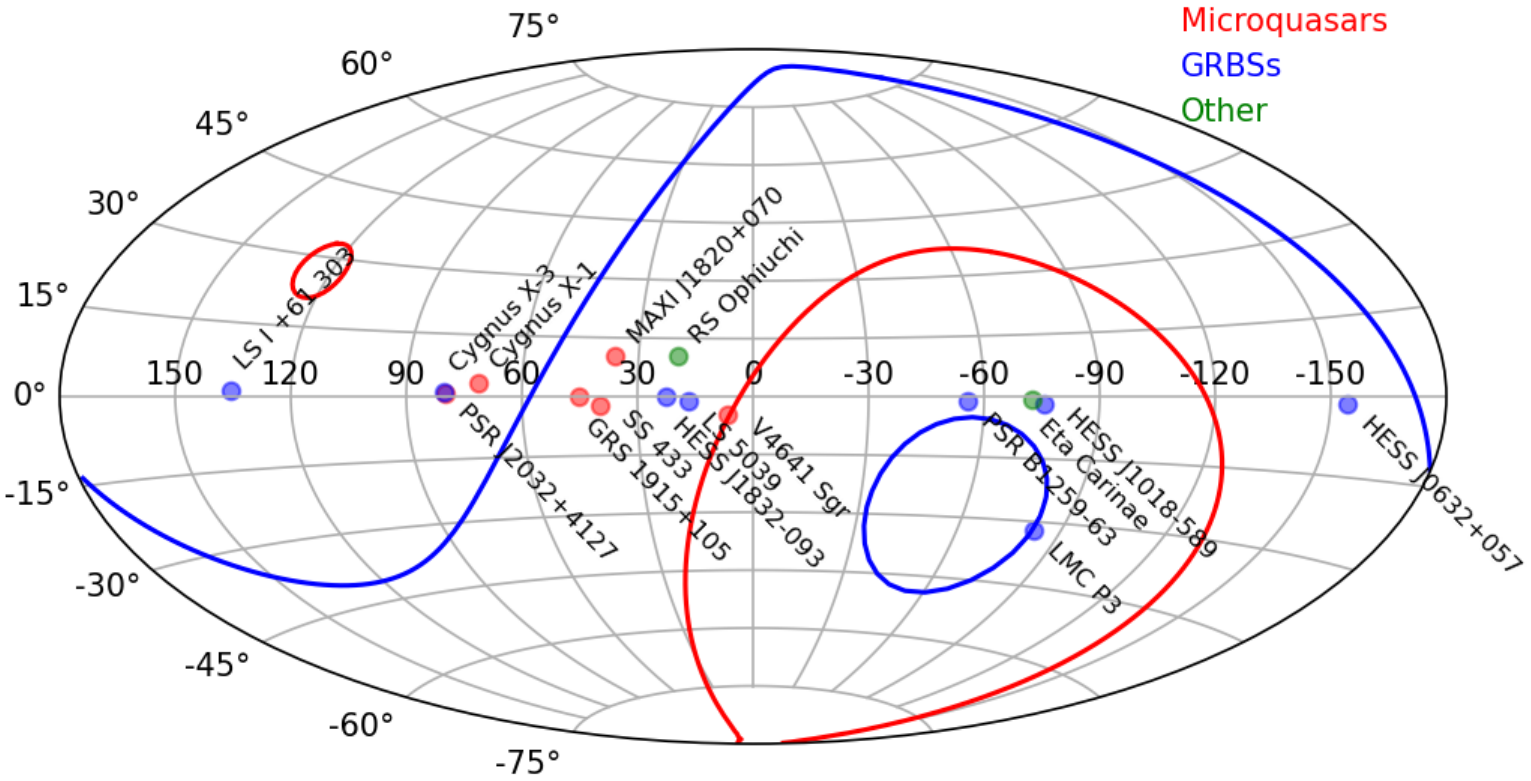

TeVCAT + Cygnus X-3

H.E.S.S. @23°S, zenith angle $< 45°$

Binary Systems@VHE γ rays

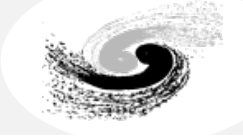

System	Star	Star*	P	VHE	HE	X-ray
PSR B1259-63/LS2883	psr	O/Be	1237d	periodic	variable	periodic
LS 5039	psr(?)	O	3.9d	periodic	periodic	periodic
LS I +61+303	psr(?)	Be	27d	variable	periodic	variable
HESS J0632+057	?	Be	320d	variable	steady(?)	variable
HESS J1832-093	?	Be(?)	86d(?)	variable(?)	periodic(?)	periodic
1FGL J1018.6-5856	?	O	17d	variable	periodic	variable
PSR J2032+4127	psr	Be	50yr	variable	variable	variable
LMC P3	?	O	10d	periodic	periodic	variable
Cyg X-1	bh	O	5.6d	flare	flare	—
Cyg X-3	bh(?)	WR	4.8h	flare	flare	—
SS433	bh	A	13d	steady	steady(?)	steady
V4641 Sgr	bh	B	2.8d	steady(?)	—	flare
MAXI J1820+070	bh	KG	0.7d	steady(?)	—	flare
GRS 1915+105	bh	RG	33.5d	steady(?)	steady(?)	flare
η Car	BG	O	5.5yr	variable(?)	variable	variable
RS Oph	WD	RG	1.2yr	flare	flare	flare

RS Ophiuchi (Recurrent Nova)

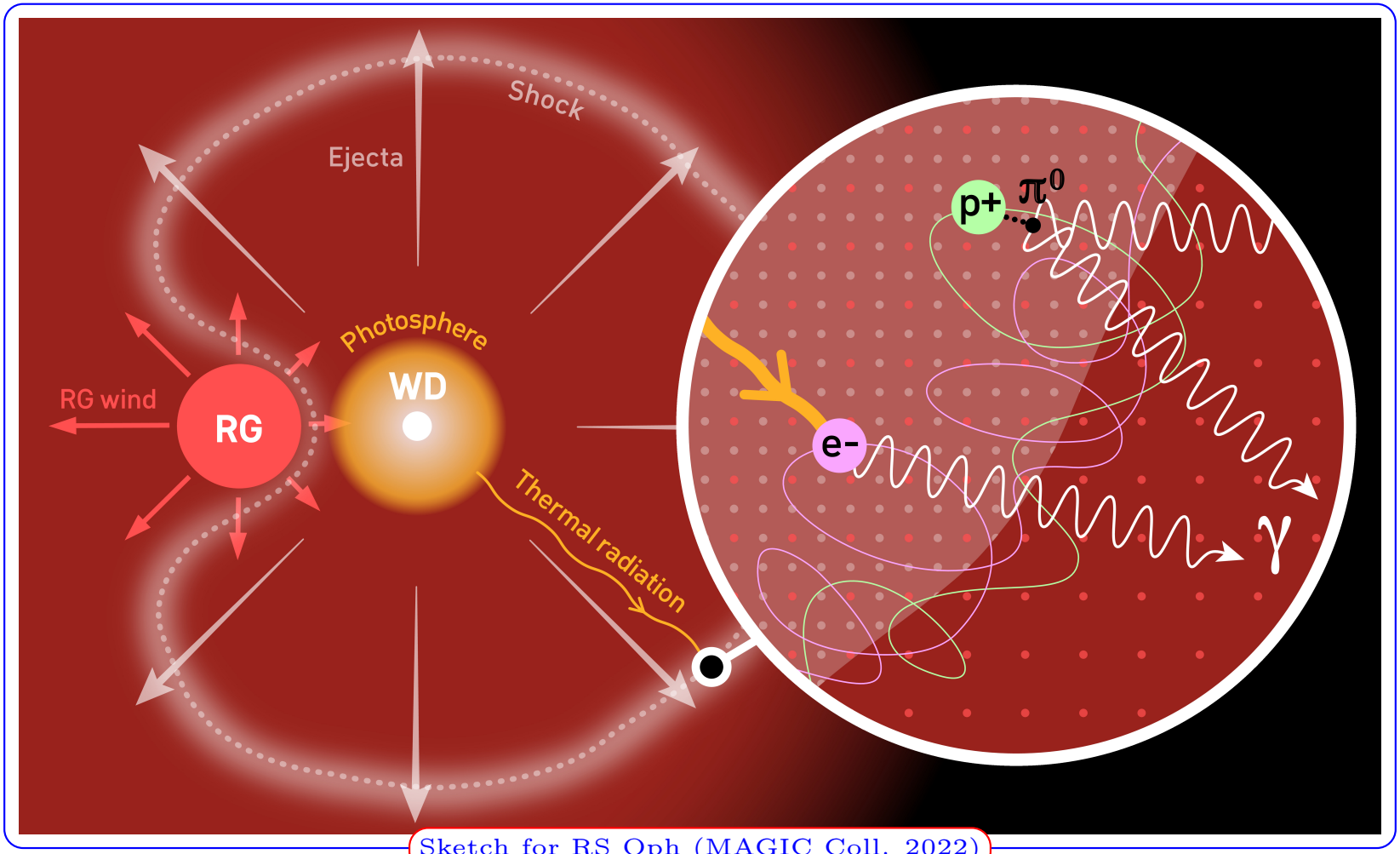

Sketch for RS Oph (MAGIC Coll. 2022)

RS Ophiuchi (Recurrent Nova)

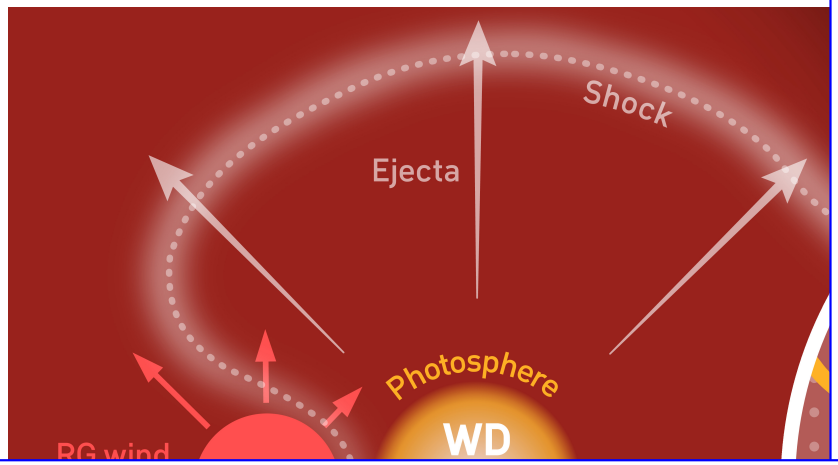

RS Oph HE/VHE spectra (H.E.S.S. Coll. 2022)

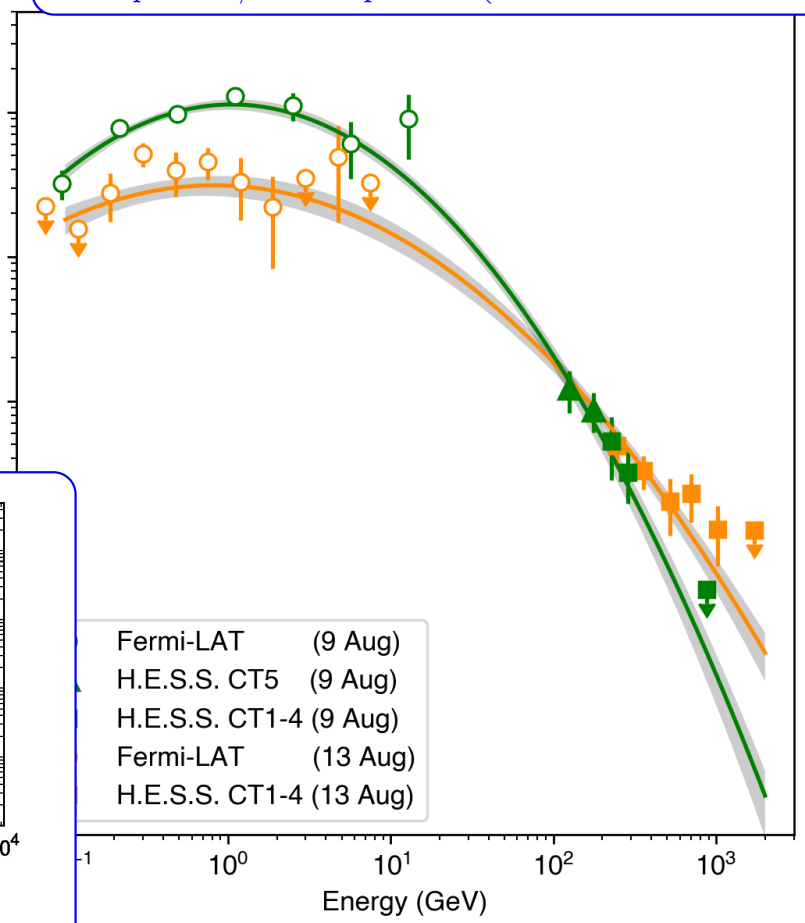

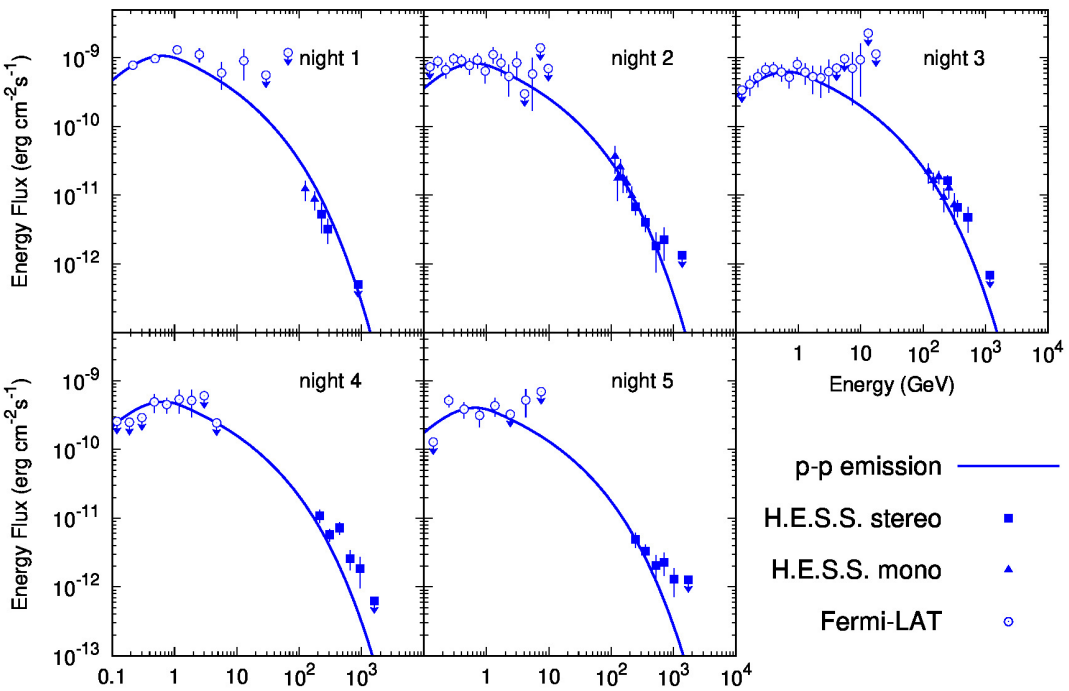

Both MAGIC and H.E.S.S. data favor pp origin of VHE emission

T CrB is a recurrent nova located in the constellation Corona Borealis, just 1 kpc away, and we wait for its explosion since 2024

Colliding Wind Binaries

NASA/C. Reed

Colliding Wind Binaries

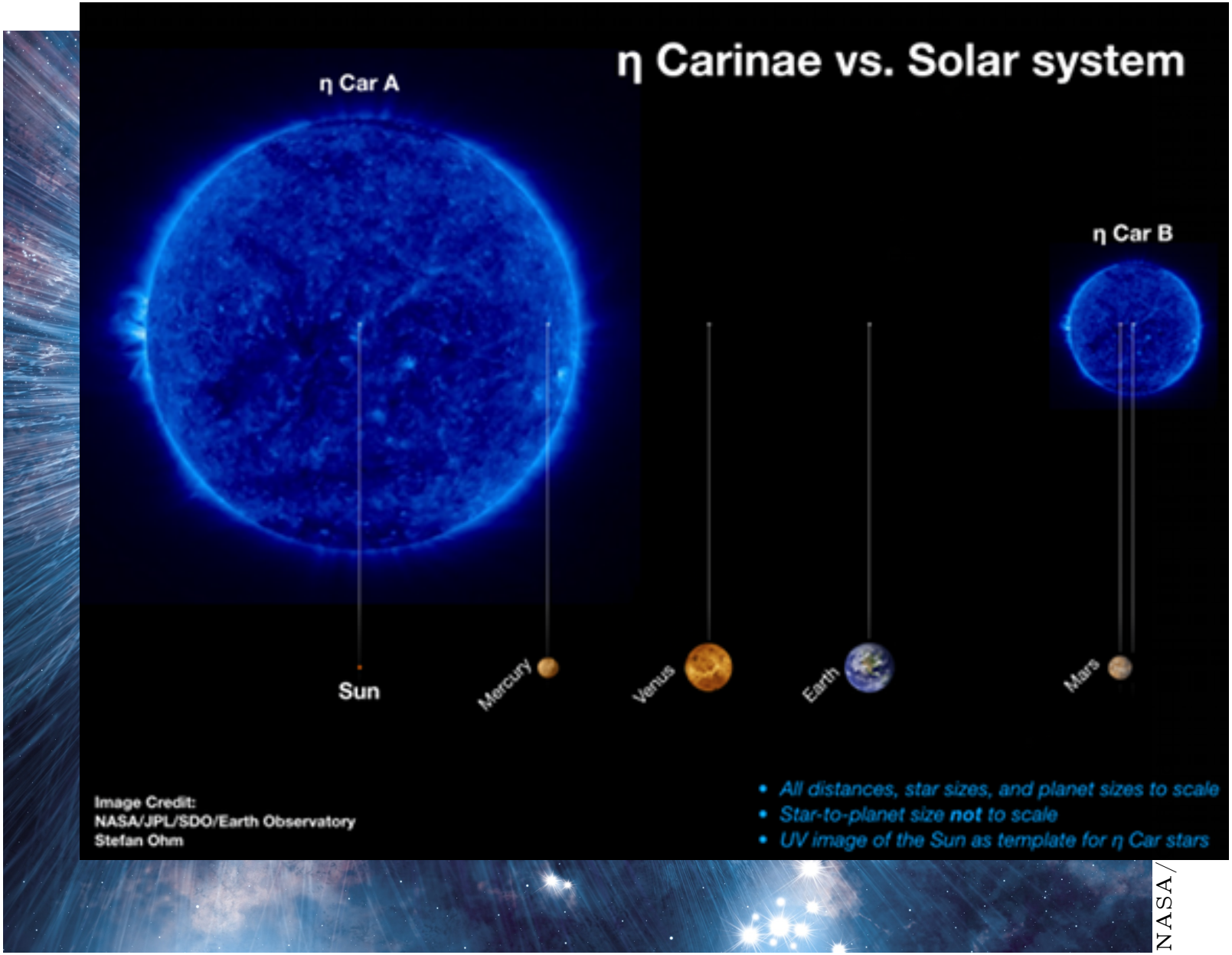

Colliding Wind Binaries

VHE spectrum (H.E.S.S. Coll. 2020)

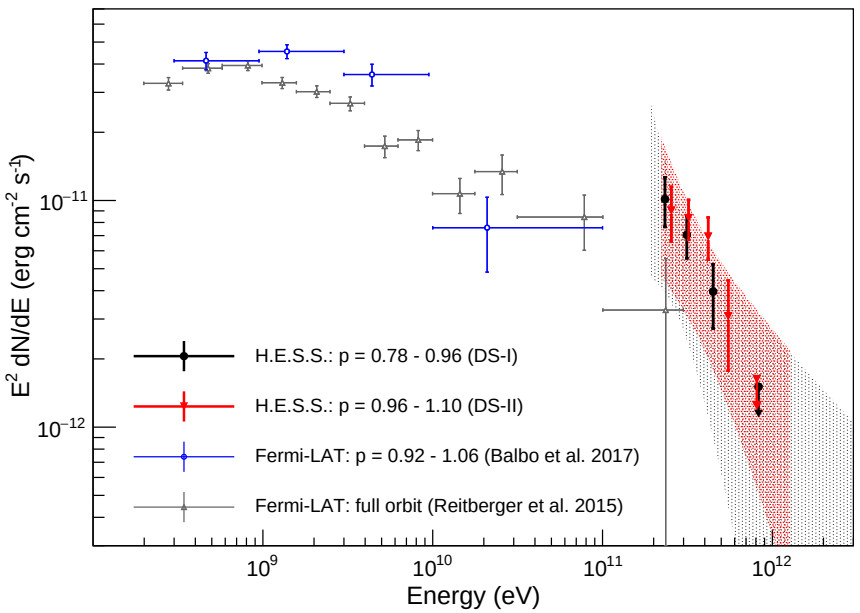

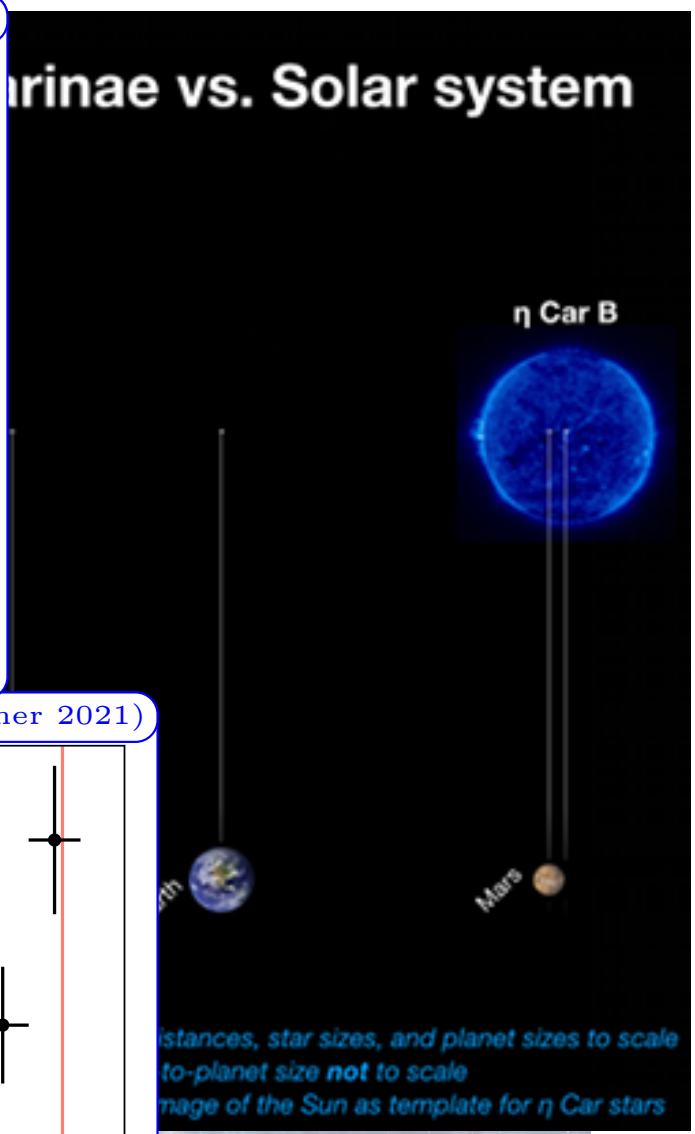

Fermi/LAT lightcurve (Marti-Devesa&Reimer 2021)

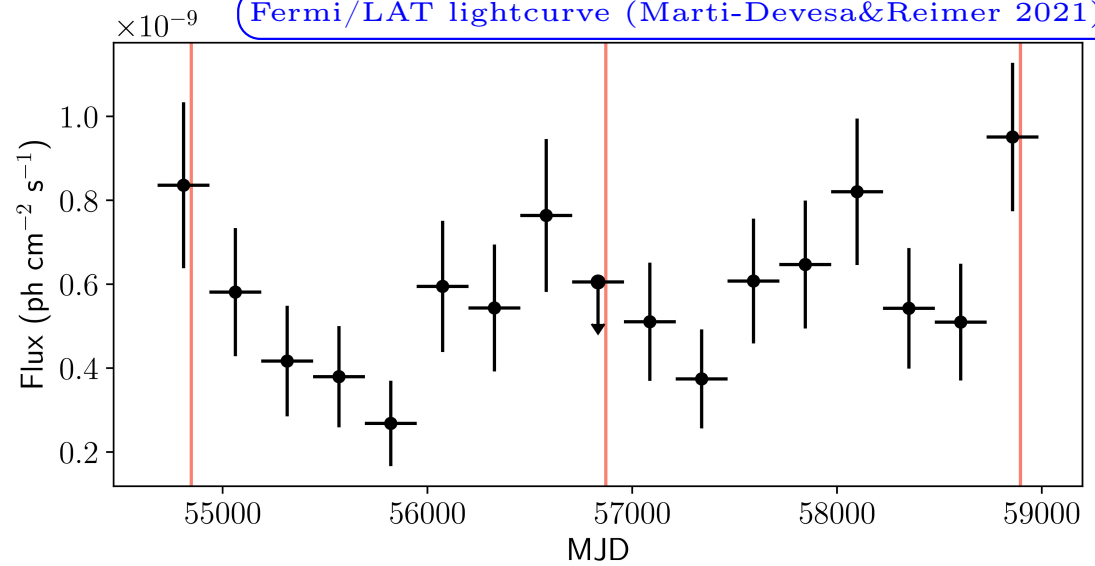

Colliding Wind Binaries

VHE spectrum (H.E.S.S. Coll. 2020)

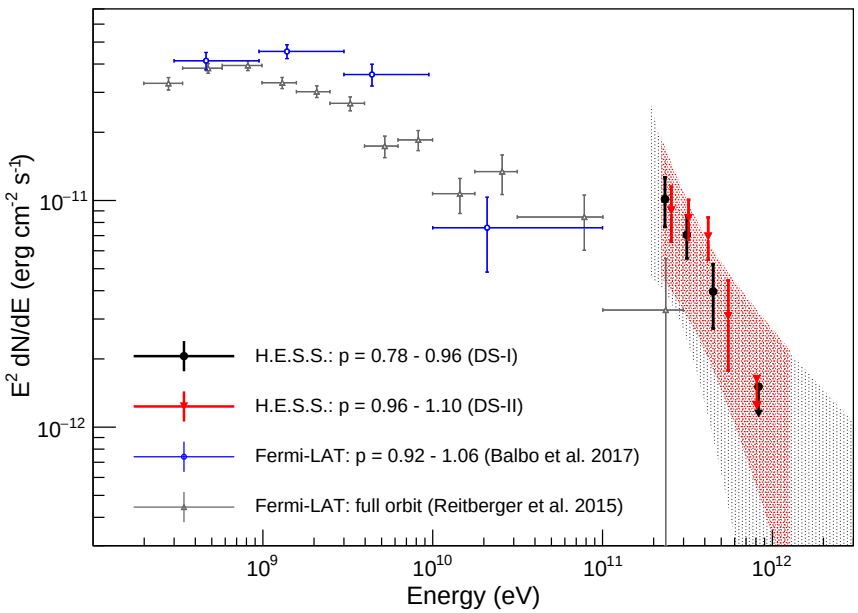

Fermi/LAT lightcurve (Marti-Devesa&Reime

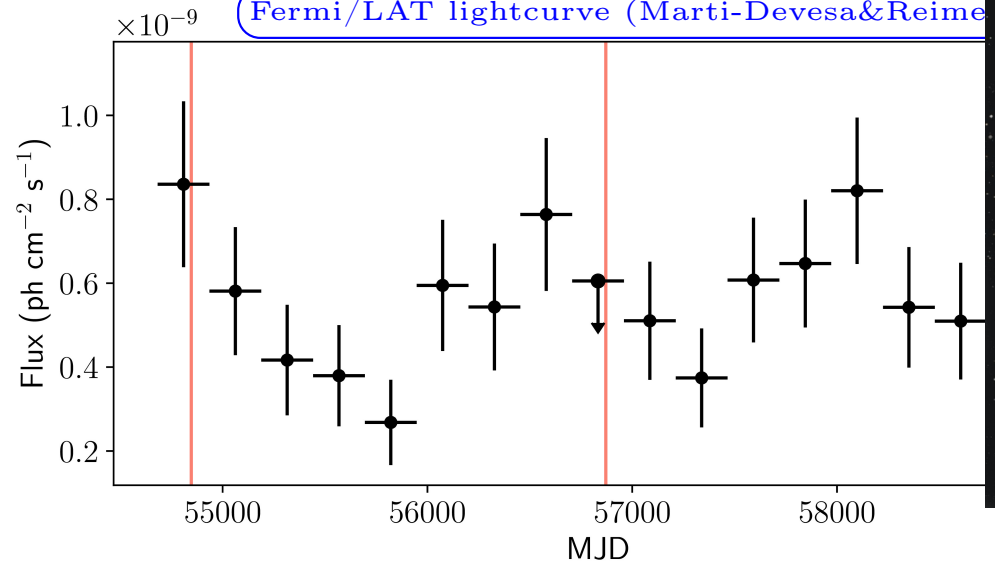

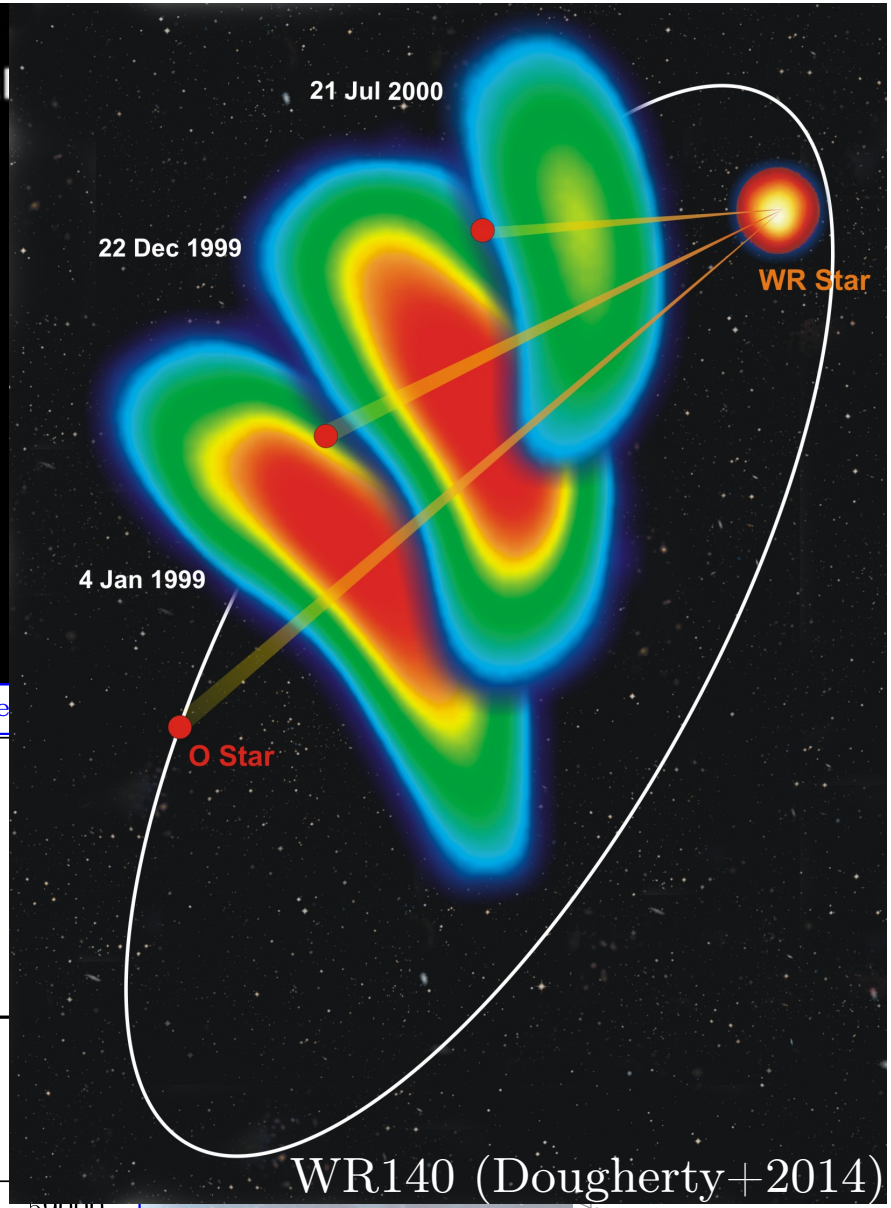

Outline

Binary Systems@VHE γ rays

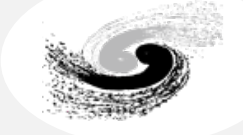

System	Star	Star*	P	VHE	HE	X-ray
PSR B1259-63/LS2883	psr	O/Be	1237d	periodic	variable	periodic
LS 5039	psr(?)	O	3.9d	periodic	periodic	periodic
LS I +61+303	psr(?)	Be	27d	variable	periodic	variable
HESS J0632+057	?	Be	320d	variable	steady(?)	variable
HESS J1832-093	?	Be(?)	86d(?)	variable(?)	periodic(?)	periodic
1FGL J1018.6-5856	?	O	17d	variable	periodic	variable
PSR J2032+4127	psr	Be	50yr	variable	variable	variable
LMC P3	?	O	10d	periodic	periodic	variable
Cyg X-1	bh	O	5.6d	flare	flare	—
Cyg X-3	bh(?)	WR	4.8h	flare	flare	—
SS433	bh	A	13d	steady	steady(?)	steady
V4641 Sgr	bh	B	2.8d	steady(?)	—	flare
MAXI J1820+070	bh	KG	0.7d	steady(?)	—	flare
GRS 1915+105	bh	RG	33.5d	steady(?)	steady(?)	flare
η Car	BG	O	5.5yr	variable(?)	variable	variable
RS Oph	WD	RG	1.2yr	flare	flare	flare

Gamma-Ray Binary Systems

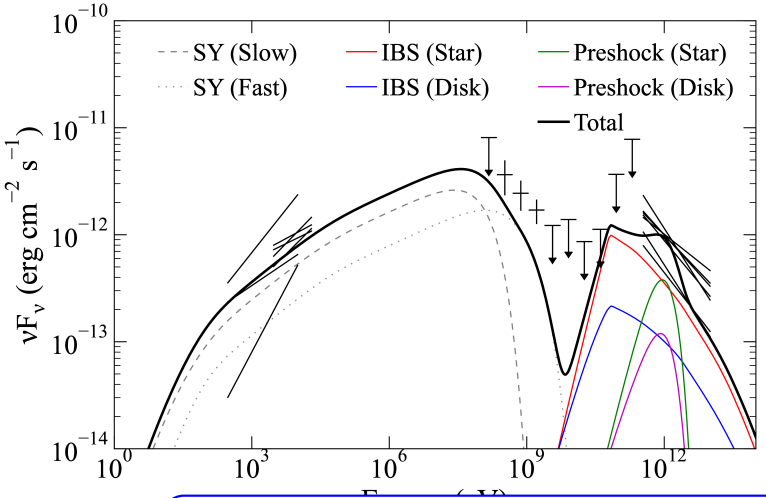

SED of HESS J0632+057 (Kim+2022)

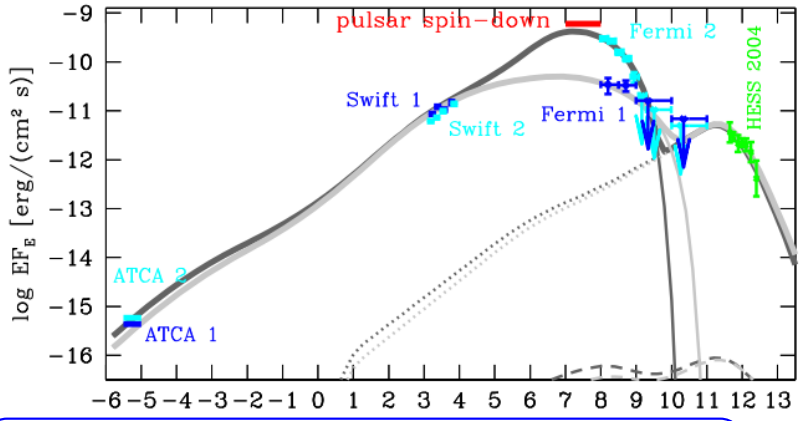

SED of PSR B1259-63/LS2883 (Abdo+2011)

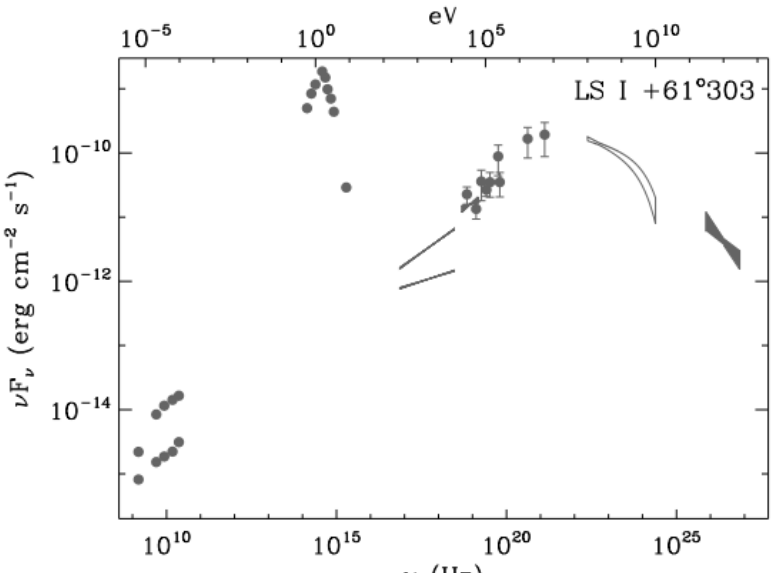

SED of LS I +61+303 (Dubus+2013)

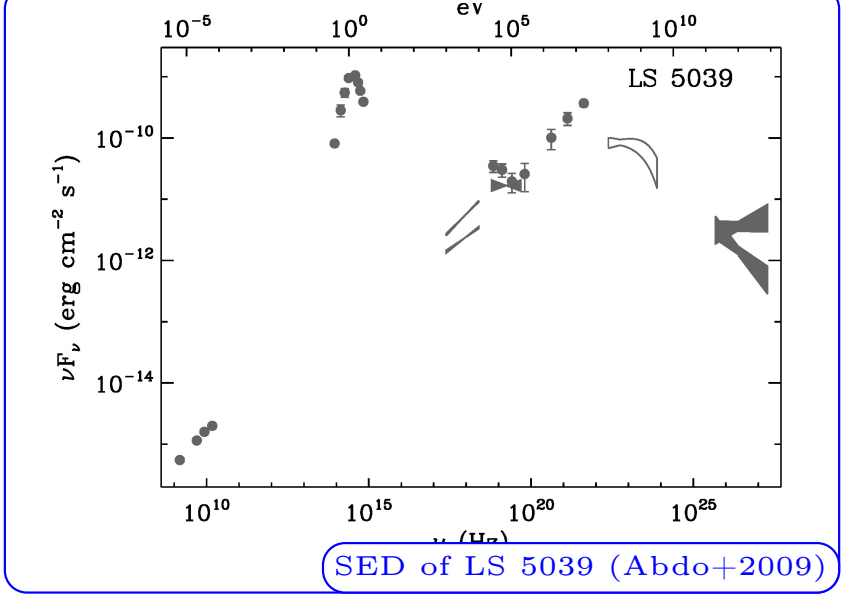

SED of LS 5039 (Abdo+2009)

Criteria for Gamma-Ray Binary:

- Hard non-thermal X-ray emission
- Detected TeV emission
- Contains luminous star
- SED is dominated in gamma-rays
- Contains non-acreting pulsar

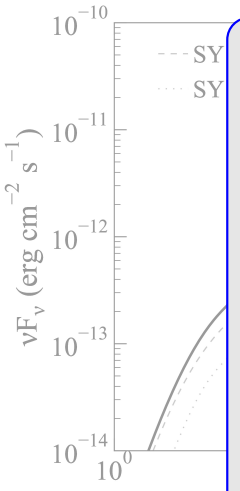

SE

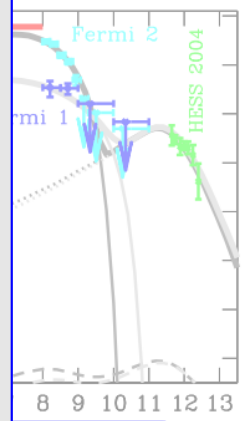

do+2011)

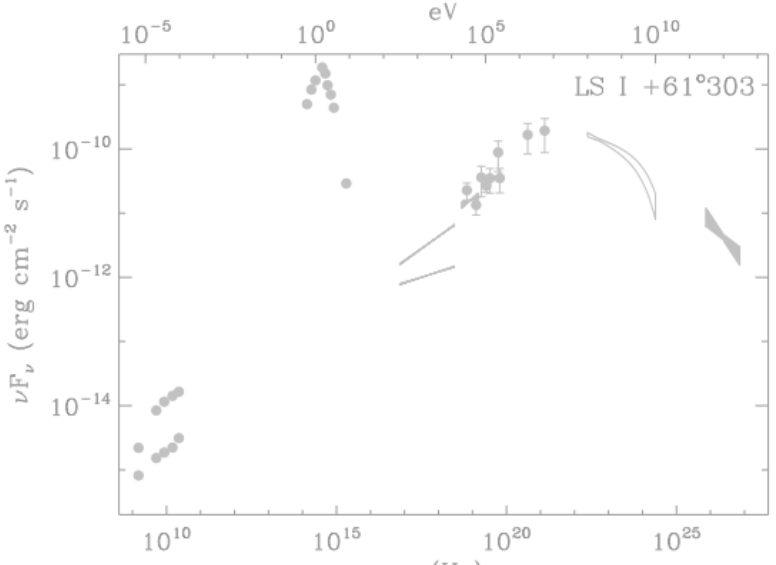

SED of LS I +61+303 (Dubus+2013)

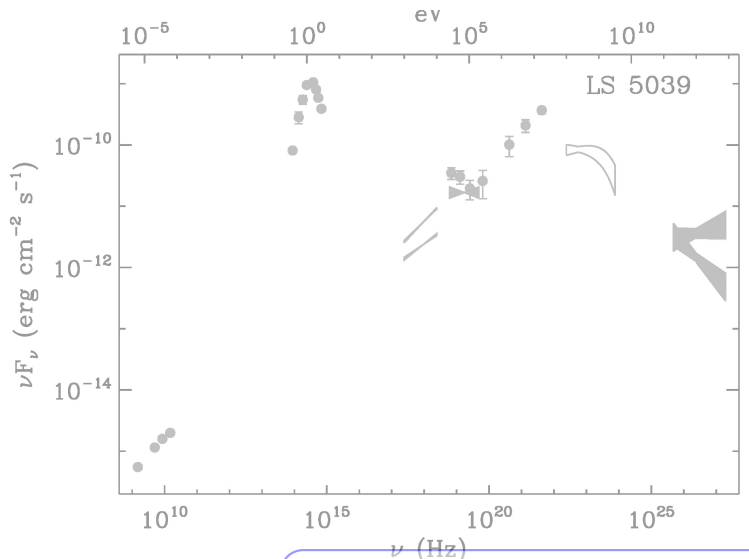

SED of LS 5039 (Abdo+2009)

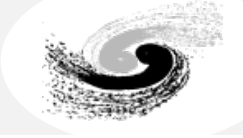

Criteria for Gamma-Ray Binary:

- Hard non-thermal X-ray emission
- Detected TeV emission
- Contains luminous star
- SED is dominated in gamma-rays
- Contains non accreting pulsar

System	X-ray	VHE	Star	SED	PSR
PSR B1259-63/LS2883	✔	✔	✔	✔	✔
LS 5039	✔	✔	✔	✔	✔?
LS I +61+303	✔	✔	✔	✔	✔?
HESS J0632+057	✔	✔	✔	✔	✘
1FGL J1018.6-5856	✔	✔	✔	✔	✘
HESS J1832-093	✔	✔	✔	✔	✘
PSR J2032+4127	✔	✔	✔	✔	✔
LMC P3	✔	✔	✔	✔	✘

Note that ✔ means YES; ✘ means we don't know

Criteria for Gamma-Ray Binary:

- Hard non-thermal X-ray emission
- Detected TeV emission
- Contains luminous star
- SED is dominated in gamma-rays
- Contains non accreting pulsar

System	X-ray	VHE	Star	SED	PSR
PSR B1259-63/LS2883	✔	✔	✔	✔	All contain PSR? (or Magnetar!)
LS 5039	✔	✔	✔	✔	
LS I +61+303	✔	✔	✔	✔	
HESS J0632+057	✔	✔	✔	✔	
1FGL J1018.6-5856	✔	✔	✔	✔	
HESS J1832-093	✔	✔	✔	✔	
PSR J2032+4127	✔	✔	✔	✔	
LMC P3	✔	✔	✔	✔	

Note that ✔ means YES; ✘ means we don't know

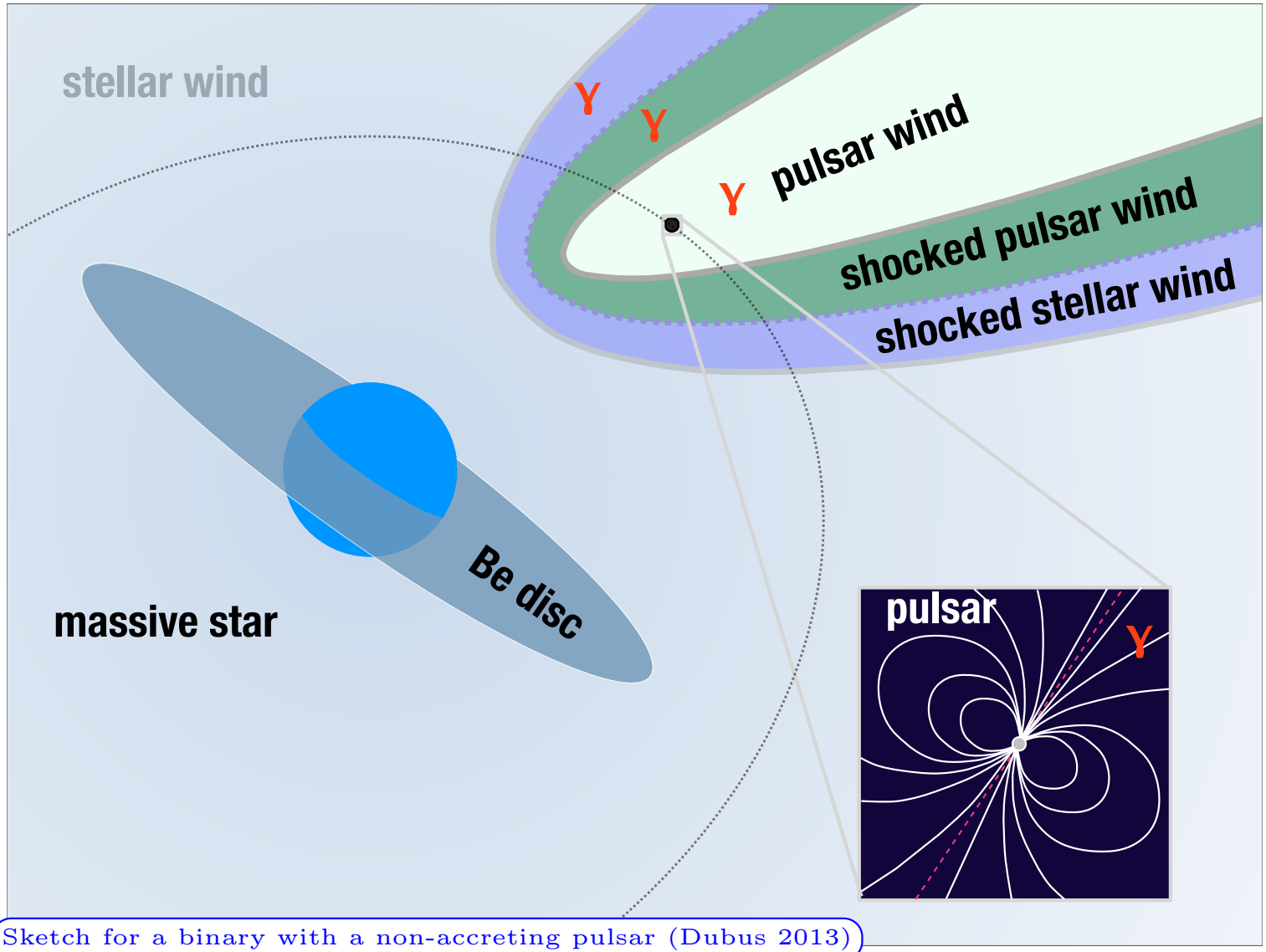

Sketch for a binary with a non-accreting pulsar (Dubus 2013)

Note that ✔ means YES; ✘ means we don't know

Outline

Binary Systems@VHE γ rays

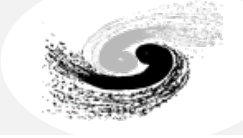

System	Star	Star*	P	VHE	HE	X-ray
PSR B1259-63/LS2883	psr	O/Be	1237d	periodic	variable	periodic
LS 5039	psr(?)	O	3.9d	periodic	periodic	periodic
LS I +61+303	psr(?)	Be	27d	variable	periodic	variable
HESS J0632+057	?	Be	320d	variable	steady(?)	variable
HESS J1832-093	?	Be(?)	86d(?)	variable(?)	periodic(?)	periodic
1FGL J1018.6-5856	?	O	17d	variable	periodic	variable
PSR J2032+4127	psr	Be	50yr	variable	variable	variable
LMC P3	?	O	10d	periodic	periodic	variable
Cyg X-1	bh	O	5.6d	flare	flare	—
Cyg X-3	bh(?)	WR	4.8h	flare	flare	—
SS433	bh	A	13d	steady	steady(?)	steady
V4641 Sgr	bh	B	2.8d	steady(?)	—	flare
MAXI J1820+070	bh	KG	0.7d	steady(?)	—	flare
GRS 1915+105	bh	RG	33.5d	steady(?)	steady(?)	flare
η Car	BG	O	5.5yr	variable(?)	variable	variable
RS Oph	WD	RG	1.2yr	flare	flare	flare

What are microquasars?

Artistic view (credit NASA)

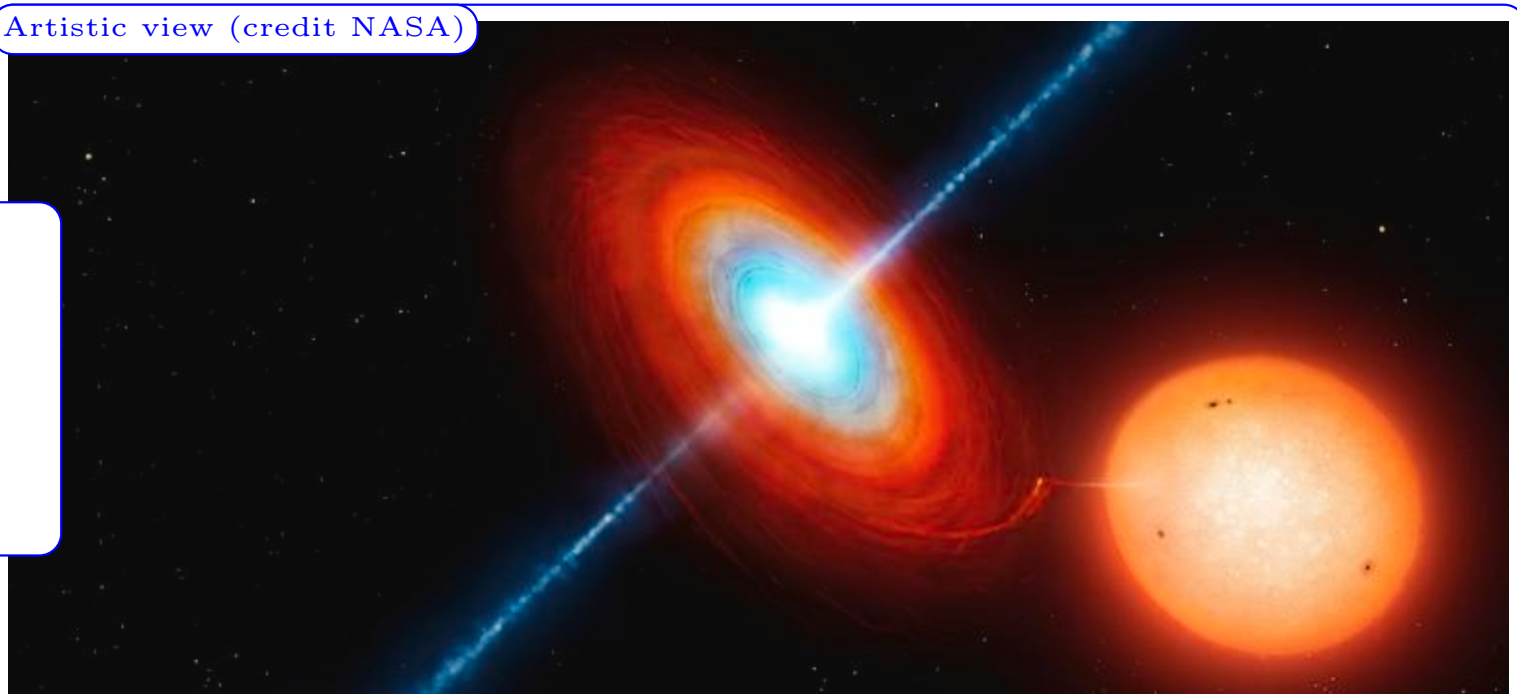

Key elements:

- Compact object
- Optical star
- Intense accretion
- Relativistic jet

A microquasar is a compact stellar system composed of a stellar-mass black hole or neutron star accreting matter from a companion star. The resulting accretion disk produces strong X-ray emission, indicative of a high accretion rate, and the system launches two powerful, relativistic jets moving at speeds close to that of light.
The term microquasar draws a phenomenological analogy with quasars: while this analogy has not yet led to a direct breakthrough in either domain, microquasars nevertheless serve as unique nearby laboratories for investigating accretion and jet-launching processes that.

What are microquasars?

Let us "zoom out" and consider microquasars on Galactic scale

- There are $\sim 2 \times 10^{11}$ stars in MW
- A significant fraction of them in binary system
- To create a BH/NS the progenitor star needs to be massive
- 1% of stars are massive
- "almost all" massive stars in binary systems
- there could be 10^9 massive binary systems in MW

What are these systems? How many of them are microquasars? We know about 20 microquasars in MW, which makes them quite a rare class of objects!

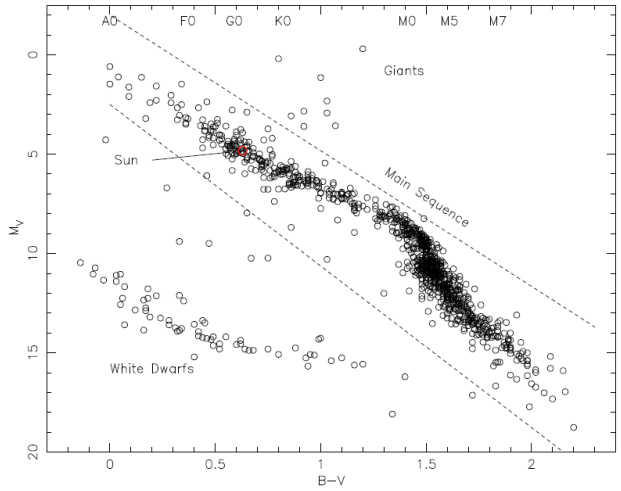

The nearest 1000 stars from the Gliese & Jahreiss 3rd catalogue of nearby stars

What are microquasars?

Whate are all these massive star binaries?

- Colliding wind binaries
- Live for $\sim 10^6$ yr $\Rightarrow$ one of the companions dies
- Disrupted, high eccentricity, large separation systems $\Rightarrow$ do not show clear binary features
- CO: black hole $\Rightarrow$ accretion powered source

  high accretion rate$\Rightarrow$ X-ray binary
- CO: NS $\Rightarrow$ there are several options

  strong wind $\Rightarrow$ binary pulsar system
  low accretion rate $\Rightarrow$ reccurent nova
  high accretion rate$\Rightarrow$ X-ray binary

There are quite a lot of X-ray binary systems...
How many with black holes? 20-70
How many microquasars? $\sim$20

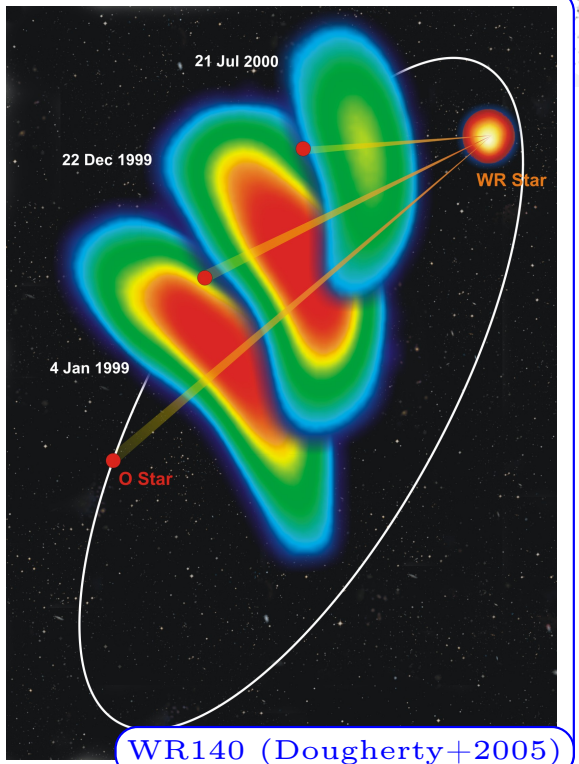

WR140 (Dougherty+2005)

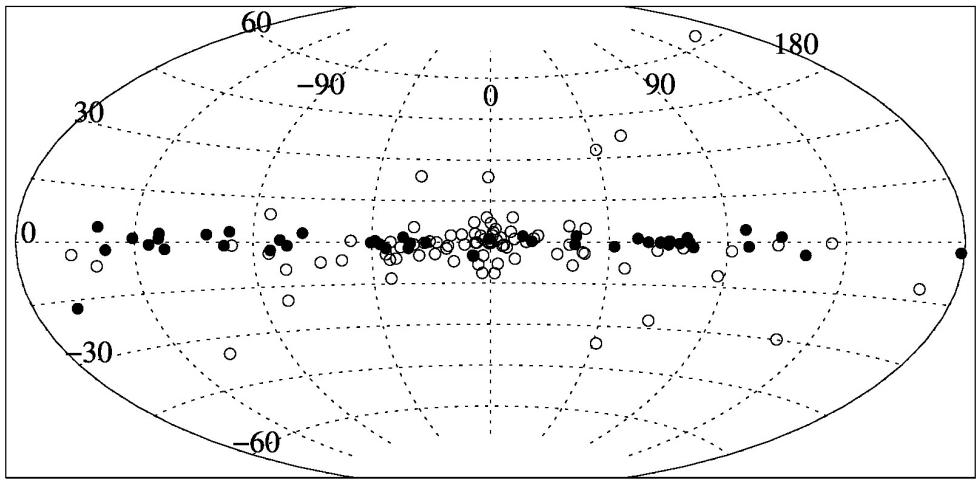

Distribution of X-ray binaries in the Galaxy

What are microquasars?

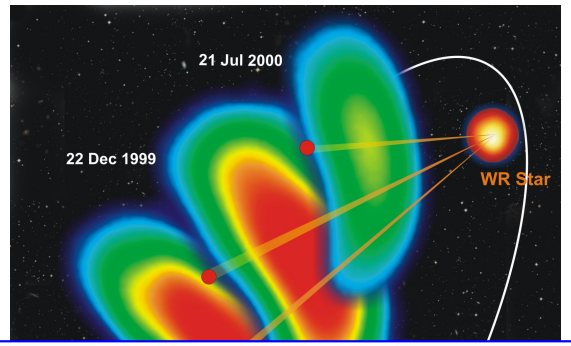

Whate are all these massive star binaries?

- Colliding wind binaries
- Live for $\sim 10^6$ yr $\Rightarrow$ one of t companions dies
- Disrupted, high eccentricity, la separation systems $\Rightarrow$ do not sh clear binary features
- CO: black hole $\Rightarrow$ accretion po ered source

  high accretion rate$\Rightarrow$ X-ray bin
- CO: NS $\Rightarrow$ there are several tions

  strong wind $\Rightarrow$ binary pulsar s tem
  low accretion rate $\Rightarrow$ reccur nova
  high accretion rate$\Rightarrow$ X-ray bin

There are quite a lot of X-ray bina systems...
How many with black holes? 20-70
How many microquasars? $\sim$20

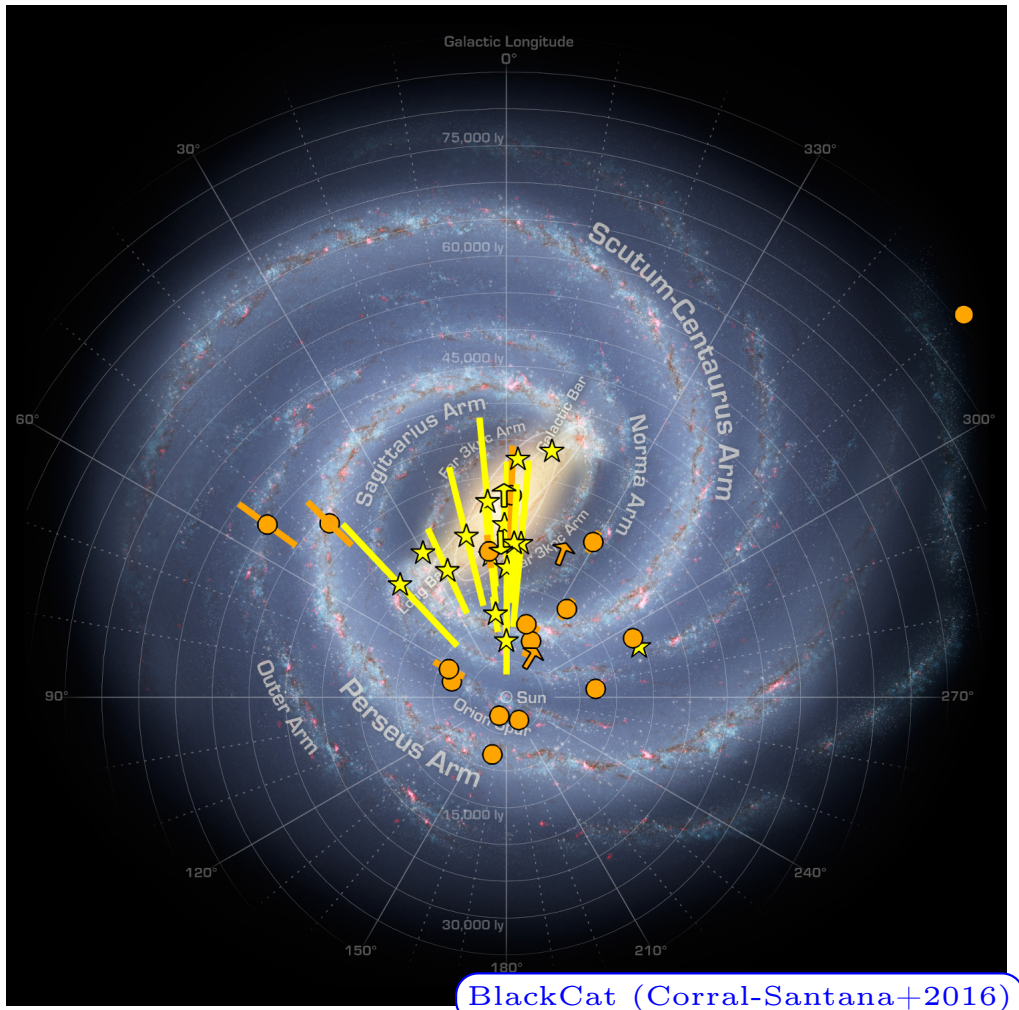

BlackCat (Corral-Santana+2016)

Distribution of X-ray binaries in the Galaxy

What are microquasars?

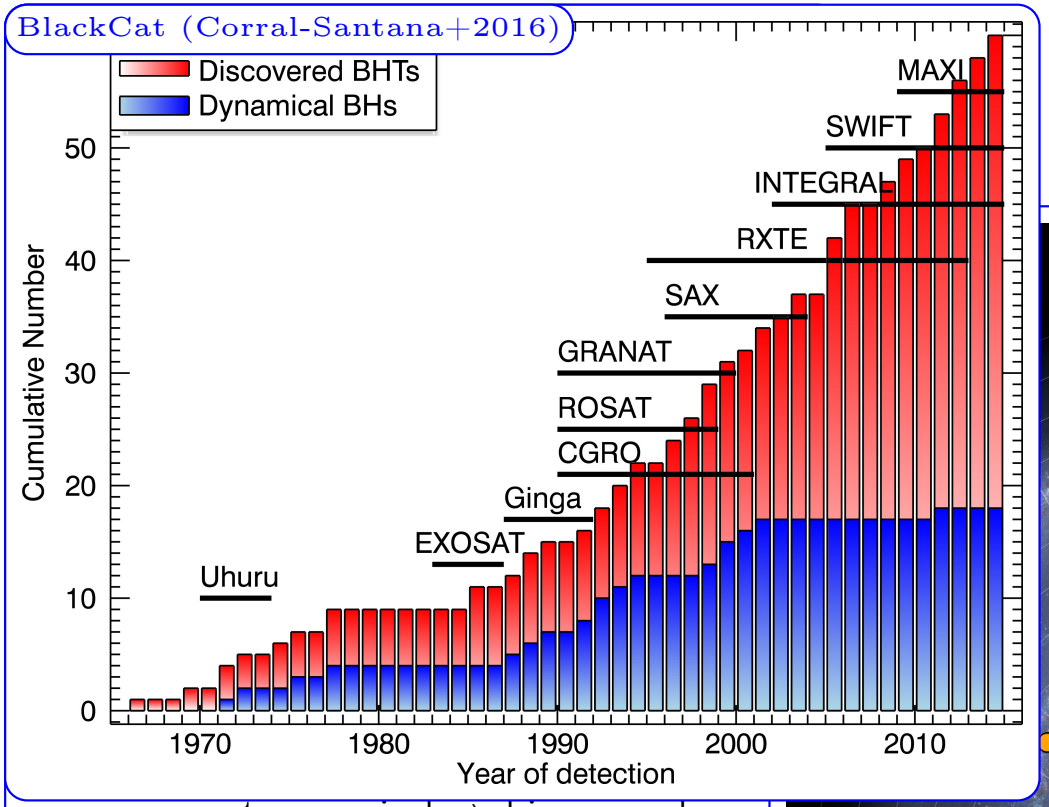

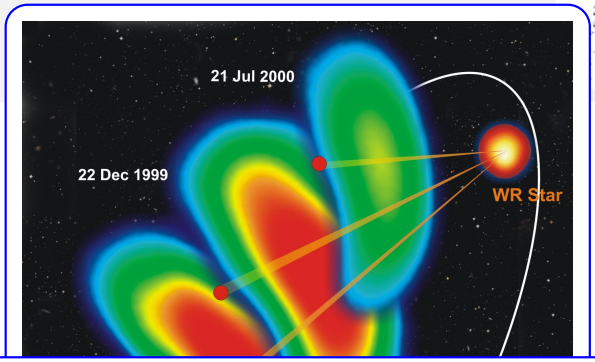

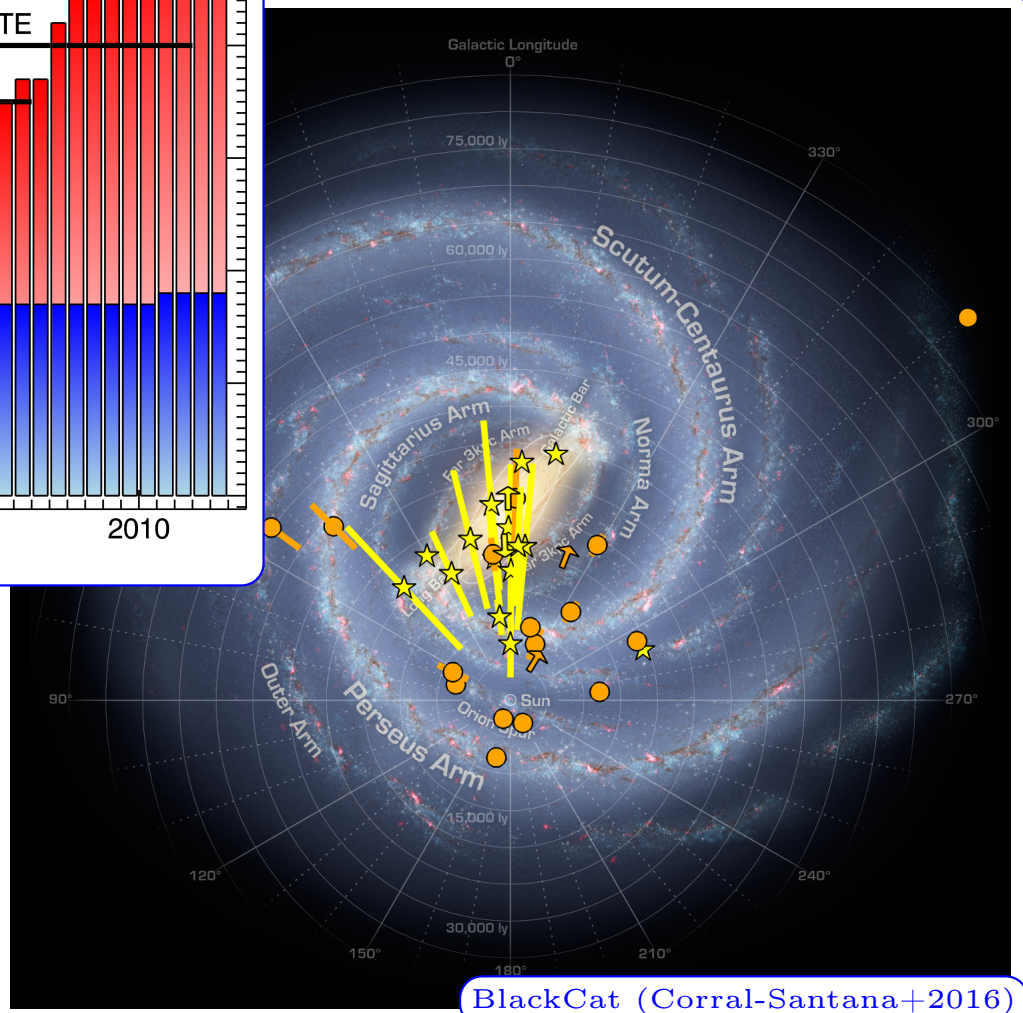

strong wind ⇒ binary pulsar s
tem
low accretion rate ⇒ reccur
nova
high accretion rate⇒ X-ray bin

There are quite a lot of X-ray bina
systems...
How many with black holes? 20-70
How many microquasars? ∼20

Census

Microquasars

- black holes
  - GRS 1915+105
  - Cygnus X-1
  - V404 Cygni
  - XTE J1550-564
  - GRO J1655-40
  - XTE J1118+480
  - V4641 Sgr
  - V691 CrA (GRS 1716-249)
  - GX 339-4
  - MAXI J1820+070
  - V406 Vul(?)
- unknown
  - 4U 1755-33
  - Cygnus X-3
  - SS 433
  - CI Cam (XTE J0421+560)
  - 4U 1630-47
- NSs
  - Scorpius X-1
  - Cir X-1

Census

Microquasars

black holes
- GRS 1915+105
- Cygnus X-1
- V404 Cygni
- XTE J1550-564
- GRO J1655-40
- XTE J1118+480
- V4641 Sgr
- V691 CrA (GRS 1716-249)
- GX 339-4
- MAXI J1820+070
- V406 Vul(?)

unknown
- 4U 1755-33
- Cygnus X-3
- SS 433
- CI Cam (XTE J0421+560)
- 4U 1630-47

NSs
- Scorpius X-1
- Cir X-1

Galactic black holes (dynamic)

microquasars

V4641 Sgr	V518 Per
Cygnus X-1	H 1705-25
V404 Cyg	GRS 1009-45
V406 Vul(?)	GS 2000+25
XTE J1118+480	MAXI J1305-704
XTE J1550-564	GRO J1719-24
GX 339-4	GRS 1124-683
GRS 1915+105	NGC 3201 #12560
MAXI J1820+070	NGC 3201 #21859
V691 CrA	A0620-00
GRO J1655-40	XTE J1650-500
4U 1543-475	GS 1354-64

Note that each of these systems has several different names. Furthermore, there could be a discrepancy in the classification of a specific binary system as a microquasar.

Black Holes in Our Galaxy

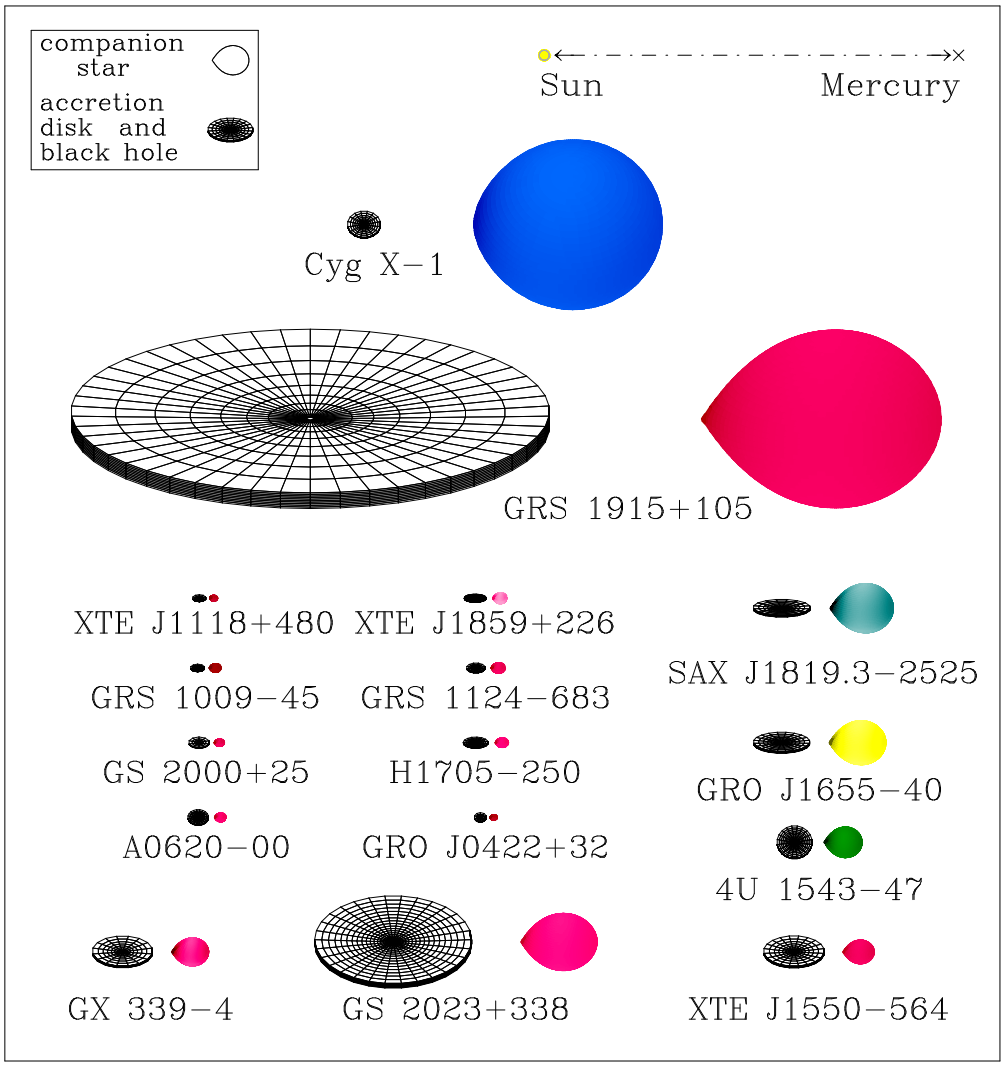

courtesy of J. Orosz

Binary systems are (all) different:

- Mass of the BH
- Mass of the donor star
- Size of the orbit
- Eccentricity of the orbit
- Inclination of the orbit
- Age of the system
- Environment

Stellar-Mass Black Holes seen with LHAASO

- Visibility from the LHAASO site (29°N) for zenith angle $< 55°$
- There are 14 binaries (probably) with black holes that can be seen with LHAASO
- Among these 14 binaries, 8 are microquasars

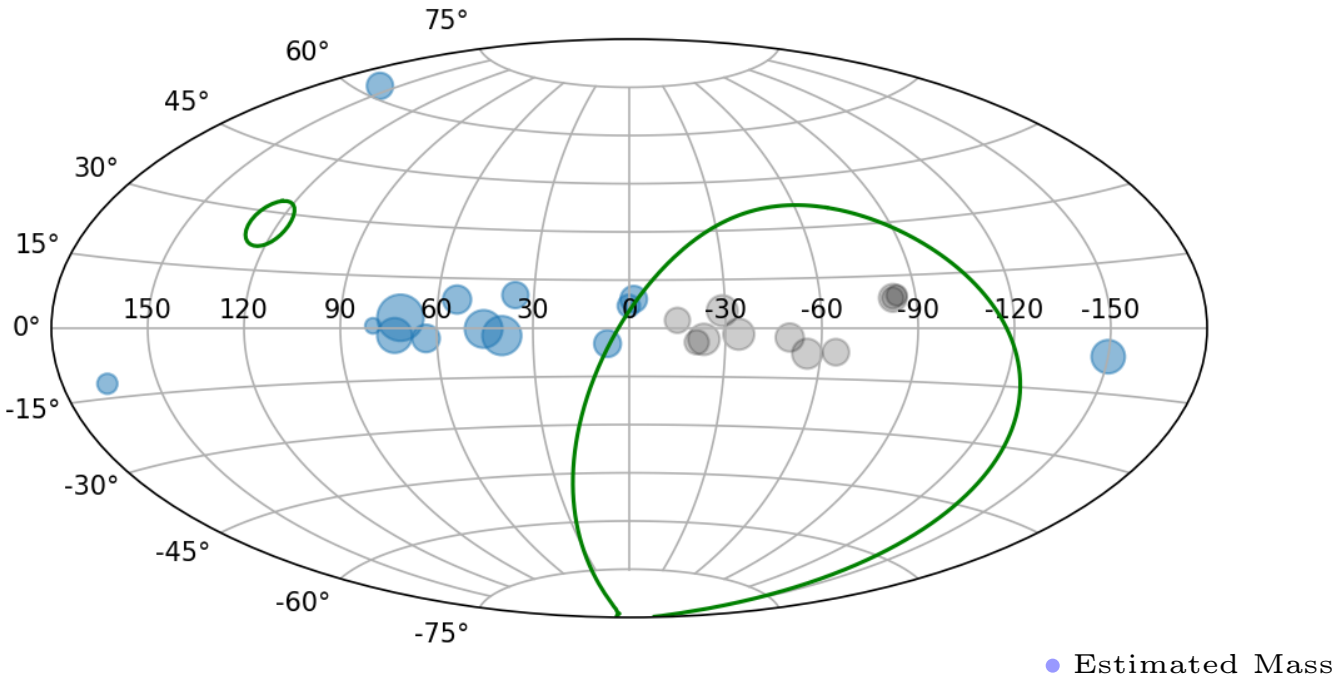

Stellar-Mass Black Holes seen with LHAASO

Object	$M_{BH}[M_\odot]$	$\sim M_*[M_\odot]$	P[d]	D[kp]
XTE J1118+480	6.8 ± 0.4	6	0.17	1.7
Cyg X-1	21.2 ± 2.2	40	5.6	2.2
V404 Cyg	12 ± 2	6	6.5	2.4
GRO J0422+32	4 ± 1	1	0.21	2.6
GS 2000+25	7.5 ± 0.3	5	0.35	2.7
V406 Vul	7.8 ± 1.9	0.5	0.276	4.2
GRS 1915+105	14 ± 4.0	1	33.5	9.4
MAXI J1820+070	6.75 ± 0.5	0.5	0.68	3.0
SS433	17 ± 13	30	13	4.6
A0620-00	11 ± 2	3	0.33	1.1
GRO J1719-24	> 4.9	1.6	0.6	2.6
H 1705-25	6.95 ± 1.35	0.4	0.5	8.3
V4641 Sgr	7.1 ± 0.3	7	2.82	6.2
Cyg X-3	2.4 ± 1.1	10	0.2	9

Stellar-Mass Black Holes seen with LHAASO

Object	$M_{BH}[M_\odot]$	$\sim M_*[M_\odot]$	P[d]	D[kp]	μQ?	detected?
XTE J1118+480	6.8 ± 0.4	6	0.17	1.7	✘	✘
Cyg X-1	21.2 ± 2.2	40	5.6	2.2	✔	✔
V404 Cyg	12 ± 2	6	6.5	2.4	✔	✘
GRO J0422+32	4 ± 1	1	0.21	2.6	✘	✘
GS 2000+25	7.5 ± 0.3	5	0.35	2.7	✘	✘
V406 Vul	7.8 ± 1.9	0.5	0.276	4.2	?	✘
GRS 1915+105	14 ± 4.0	1	33.5	9.4	✔	✔
MAXI J1820+070	6.75 ± 0.5	0.5	0.68	3.0	✔	✔
SS433	17 ± 13	30	13	4.6	✔	✔
A0620-00	11 ± 2	3	0.33	1.1	✘	✘
GRO J1719-24	> 4.9	1.6	0.6	2.6	✘	✘
H 1705-25	6.95 ± 1.35	0.4	0.5	8.3	✘	✘
V4641 Sgr	7.1 ± 0.3	7	2.82	6.2	✔	✔
Cyg X-3	2.4 ± 1.1	10	0.2	9	✔	✔

Stellar-Mass Black Holes seen with LHAASO

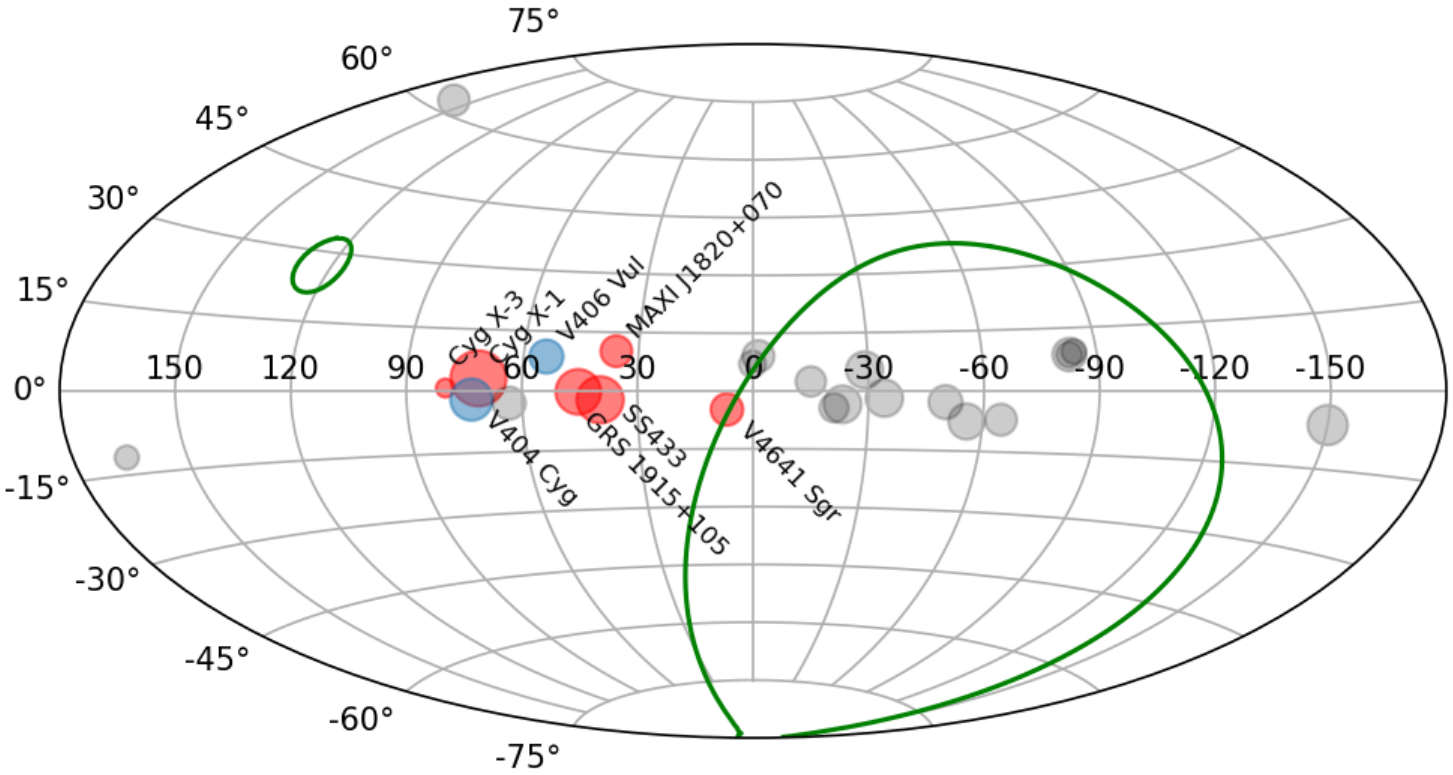

The mass of the black hole might to be an important factor for detection, but not critical. What is then the defining criterion?

Outline

Why Galactic jets are good accelerators?

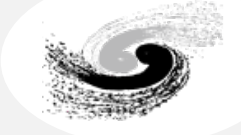

Hillas criterion

- Particle energy is changed by electric field:

$$\mathrm{E_{max}} \sim \mathrm{e}\mathcal{E}\mathrm{R}$$

- Conductivity of space plasma is typically very large, thus

$$\vec{\mathcal{E}} = \vec{\beta} \times \vec{\mathcal{B}}$$

- The energy gain at crossing the source

$$\mathrm{E_{max}} \sim \mathrm{e}\beta\mathcal{B}\mathrm{R}$$

- The Poynting flux carries a fraction of the total source luminosity:

$$\frac{\mathrm{c}\beta}{4\pi}\mathcal{B}^2 4\pi \mathrm{R}^2 = \sigma \mathrm{L}$$

- Maximum energy:

$$\mathrm{E_{max}} \sim \sqrt{\sigma\beta}\sqrt{\frac{\mathrm{e}^2\mathrm{L}}{\mathrm{c}}}$$
$$\approx 5\sigma_{-1}^{1/2}\beta_{-1}^{1/2}\mathrm{L}_{39}^{1/2}\ \mathrm{PeV}$$

1984ARA&A..22..425H

Ann. Rev. Astron. Astrophys. 1984. 22 : 425–44

THE ORIGIN OF ULTRA-HIGH-ENERGY COSMIC RAYS

A. M. Hillas

Physics Department, University of Leeds, Leeds LS2 9JT, England

1. WHY BOTHER WITH ULTRA-HIGH-ENERGY COSMIC RAYS?

For efficient acceleration, one needs

- High luminosity, L
- Fast outflow, β
- High magnetization, σ

(obviously)

Why Galactic jets are good accelerators?

Hillas criterion

- Particle energy is changed by electric field:

$$\mathrm{E_{max}} \sim \mathrm{e}\mathcal{E}\mathrm{R}$$

- Conductivity of space plasma is typically very large, thus

$$\vec{\mathcal{E}} = \vec{\beta} \times \vec{\mathcal{B}}$$

- The energy gain at crossing the source

$$\mathrm{E_{max}} \sim \mathrm{e}\beta\mathcal{B}\mathrm{R}$$

- The Poynting flux carries a fraction of the total source luminosity:

$$\frac{\mathrm{c}\beta}{4\pi}\mathcal{B}^2 4\pi\mathrm{R}^2 = \sigma\mathrm{L}$$

- Maximum energy:

$$\mathrm{E_{max}} \sim \sqrt{\sigma\beta}\sqrt{\frac{\mathrm{e}^2\mathrm{L}}{\mathrm{c}}}$$
$$\approx 5\sigma_{-1}^{1/2}\beta_{-1}^{1/2}\mathrm{L}_{39}^{1/2}\ \mathrm{PeV}$$

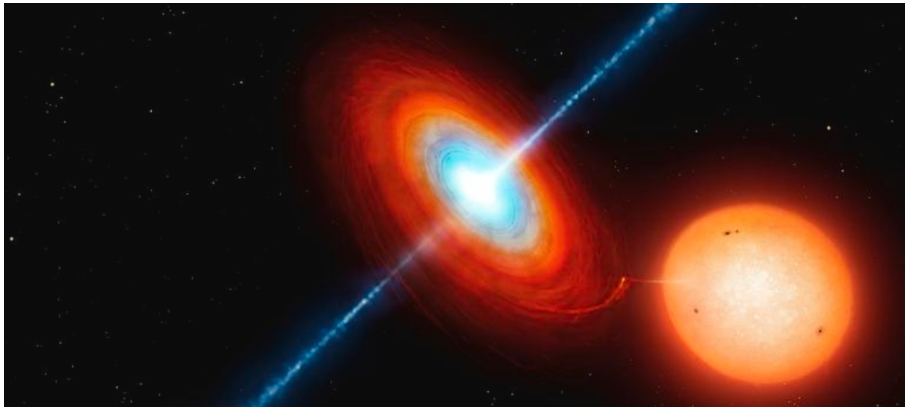

For microquasars we have

- Eddington luminosity for a stellar mass black hole, $\mathrm{L} > 10^{38}\mathrm{erg\,s^{-1}}$
- Mildly relativistic jet, $\beta \sim 1$
- Relativistic jets are believed to be launched by electromagnetic processes, $\sigma \sim 0.1$

Why Galactic jets are good accelerators?

Hillas criterion

- Particle energy is changed by electric field:

$$\mathrm{E_{max}} \sim \mathrm{e}\mathcal{E}\mathrm{R}$$

- Conductivity of space plasma is typically very large, thus

$$\vec{\mathcal{E}} = \vec{\beta} \times \vec{\mathcal{B}}$$

- The energy gain at crossing the source

$$\mathrm{E_{max}} \sim \mathrm{e}\beta\mathcal{B}\mathrm{R}$$

- The Poynting flux carries a fraction of the total source luminosity:

$$\frac{\mathrm{c}\beta}{4\pi}\mathcal{B}^2 4\pi\mathrm{R}^2 = \sigma\mathrm{L}$$

- Maximum energy:

$$\mathrm{E_{max}} \sim \sqrt{\sigma\beta}\sqrt{\frac{\mathrm{e}^2\mathrm{L}}{\mathrm{c}}}$$
$$\approx 5\sigma_{-1}^{1/2}\beta_{-1}^{1/2}\mathrm{L}_{39}^{1/2}\ \mathrm{PeV}$$

Wang et al (2025)

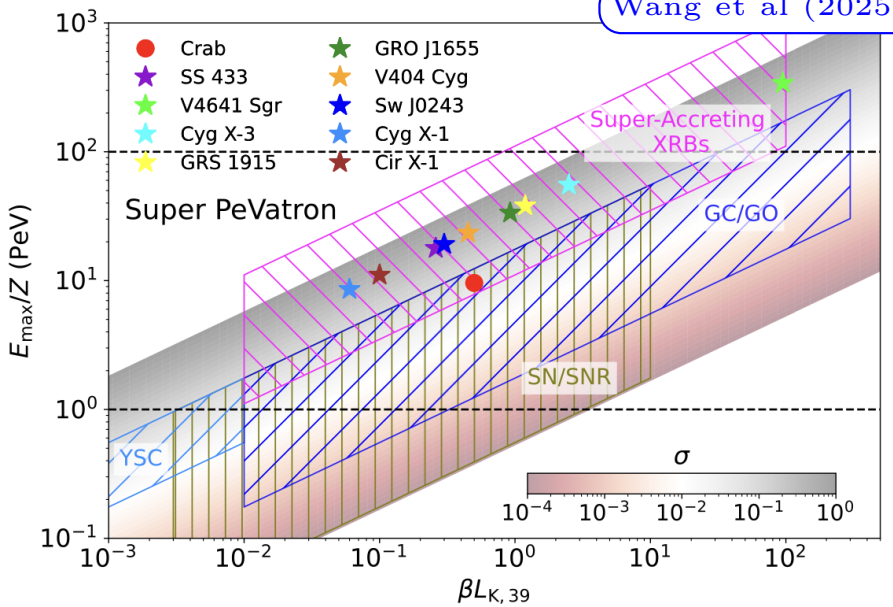

Let's check some common sources

- Super PeVatron sources during powerful flares
- $\beta\mathrm{L} \lesssim 10^{41}\mathrm{erg}$
- $\mathrm{E_{max}} \gtrsim 10^2\ \mathrm{PeV}$

Cosmic Ray Spectrum

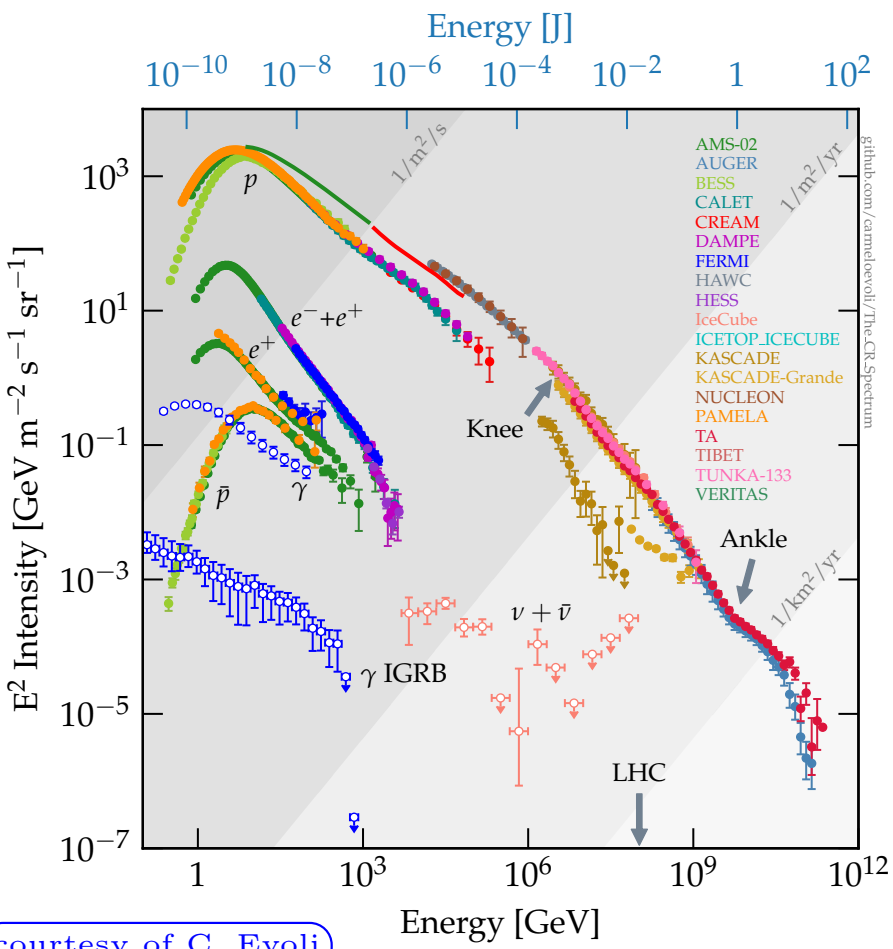

courtesy of C. Evoli

While SNRs remain the leading candidates for Galactic cosmic-ray factories, several pressing issues challenge this paradigm:

- It is unclear whether (all) SNRs can accelerate cosmic rays up to PeV energies.
- The spectrum around the knee exhibits features that may indicate contributions from multiple source classes.
- The contribution from Galactic sources might remain significant well above the knee.

These considerations motivate the search for alternative (super-)PeVatron candidates.

Microquasars have been suggested as the main Galactic PeVatrons (e.g., Kaci+2025)

LHAASO Collaboration (2025)

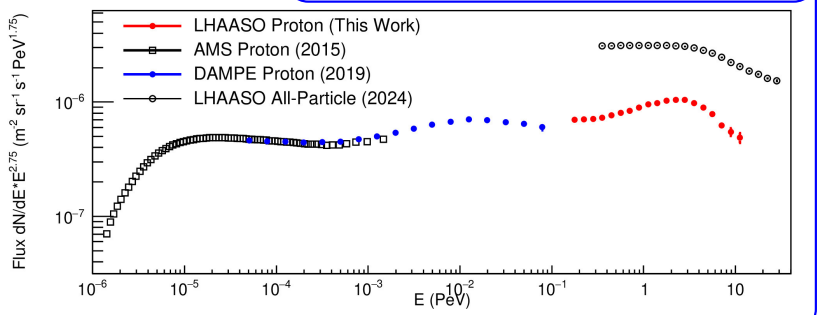

Acceleration vs Losses

$$E_{max} \sim \sqrt{\beta\sigma}\sqrt{\frac{e^2 L}{c}}$$

Doesn't depend on the size!

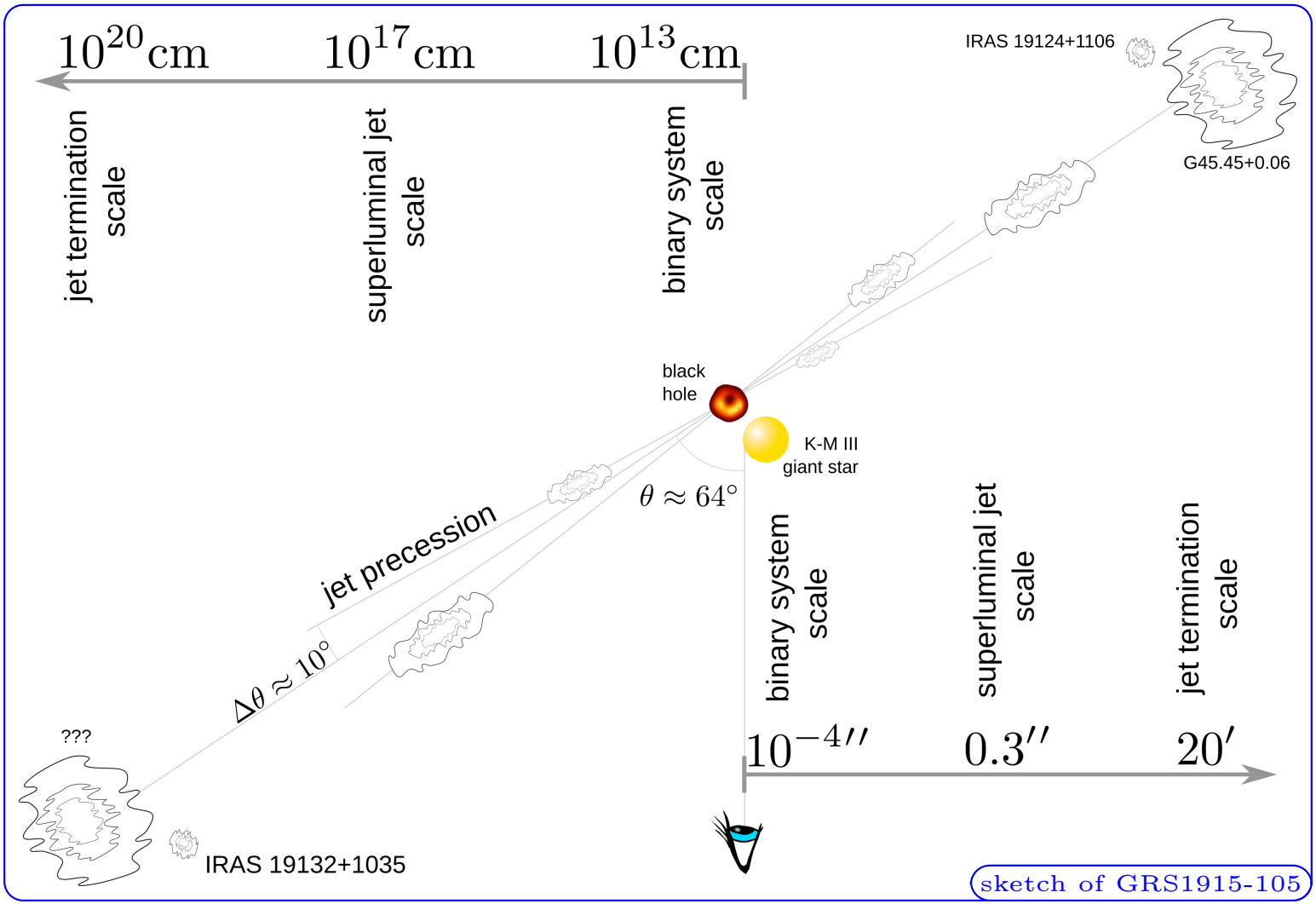

Acceleration vs Losses

$$E_{max} \sim \sqrt{\beta\sigma}\sqrt{\frac{e^2 L}{c}}$$ ← Doesn't depend on the size!

The maximum drop of electric potential is, however, only one of the conditions required for acceleration to this limit. Other constraints involve the acceleration time, $t_{acc} = \eta_{acc} r_{\mathcal{G}}/c$:

- Source age:

$$t_{acc} < t_{age}$$

- Confinement:

$$t_{acc} < t_{esc}$$

- Cooling:

$$t_{acc} < t_{cool}$$

Non of these is a necessary condition – one still needs an acceleration processes that can operate with efficiency η_{acc}.

$\mathcal{B}R \propto \sqrt{L}$

- Source age: $t_{age} = R/\beta c$

$$E_{max} < \frac{e\mathcal{B}R}{\eta_{acc}} \frac{ct_{age}}{R} = \frac{e\mathcal{B}R}{\eta_{acc}\beta}$$

- Conf. 1: $t_{esc} = R/\beta c$

$$E_{max} < \frac{e\mathcal{B}R}{\eta_{acc}\beta}$$

- Conf. 2: $t_{esc} = R^2/6\eta_D D_B$, where $D_B = r_{\mathcal{G}} c/3$

$$E_{max} < \frac{e\mathcal{B}R}{\sqrt{2\eta_{acc}\eta_D}}$$

- Radiative cooling: $t_{cool} \propto R^2$

$$E_{max} < \frac{e\mathcal{B}R}{\eta_{acc}} \frac{ct_0}{R_0} \frac{R}{R_0}$$

Constraint from cooling can be important on "small scales"

What is acceleration efficiency?

- Acceleration time: $t_{acc} = E/\dot{E}$
- Magnetic field $\mathcal{B}$ doesn't change particle energy
- Energy gain for a particle: $mc^2\dot{\gamma} = q\vec{v}\vec{\mathcal{E}}$
- Energy gain for ensemble of particles: $\dot{E} = q\overline{\vec{v}\vec{\mathcal{E}}}$
- Acceleration efficiency is dimensionless parameter: $t_{acc} = \eta r_{\mathcal{G}}/c$
- Naive algebra yields: $\eta^{-1} = \frac{\overline{a\vec{v}\vec{\mathcal{E}}}}{E}\frac{E}{q\mathcal{B}c} = \frac{\overline{\vec{v}\vec{\mathcal{E}}}}{\mathcal{B}c}$
- Typically $\mathcal{E} = \frac{v}{c}\mathcal{B} < \mathcal{B}$
- Trajectories are not straight lines: $\overline{\vec{v}\vec{\mathcal{E}}} \ll c\mathcal{E}$
- Thus, we should expect $\eta_{acc} \gg 1$

(for DSA $\eta_{acc} = 2\pi\left(\frac{c}{v}\right)^2 = 2\pi\left(\frac{c}{v}\right)\left(\frac{c}{v}\right)$)

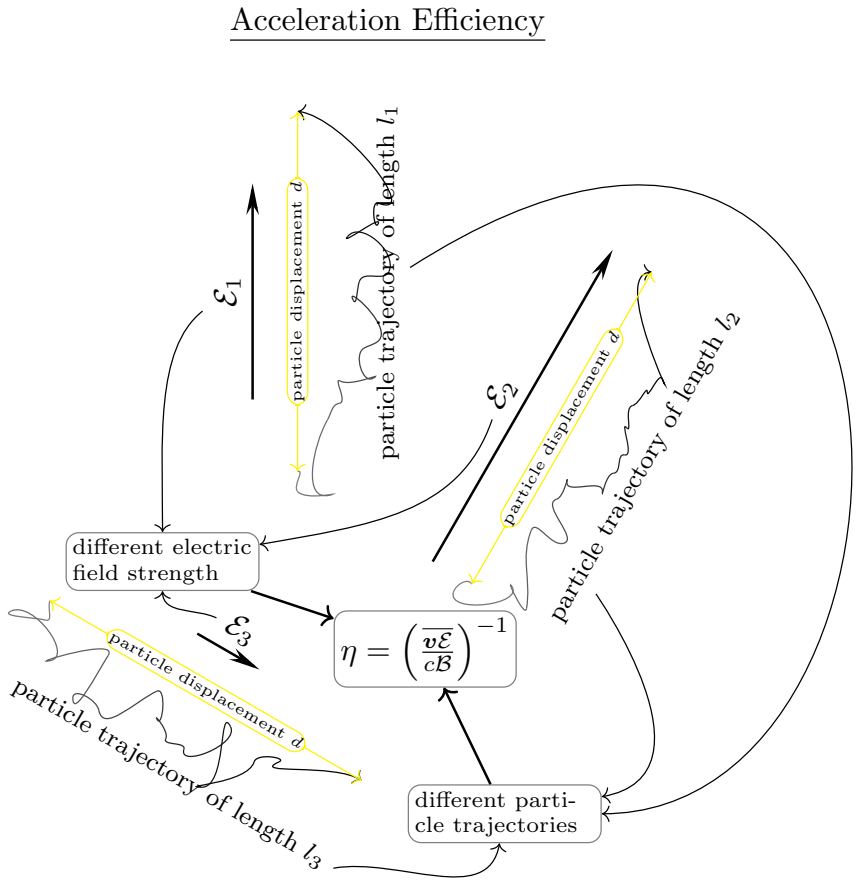

It looks an impossible task to get $\eta_{acc} \to 1$ under realistic conditions

Radiation processes in microquasars

Basic physical parameters:

- Jet power: $L \sim 10^{39} \mathrm{erg\,s^{-1}}$
- Jet bulk speed: $v_{blk} \approx 0.3c$
- Jet opening angle: $\Delta\Omega \approx 0.3$
- Jet magnetization: $\sigma \approx 0.03$
- Star luminosity: $L_\star \sim 10^{38} \mathrm{erg\,s^{-1}}$
- Star temperature: $T_\star \approx 3 \times 10^4\,\mathrm{K}$
- Disk luminosity: $L_d \sim 10^{38} \mathrm{erg\,s^{-1}}$
- Disk temperature: $T_d \approx 6 \times 10^7\,\mathrm{K}$
- Wind mass-loss rate: $\dot{M}_\star \sim 10^{-9} M_\odot\,\mathrm{yr^{-1}}$
- Wind speed: $v_\star \sim 10^3\,\mathrm{km\,s^{-1}}$

Key parameters for electrons

- $\mathcal{B} = 0.2 R_{15}^{-1}\,\mathrm{G}$
- $w_B = 2 \times 10^{-3} R_{15}^{-2}\,\mathrm{erg\,cm^{-3}}$
- $w_\star = 3 \times 10^{-4} R_{15}^{-2}\,\mathrm{erg\,cm^{-3}}$
- $w_d = 3 \times 10^{-4} R_{15}^{-2}\,\mathrm{erg\,cm^{-3}}$
- $w_{bgr} \sim 10^{-11}\,\mathrm{erg\,cm^{-3}}$

Key parameters for protons

- $n_{wind} = 30 R_{15}^{-2}\,\mathrm{cm^{-3}}$
- $n_{ism} = 1\,\mathrm{cm^{-3}}$
- $n_\star = 2 \times 10^7 R_{15}^{-2}\,\mathrm{cm^{-3}}$
- $n_d = 10^4 R_{15}^{-2}\,\mathrm{cm^{-3}}$

Acceleration and radiation regime

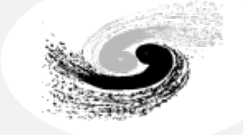

Acceleration time

- DSA in mildly relativistic jet, $\eta_{\rm acc} \sim 10^3$, and the acceleration time is determined by magnetic field strength

$$t_{\rm acc} = 10^2 \eta_{\rm acc} E_{\rm PeV} \mathcal{B}_{\rm G}^{-1}\,{\rm s} = 5\times 10^2 \eta_{\rm acc} E_{\rm PeV} R_{15}\,{\rm s}$$

Cooling time

- Synchrotron

$$t_{\rm syn} = 0.4 E_{\rm PeV}^{-1} \mathcal{B}_{\rm G}^{-2}\,{\rm s}$$

- Thomson similar to synchrotron
- Klein-Nishina is gradually less efficient
- Hadronic pp

$$t_{\rm pp} \approx 10^5 n_{\rm p,10}\,{\rm s}$$

- Hadronic pγ

$$t_{\rm p\gamma} \approx 10^7 n_{\rm ph,10}\,{\rm s}$$

Escape time

- Advection (in the jet)

$$t_{\rm adv} = 10^5 R_{15}\,{\rm s}$$

- Diffusion (in the termination region)

$$t_{\rm diff} = 10^9 R_{\rm pc}^2 D_{30}^{-1}\,{\rm s}$$

This has the following implications:

- Losses constrain electrons electron energy:

$$E_{\rm max} < \frac{60\,{\rm TeV}}{\sqrt{\eta_{\rm acc}\mathcal{B}_{\rm G}}}$$

- Multi-TeV electrons are in fast cooling regime (synchrotron dominates unless background photons are important)
- Escape dominates losses for protons
- For $R < 10\,{\rm pc}$ pγ dominates (provided protons are accelerated to sufficiently high energies)
- In the termination region pp becomes efficient

Outline

SS433@Radio

Blundell&Bowler2004

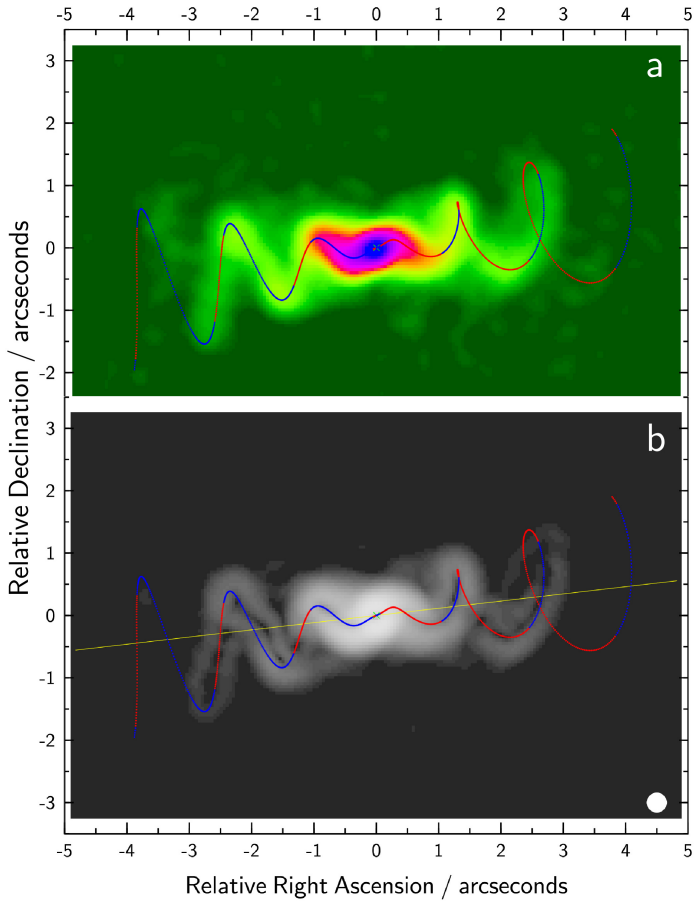

Safi-Harb+2022

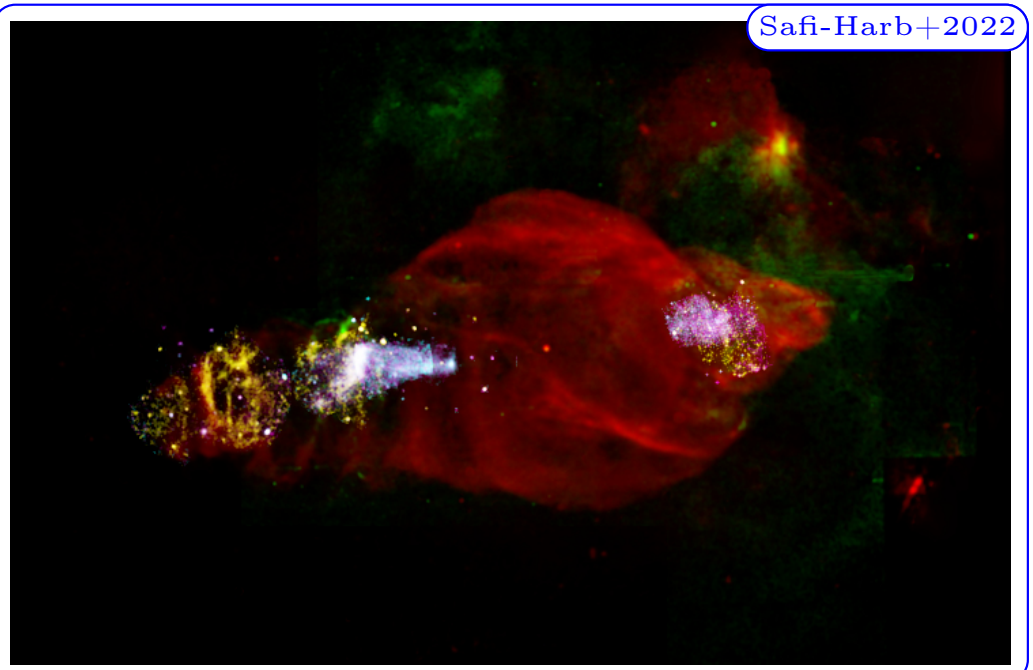

- For a source distance of 5.5 kpc, $1''$ corresponds to 3×10^{-2} pc.
- The size of W50 and the jets is on the order of ~ 100 pc.
- Thus, we observe a coherent structure extending across four orders of magnitude in scale.

SS433@X-rays

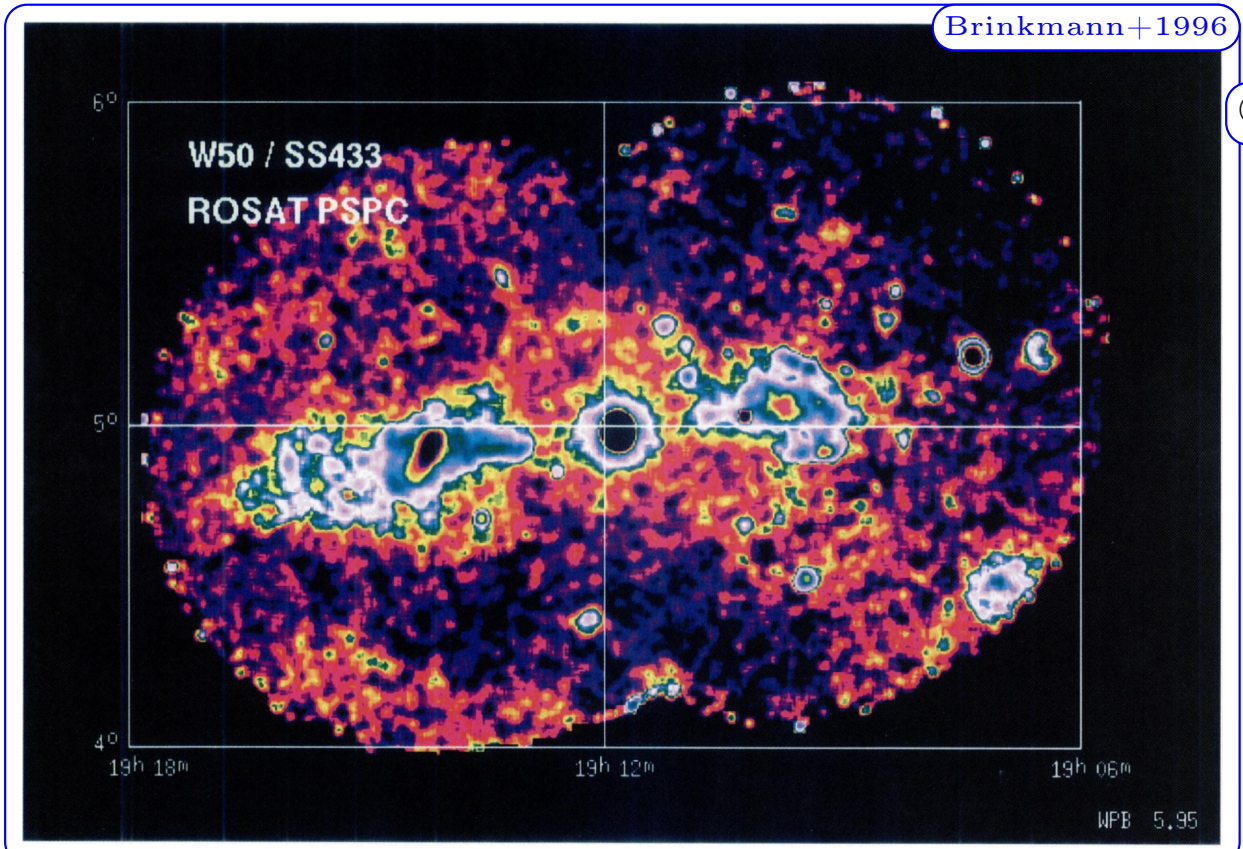

@5.5 kpc $1^\circ \rightarrow 100$ pc

- ☞ Although there is clear coherence between the small and large scales, the source does not appear continuous.
- ☞ ROSAT data already indicated a kind of discontinuity between the central source and the large-scale structure.

SS433@X-rays

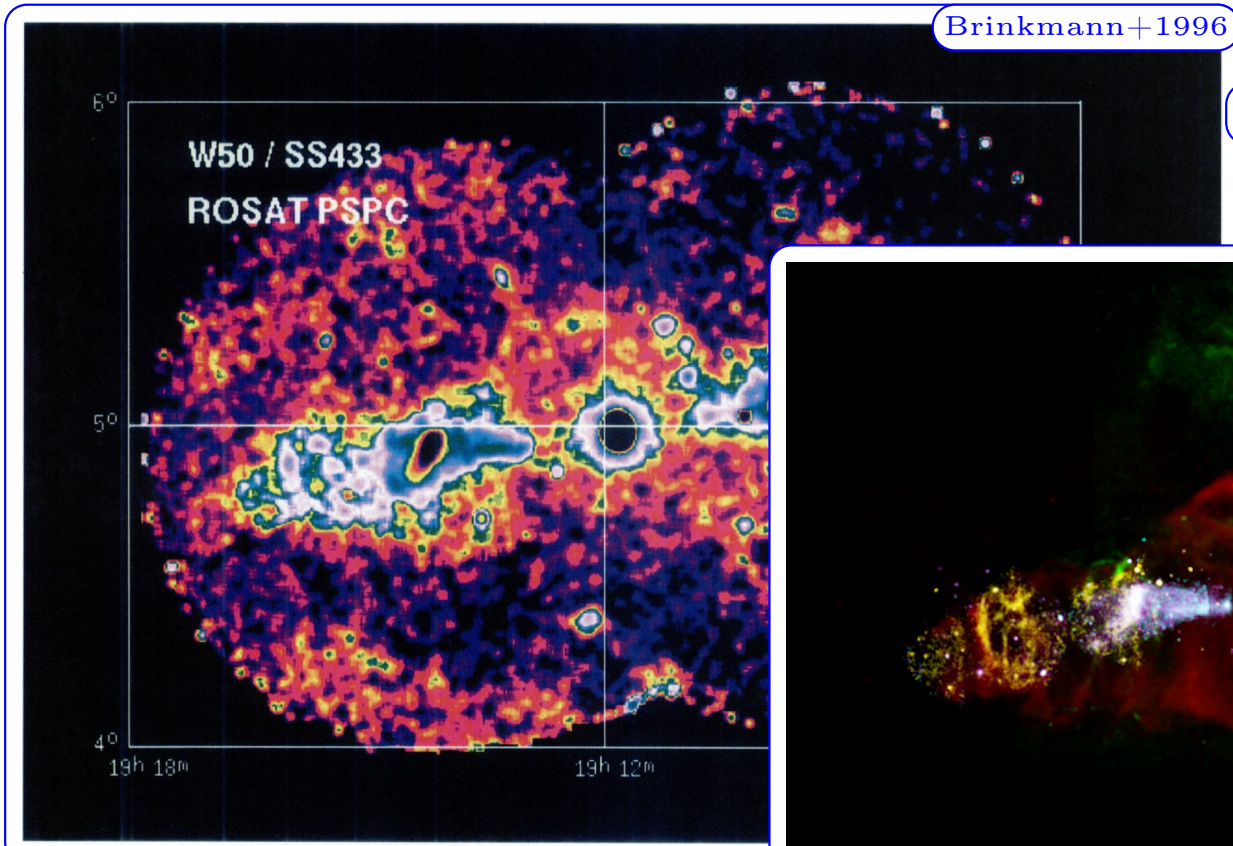

@5.5 kpc $1^\circ \rightarrow 100$ pc

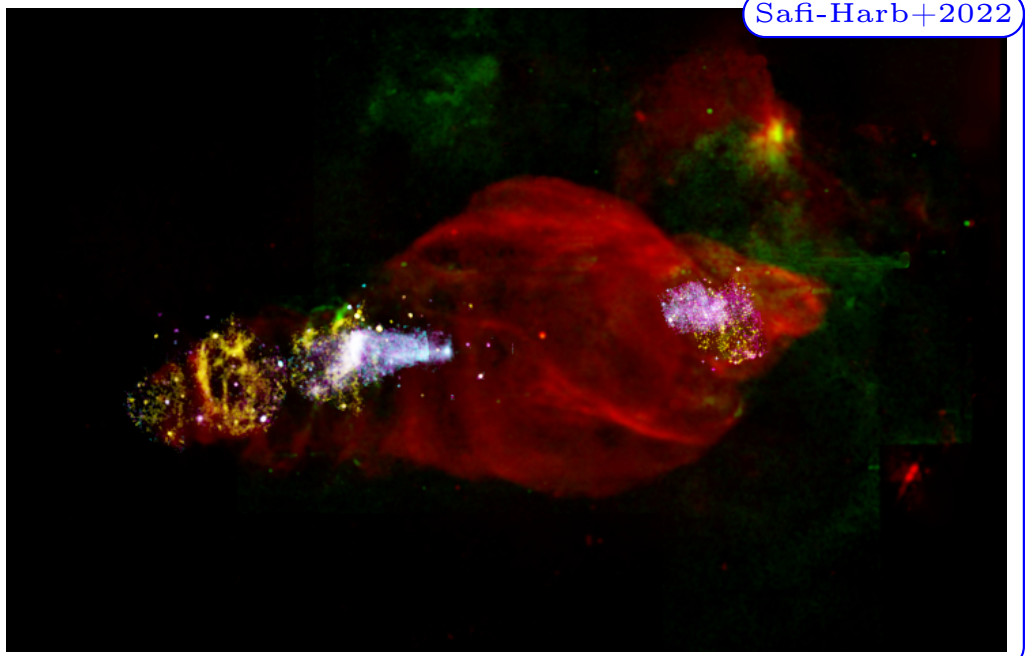

- ☞ Although there is clear coherence between the small and large scales, the source does not appear continuous.
- ☞ ROSAT data already indicated a kind of discontinuity between the central source and the large-scale structure.

SS433@GeV

Li+2020

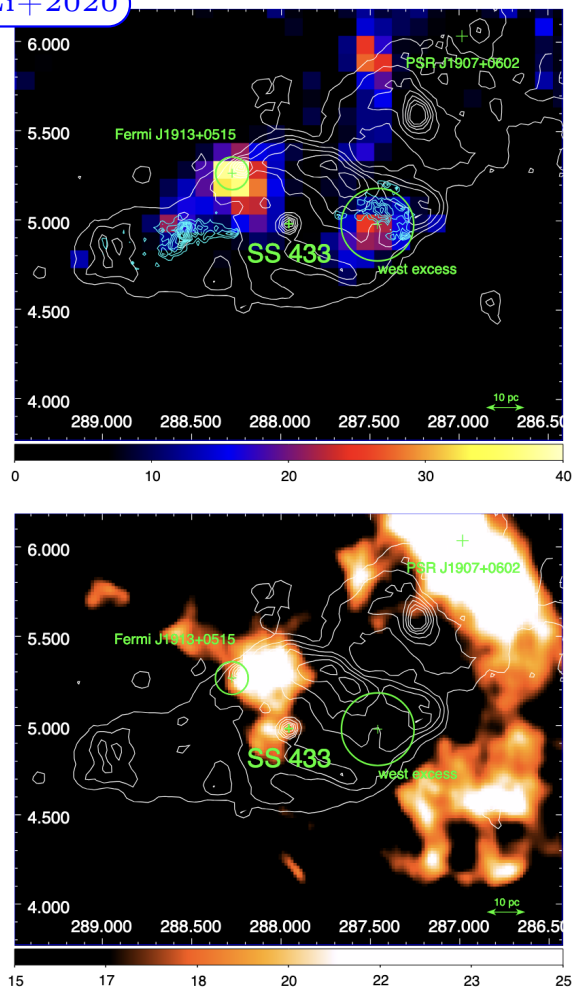

Fang+2020

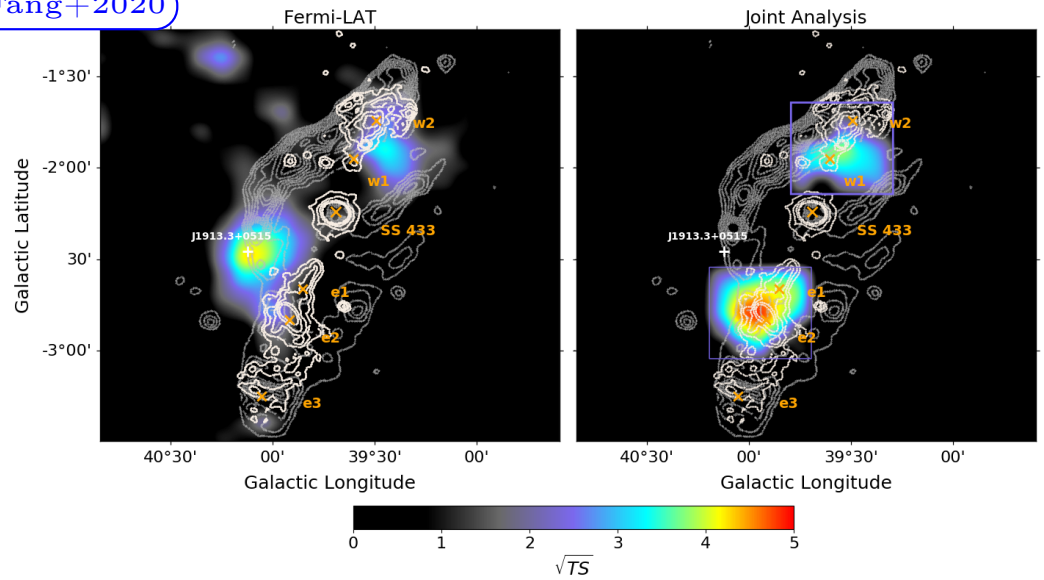

- Detection in the GeV band remains the most controversial at present.
- A consensus still needs to be established regarding the source morphology and potential variability.

SS433@GeV

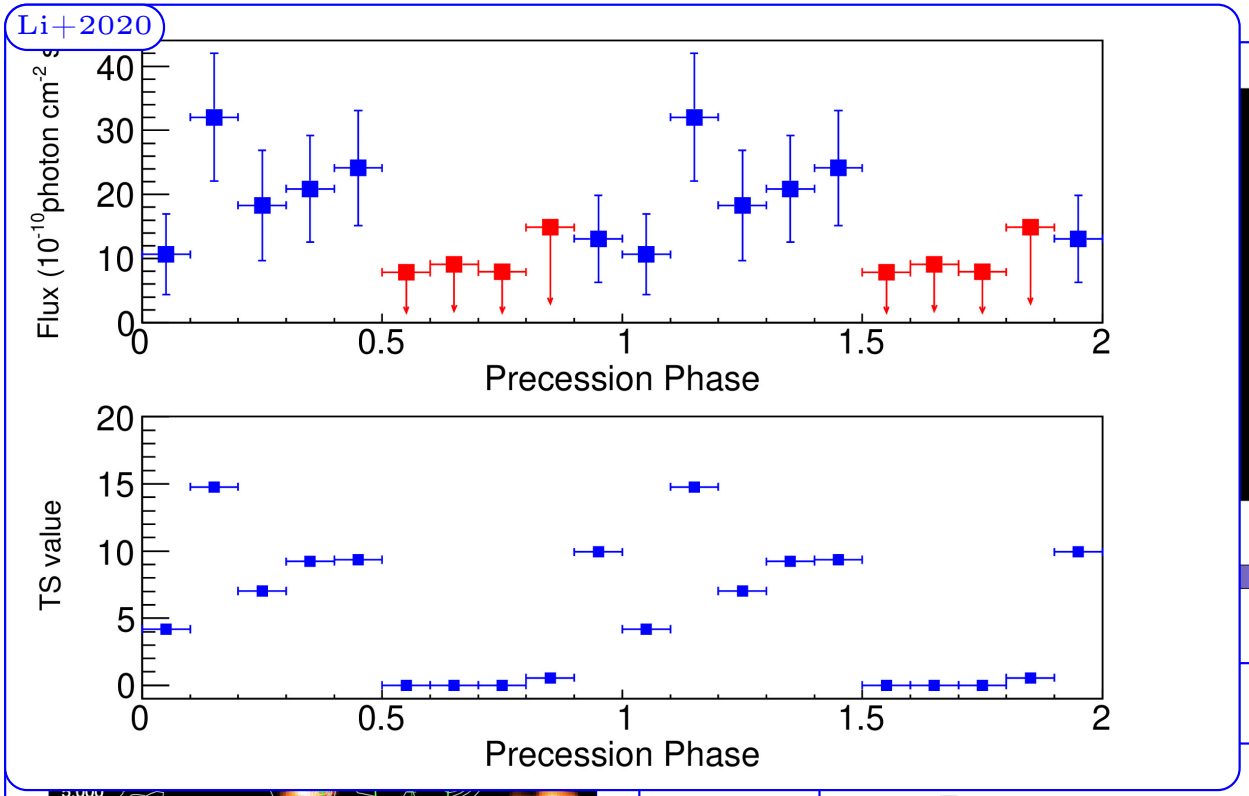

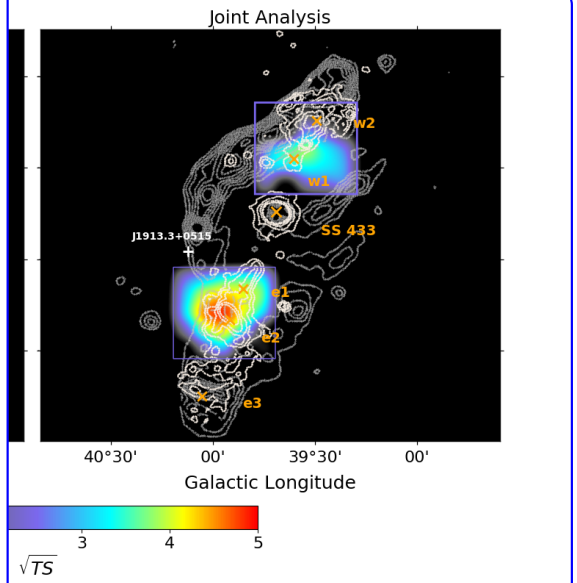

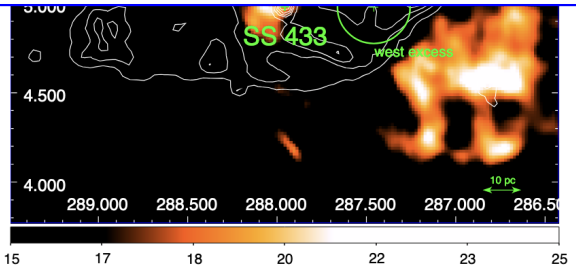

- Detection in the GeV band remains the most controversial at present.
- A consensus still needs to be established regarding the source morphology and potential variability.

HAWC Col 2018

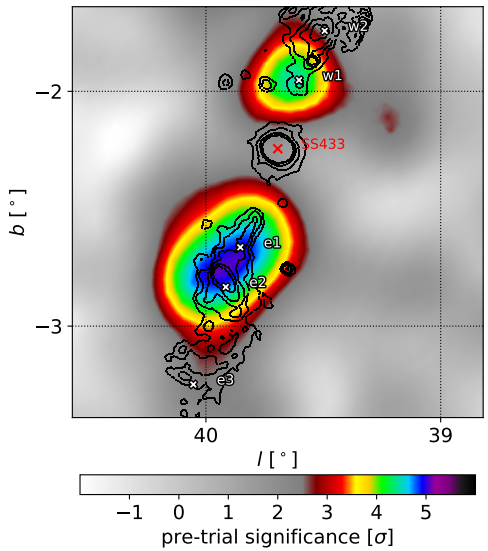

LHAASO Col 2024

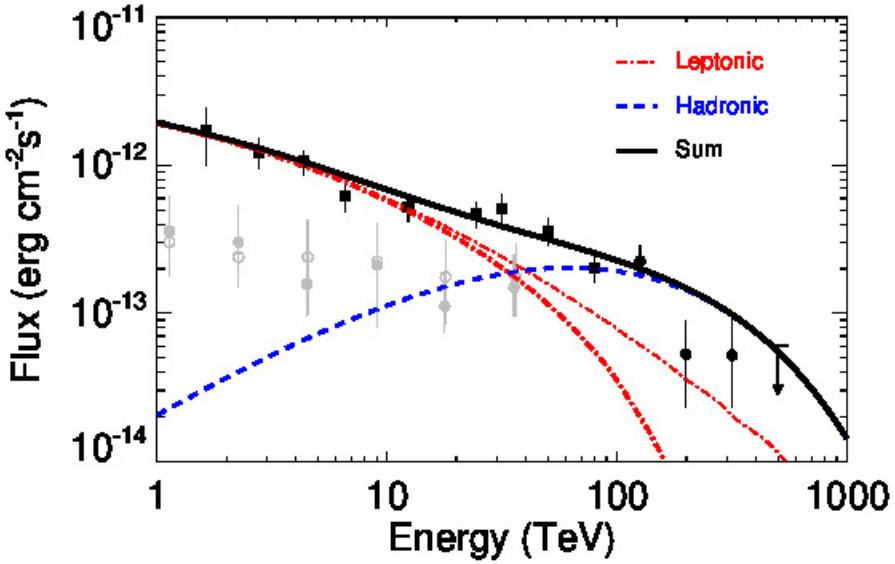

HESS Col 2024

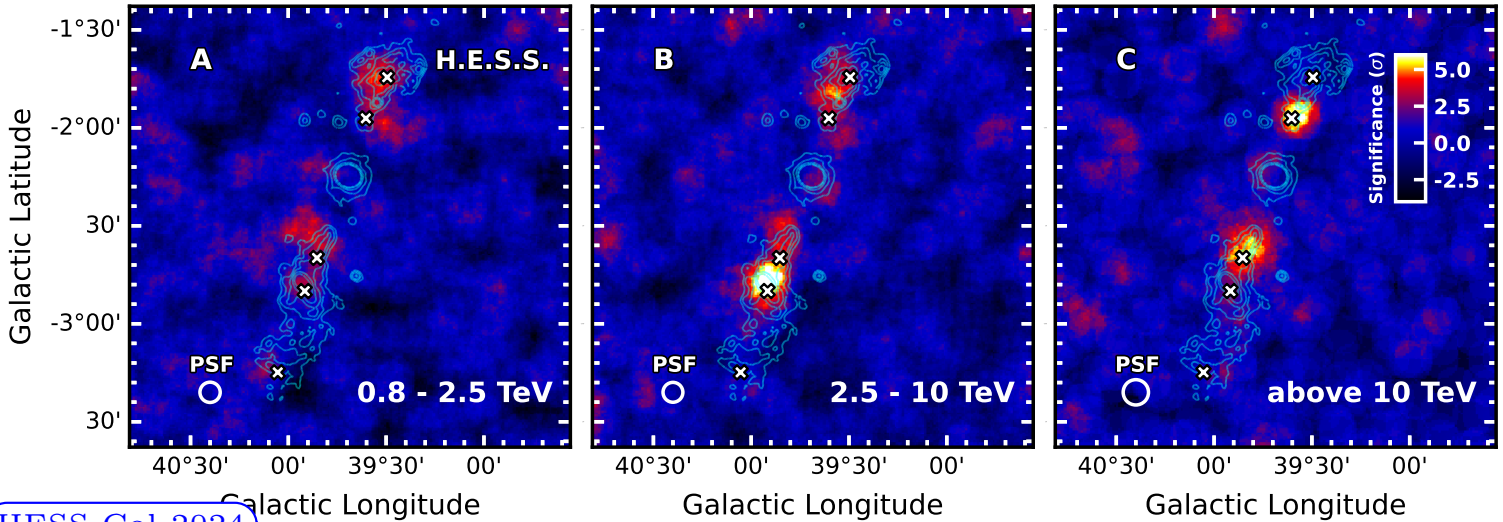

SS433@TeV

HAWC Col 2018

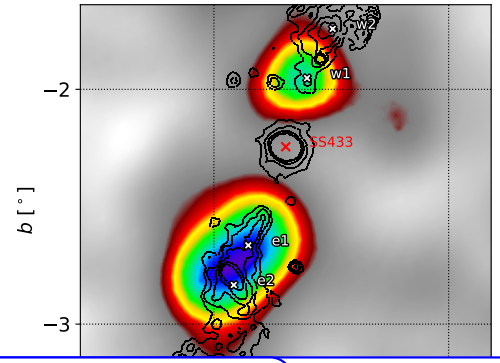

LHAASO Col 2024

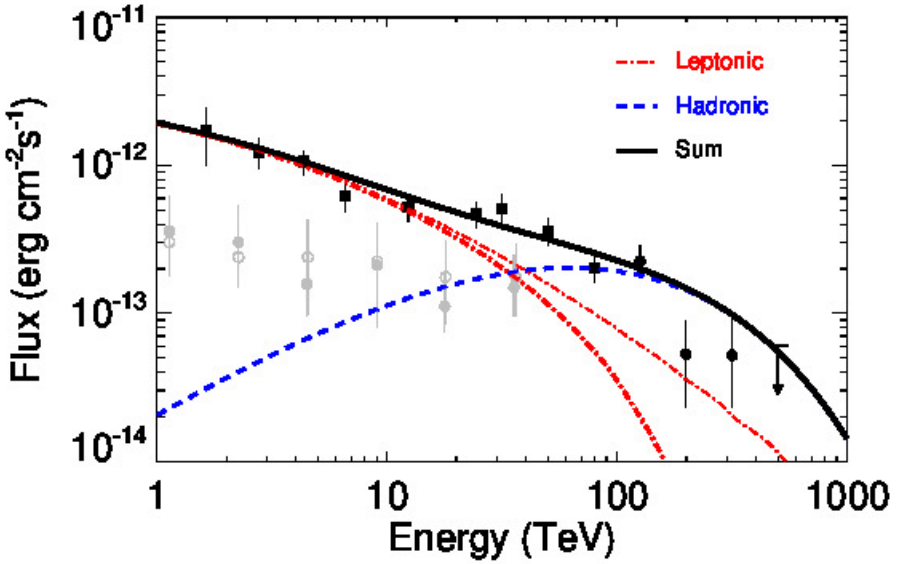

LHAASO Col 2024

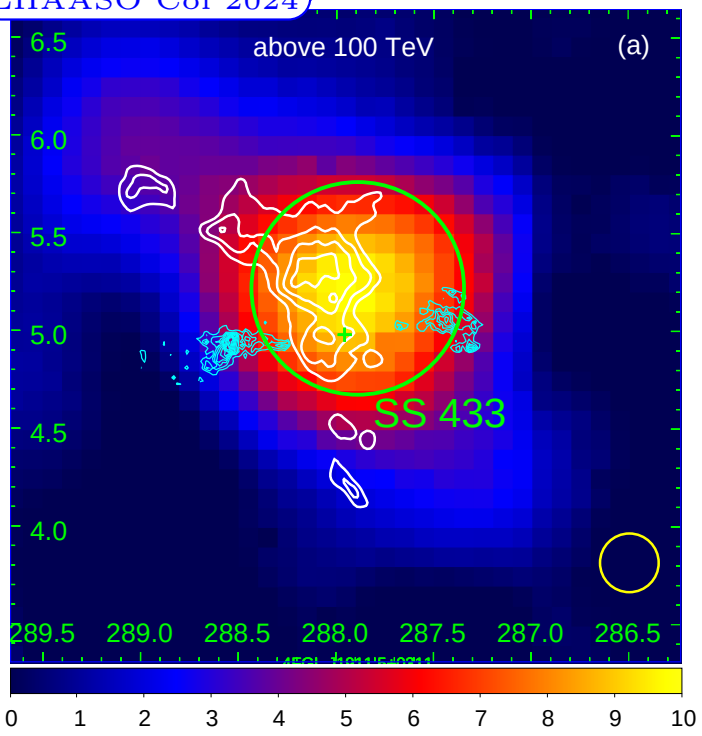

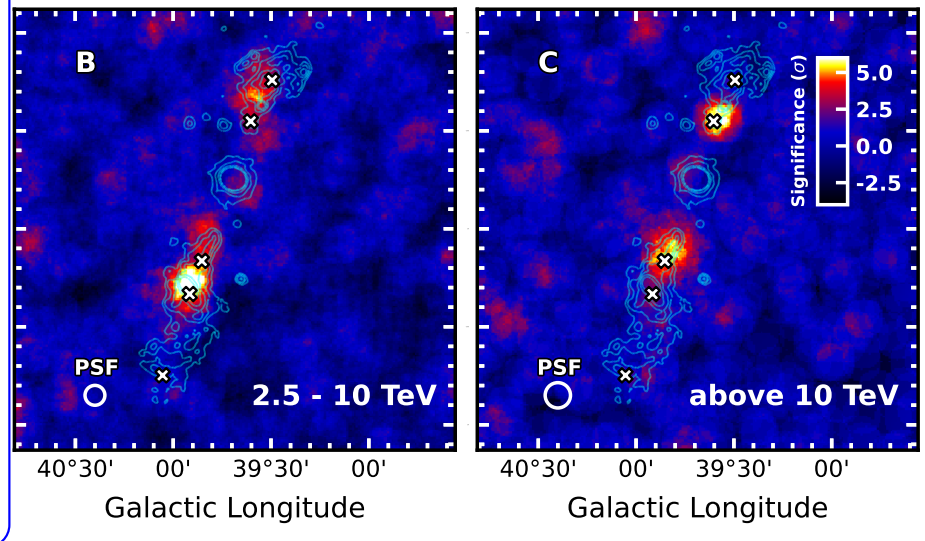

MWL view at SS433

- A jet launched (likely) on the binary scale is a defining feature of the system [radio + X-ray].
- The jet excavates a funnel extending to a distance of ~ 10 pc, where it eventually terminates or passes through a recollimation shock [X-ray + TeV].
- Electrons are accelerated to multi-TeV energies [TeV].
- Synchrotron emission from these multi-TeV electrons appears in the X-ray band, enabling detailed studies of particle transport and cooling (e.g., Tsuji+2025).
- The jet remains a coherent outflow in the downstream region over significant distances [X-ray + TeV(?)], supporting advection–cooling transport modeling (e.g., Sudoh et al. 2020).
- Proton acceleration may accompany lepton acceleration, making SS 433 a promising PeVatron candidate (e.g., Bosch-Ramon 2024).
- Is 300 TeV emission detected with LHAASO generated by UHE protons?

V4641 Sgr

HAWC Collaboration

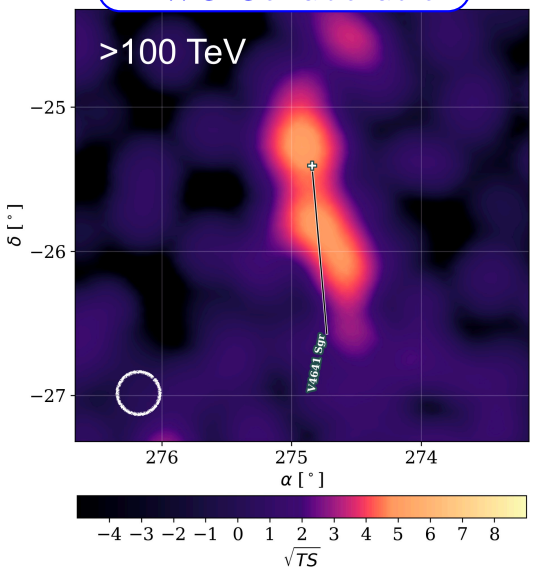

- V4641 Sgr: Microquasar ("Microblazar") showing superluminal motion in the jet with bright radio and X-ray emission
- The system harbors a $\approx 6M_\odot$ BH on a 2.8 day orbit around $\approx 3M_\odot$ B giant star
- Microquasar V4641 Sgr is probably the fastest Galactic jet
- Jet in V4641 Sgr should make just several degrees to the line of sight, thus jet extention is a factor of 10 larger than its projection

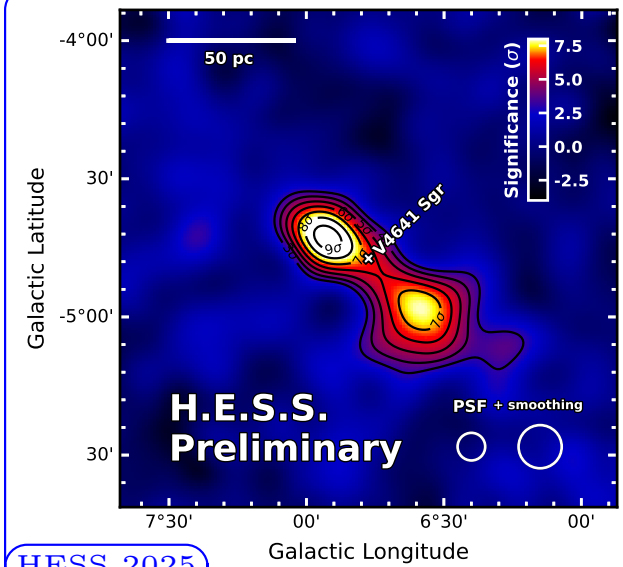

HESS 2025

VLA Shows Rapid Change in Nearest Microquasar

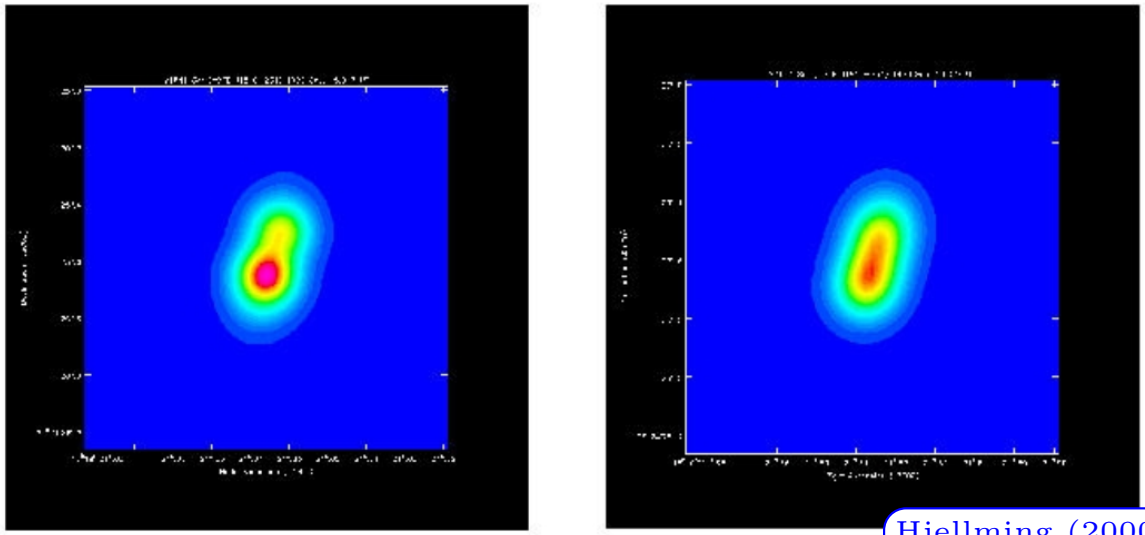

Hjellming (2000)

V4641 Sgr

HAWC Collaboration

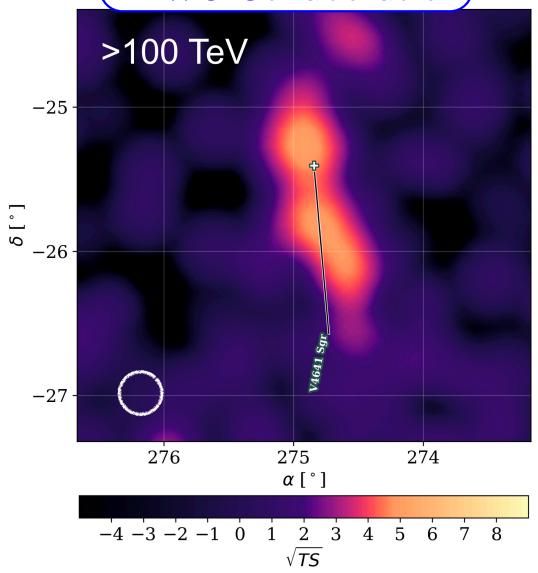

- V4641 Sgr: Microquasar ("Microblazar") showing superluminal motion in the jet with bright radio and X-ray emission
- The system harbors a $\approx 6M_\odot$ BH on a 2.8 day orbit around $\approx 3M_\odot$ B giant star
- ~~Microquasar V4641 Sgr is probably the fastest Galactic jet~~
- ~~Jet in V4641 Sgr should make just several degrees to the line of sight, thus jet extention is a factor of 10 larger than its projection~~
- Microquasar V4641 is the first source in which the radio morphology was corrected based on VHE data

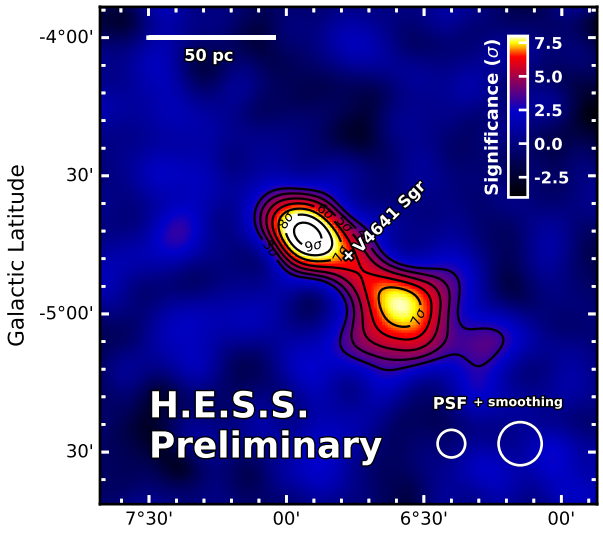

HESS 2025

Marti&Luque-Escamilla2026

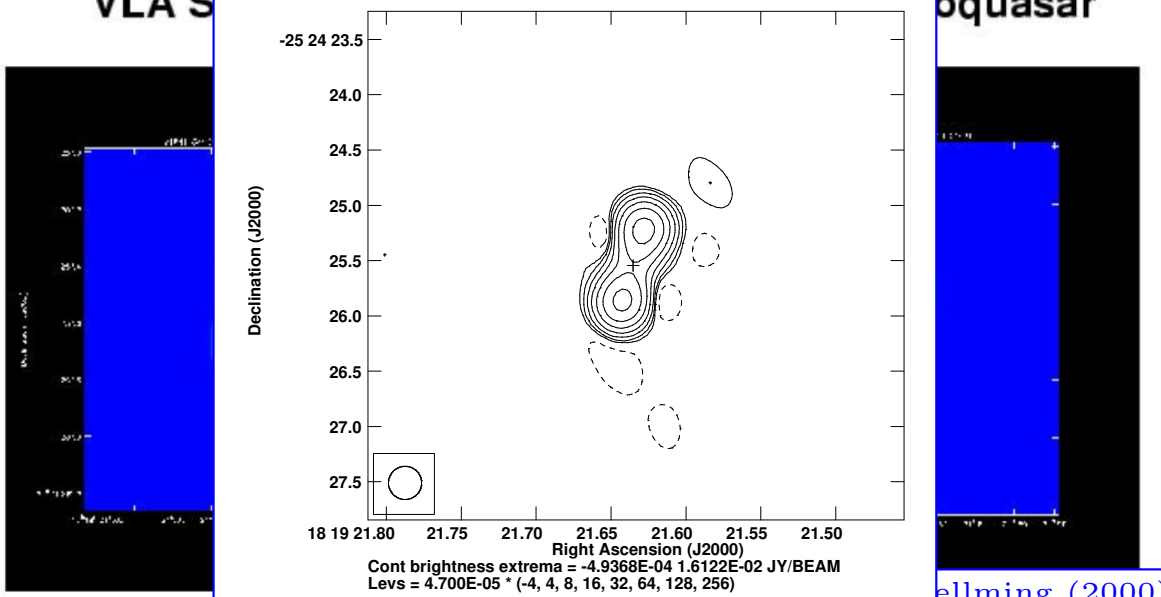

ellming (2000)

V4641 Sgr

HAWC Collaboration

HAWC Collaboration 2025

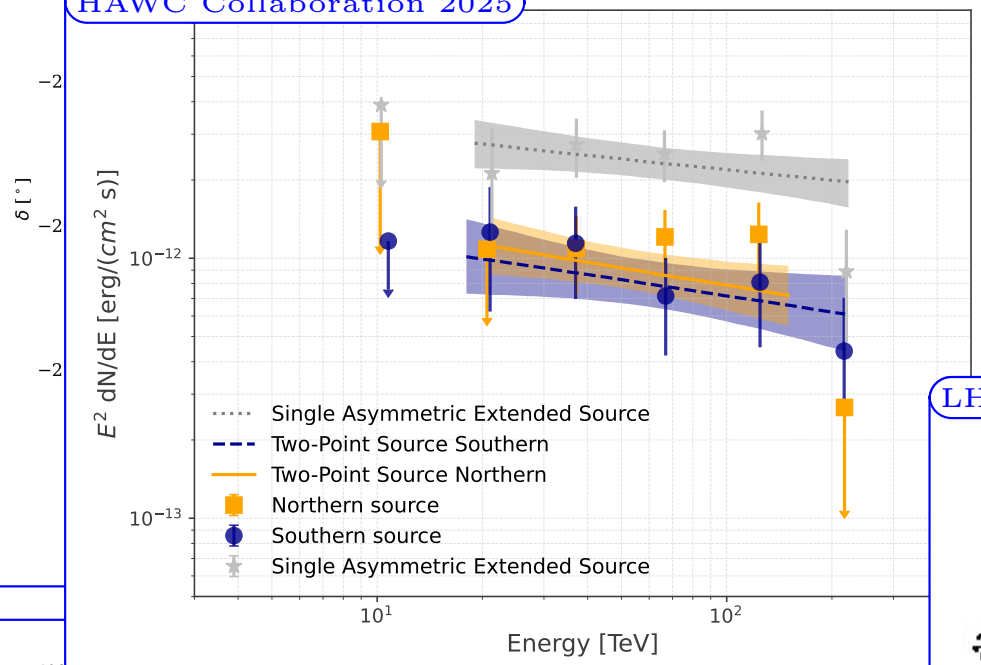

Microquasar ("Microblazar") showing superluminal
he jet with bright radio and X-ray emission

harbors a $\approx 6M_\odot$ BH on a 2.8 day orbit around
iant star

~~r V4641 Sgr is probably the fastest Galactic jet~~

~~1 Sgr should make just several degrees to the line~~
~~us jet extention is a factor of 10 larger than its~~

r-

LHAASO Collaboration 2024

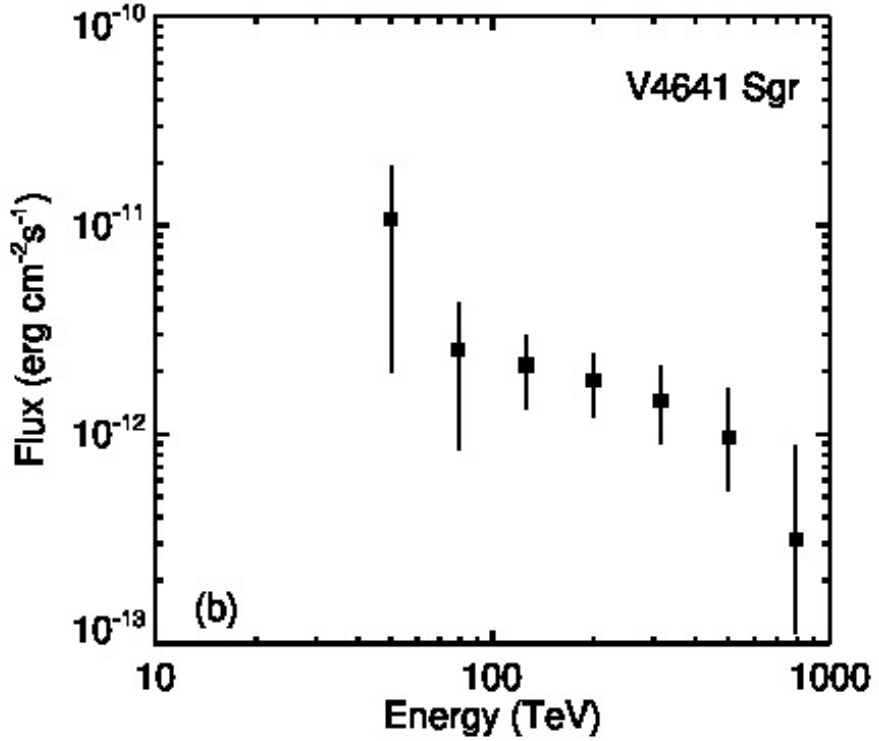

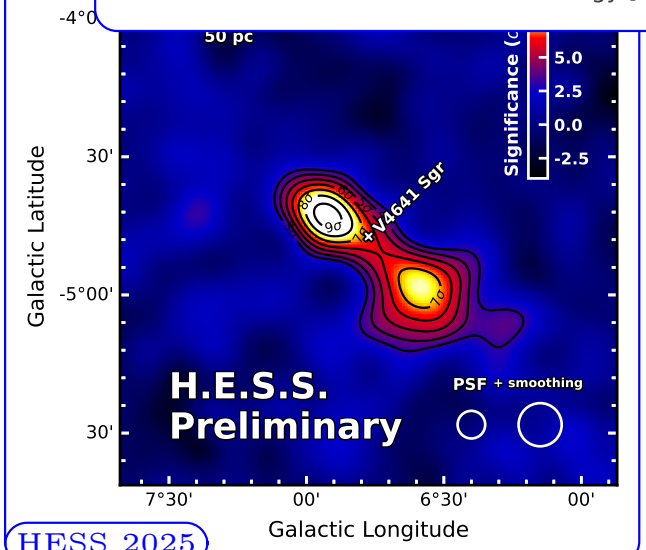

HESS 2025

MWL view at V4641 Sgr

- Compared to SS 433, our current multi-wavelength understanding of V4641 Sgr is still limited. Nevertheless, the detection at VHE/UHE energies has triggered follow-up observations, including X-rays with XRISM (Suzuki et al. 2025) and reanalysis of the archival radio data (Marti&Luque-Escamilla2026)
- The TeV source size, as revealed by HAWC and H.E.S.S., appears to be very large, but the structure aligns with the revised radio jets.
- TeV spectrum is hard and extends up to 800 TeV making V4641 Sgr one of the strongest PeVatron candidates.
- The detection of extremely powerful flares with luminosities $L > 10^{39}\,\mathrm{erg\,s^{-1}}$ (e.g., Revnivtsev et al. 2002) suggests that the source might be a super-PeVatron.

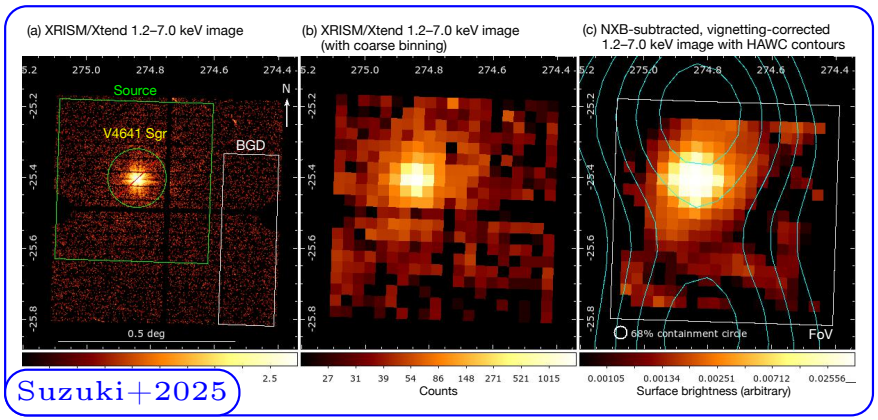

Suzuki+2025

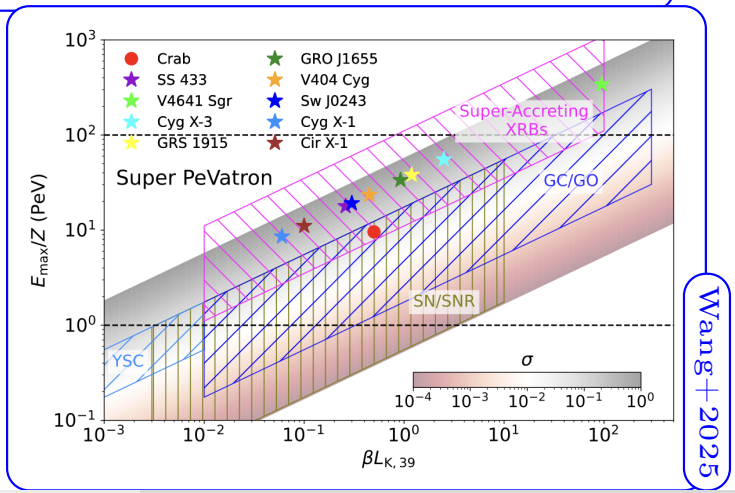

Wang+2025

GRS1915-105

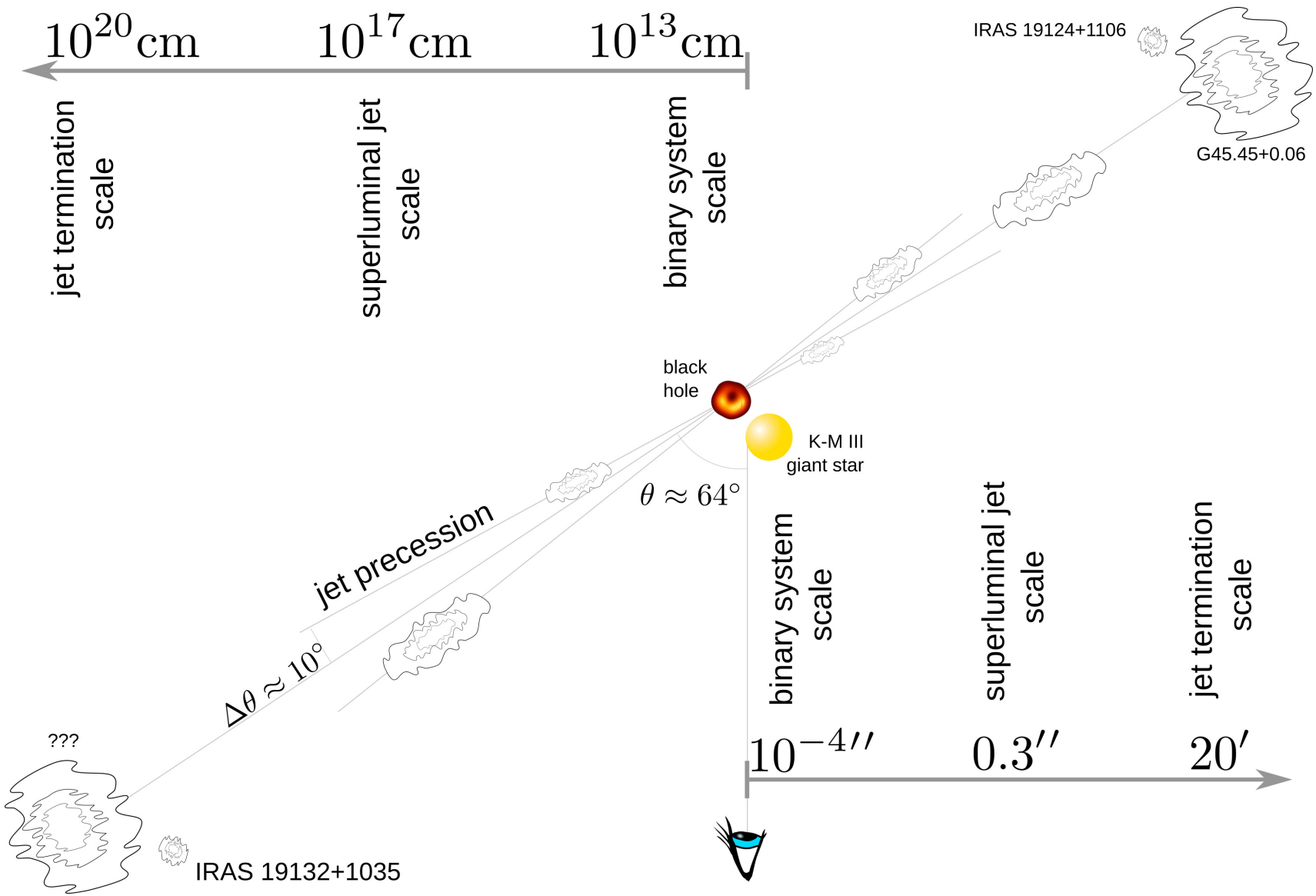
10^{20}cm
10^{17}cm
10^{13}cm
jet termination scale
superluminal jet scale
binary system scale
IRAS 19124+1106
G45.45+0.06
black hole
K-M III giant star
$\theta \approx 64°$
jet precession
$\Delta\theta \approx 10°$
???
IRAS 19132+1035
binary system scale
superluminal jet scale
jet termination scale
$10^{-4}''$
$0.3''$
$20'$

Super Luminal Motion in μQ Jets

Mirabel&Rodriquez

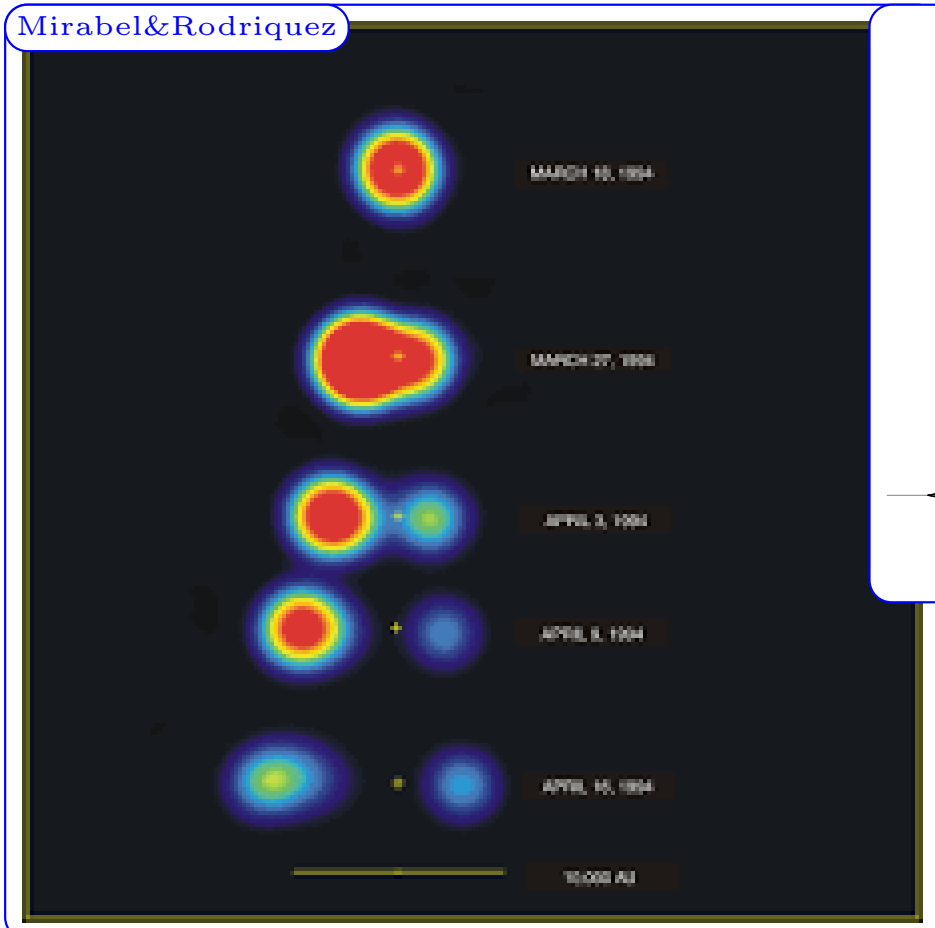

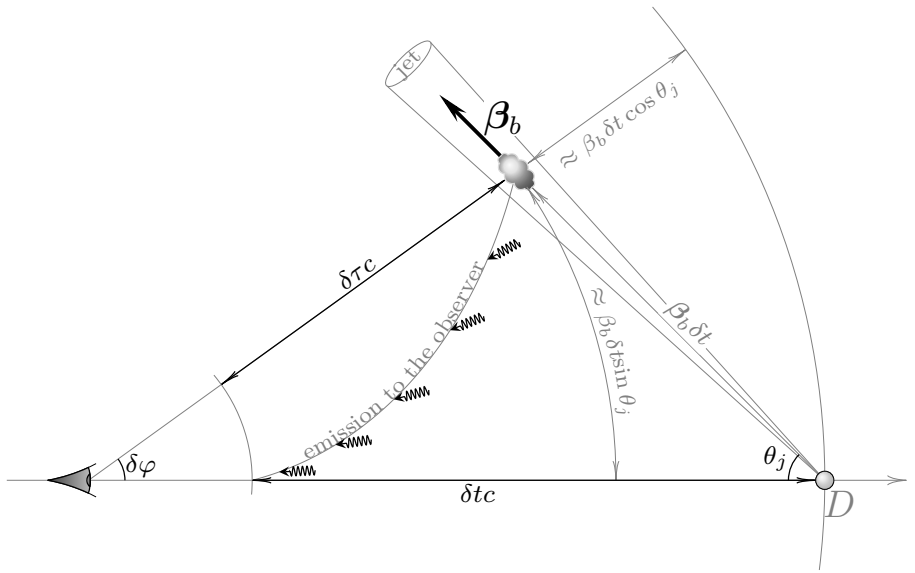

GRS1915-105 is one of the sources where one established superluminal motion in the jet. While the luminosity of the radio blobs is small, the cooling time of electrons is very long, thus the energy contained in the electrons might be very significant.

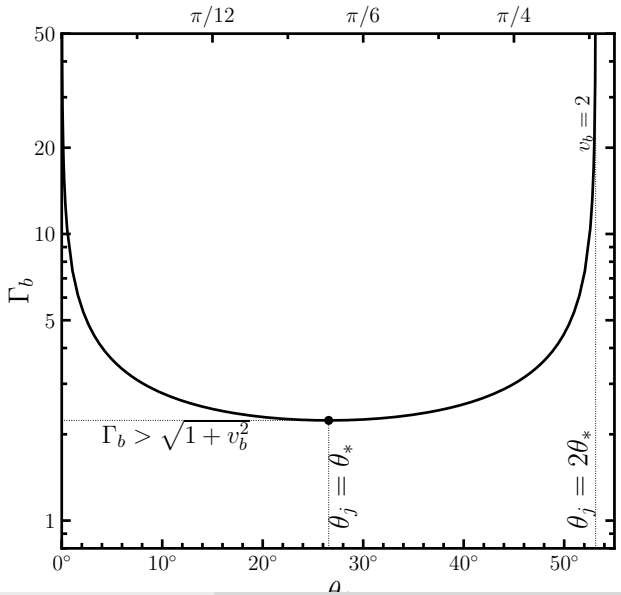

Power of Jets in GRS1915-105

- If IRAS 19132+1035 is the jet termination cavity and it can serve as the jet power calorimeter than $L_j \sim 10^{33}\,\mathrm{erg\,s^{-1}}$ (Tetarenko+2018)
- The radio blobs require $L_j > 10^{38}\,\mathrm{erg\,s^{-1}}$ is electron positron (Atoyan&Aharonian 1999)
- The radio blobs require $L_j > 10^{40}\,\mathrm{erg\,s^{-1}}$ is electron proton (Atoyan&Aharonian 1999)

Power of Jets in GRS1915-105

- If IRAS 19132+1035 is the jet termination cavity and serve as the jet power ca ter than $L_j \sim 10^{33}$ (Tetarenko+2018)
- The radio blobs require $10^{38}\,\mathrm{erg\,s^{-1}}$ is electron p (Atoyan&Aharonian 1999)
- The radio blobs require $10^{40}\,\mathrm{erg\,s^{-1}}$ is electron (Atoyan&Aharonian 1999)

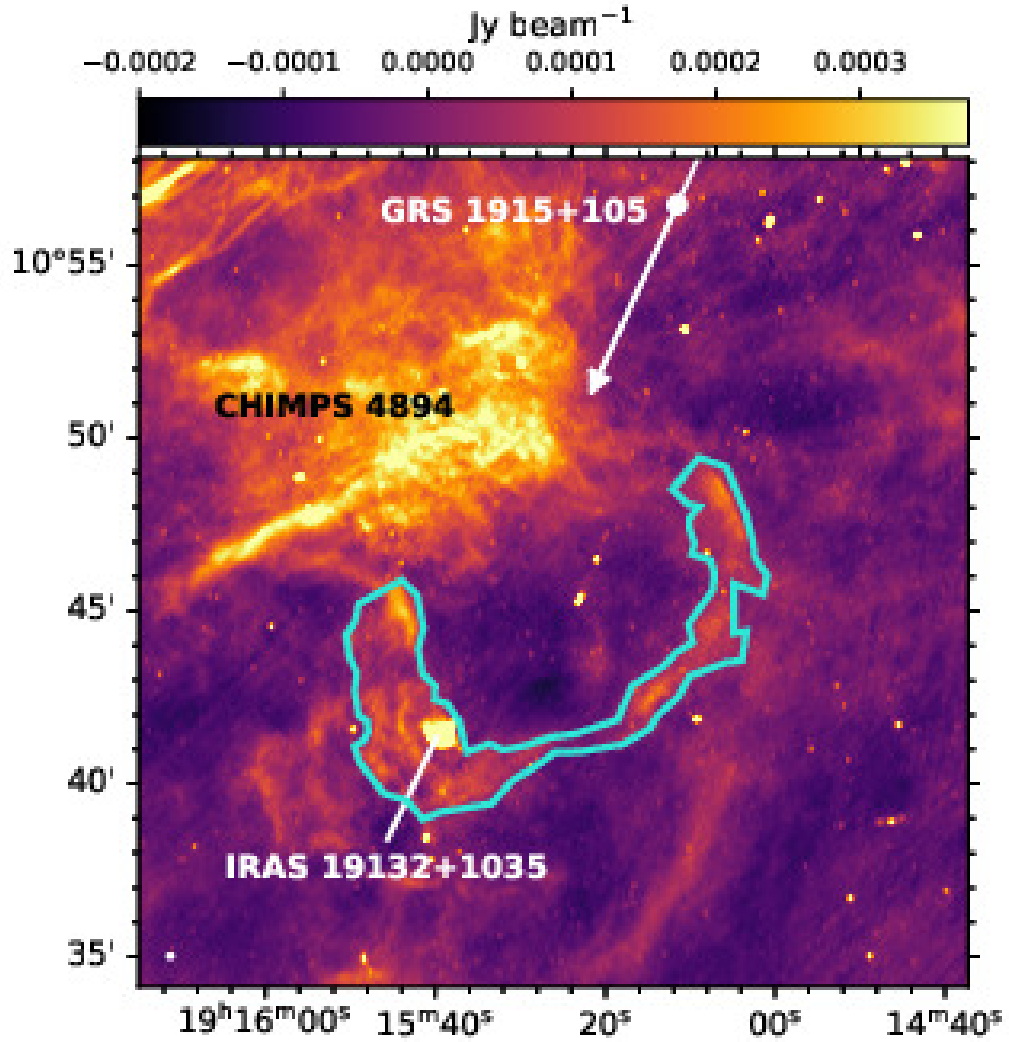

Motta+2025

Power of Jets in GRS1915-105

☞ If IRAS 19132+1035 is the jet

Source-related parameters		
Distance[m]	9.4 ± 0.7 kpc	
Jet inclination angle[m] i	60 ± 5 deg	
Jet opening angle[m] θ	1–10 deg	
Thermal Bremsstrahlung region (IRAS 19132+1035) – the IRAS region		
Diameter[m]	36 arcsec	1.6 pc
Volume[i]	6.6×10^{55} cm^3	
Integrated flux density[m]	60 ± 6 mJy	
Electron temperature[a]	10^4–3×10^6 K	
Shock-compressed gas electron density[i]	395–630 particles/cm^3	
ISM gas density[i]	100–160 particles/cm^3	
Shock front velocity	21–363 Km s^{-1}	
Region gas pressure[i] (ideal gas)	2.5×10^{-10}–7.7×10^{-8} [erg/cm^3]	
Non-thermal emission region (cylindrical hot spot) – the northern feature		
Flux density[m]	5.2 ± 0.5 mJy	
Luminosity	$2 \times 10^{+29}$ erg s^{-1}	
Radius[m]	3.9 arcsec	0.18 pc
Length[m]	17.4 arcsec	0.9 pc
Volume[i]	2.6×10^{54} cm^3	
Cylinder pressure[i] (minimum energy)	$>1.5 \times 10^{-11}$ erg/cm^3	
Cylinder magnetic density $B^i_{\rm min}$ (minimum energy)	$>2.18 \times 10^{-5}$ Gauss	
The lobe and the bow shock structure		
Bow shock structure flux density[m]	0.15 ± 0.01 mJy	
Bow shock distance from binary[m] (cavity major axis)	17 arcmin	46 pc
Lobe minor axis[m]	10 arcmin	27 pc
Bow shock structure thickness[m]	60 arcsec	2.7 pc
Lobe volume[i]	6×10^{59} cm^3	
Lobe pressure[i] (equi-partition)	$>1.3 \times 10^{-12}$ erg/cm^3	
Lobe magnetic field[i] (synchrotron emission)	$>6.4 \times 10^{-6}$ Gauss	
Jet energetics		
Jet age[i]	0.09–0.22 Myr	
Jet pressure[i] (self-similar model)	$2.8 \times 10^{-11} - 7.8 \times 10^{-10}$ [erg/cm^3]	
One-sided power transferred (self-similar)[i]	3.3×10^{37}–1.5×10^{39} erg s^{-1}	
One-sided power transferred (Enthalpy)[i]	$>1.2 \times 10^{37}$ erg s^{-1}	
One-sided power transferred (Hot spot)[i]	$>1.7 \times 10^{36}$ erg s^{-1}	
Pseudo-constant C^i_1	3.3–9	

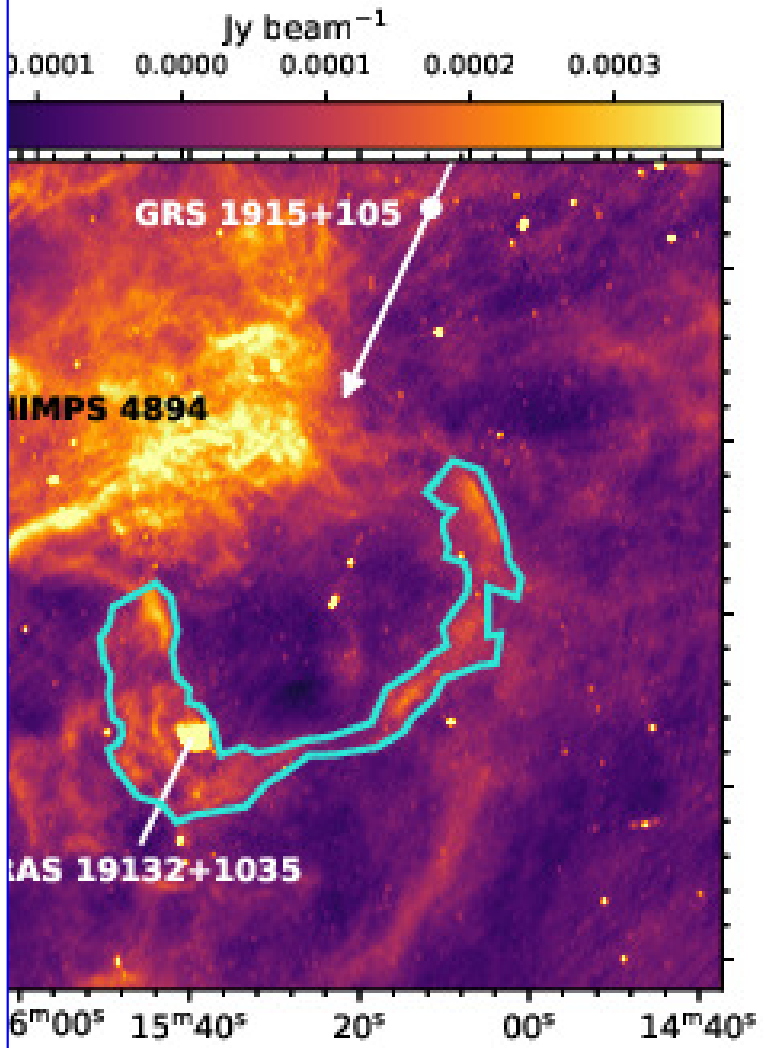

Motta+2025

LHAASO detection of GRS1915-105

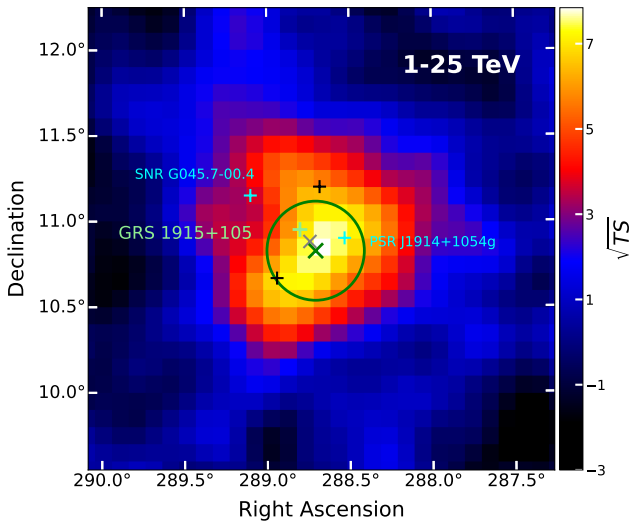

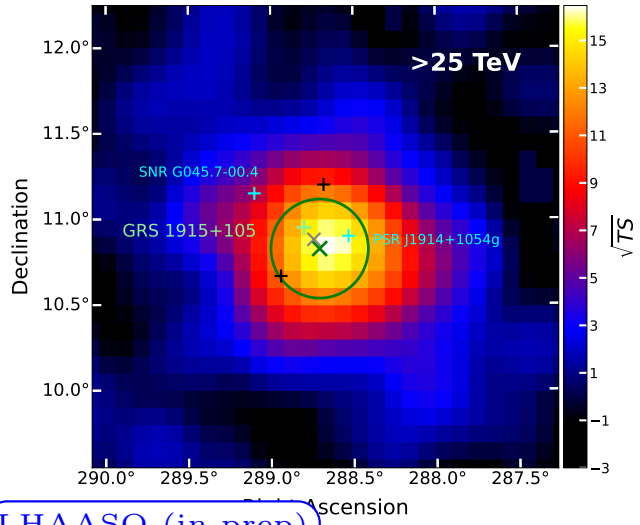

LHAASO (in prep)

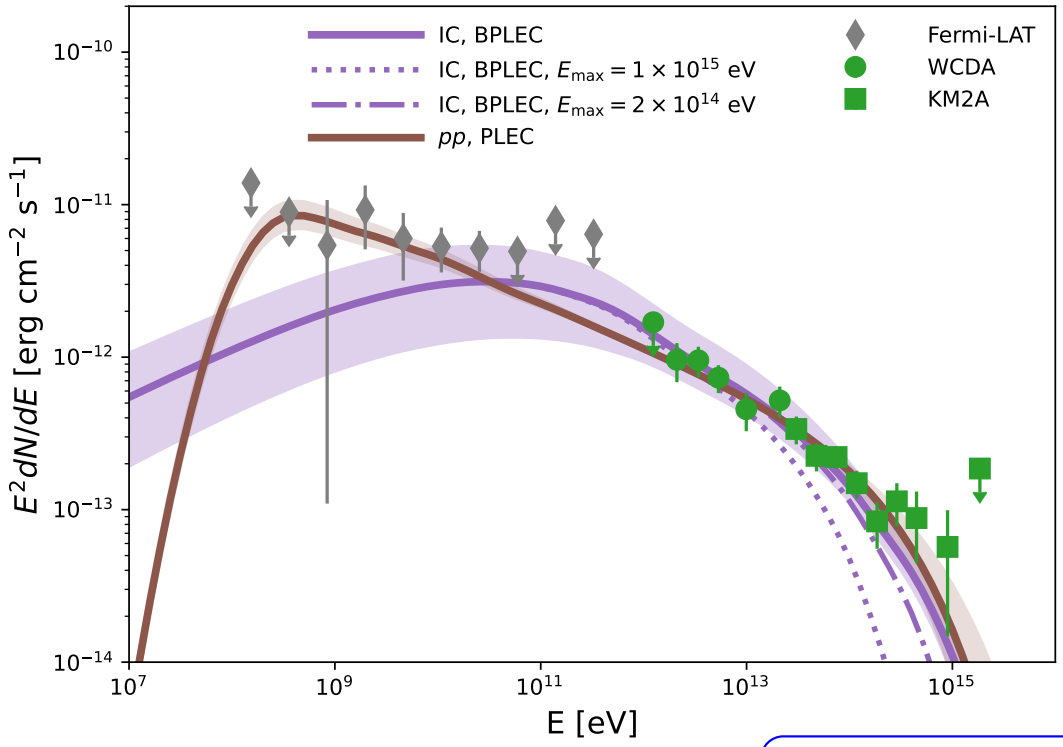

LHAASO (in prep)

- IC emission requires 3×10^{50} erg
- pp emission requires $6 \times 10^{51} \left(\frac{\mathrm{n}}{1\,\mathrm{cm}^{-3}}\right)^{-1}$ erg
- 50pc size require a fast/slow diffusion for IC/pp scenarios

MWL view of GRS1915-105

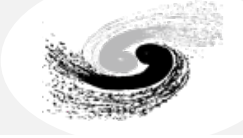

- A mildly jet or blobs launched on the binary scale is a defining feature of the system [radio].
- The jet excavates a caveat extending to a distance of ~ 50 pc, where we can see a bow shock structure [radio + IR].
- Electrons or protons are accelerated to PeV energies [TeV].
- Absence of diffuse X-ray emission implies a weak magnetic field or hadronic scenario.
- The dense environment favors the hadronic scenario [radio].
- The size implies a noticeable leakage of PeV protons from the system.

Cyg X-3: Flaring PeVatron

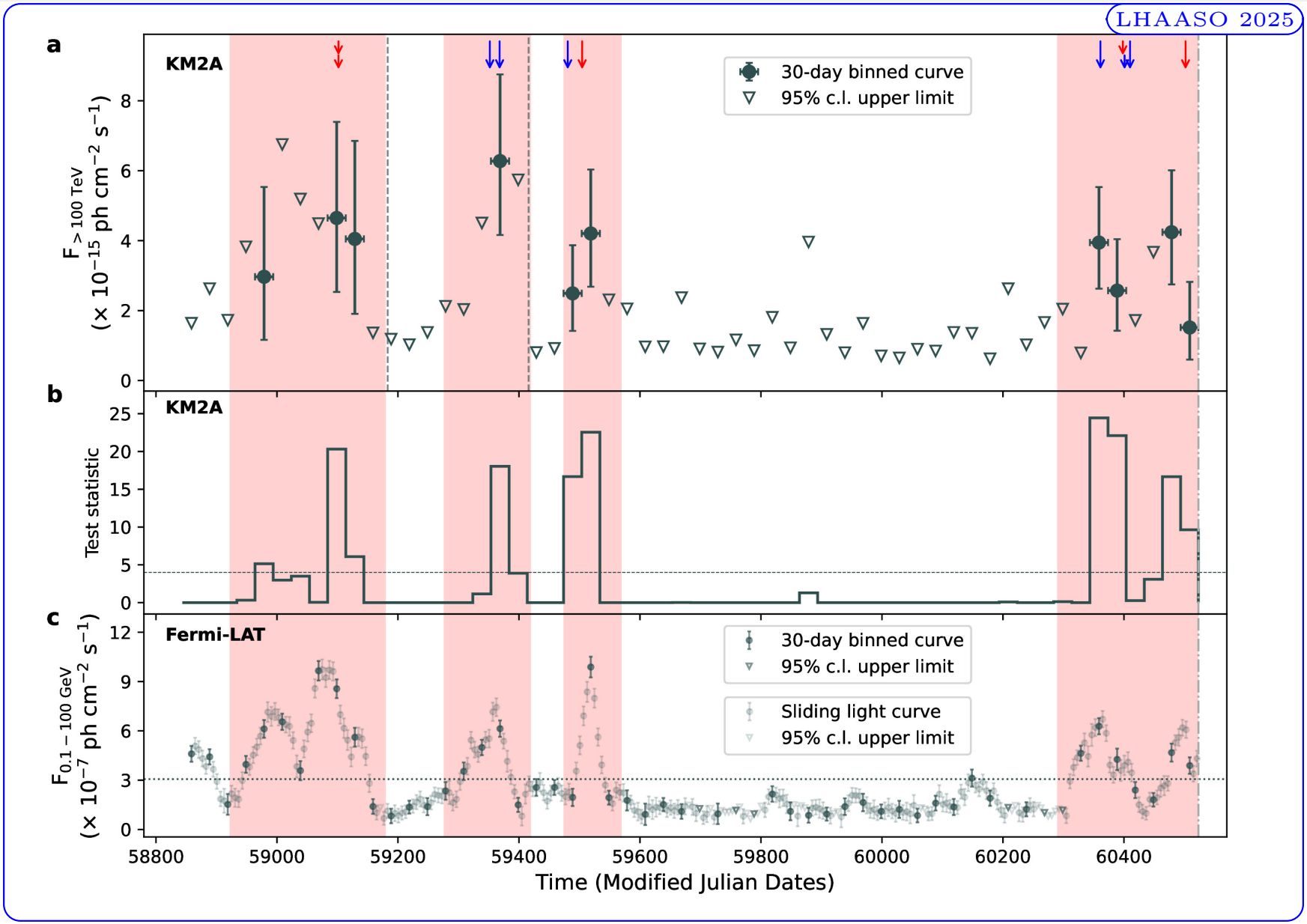

Cyg X-3: Flaring PeVatron

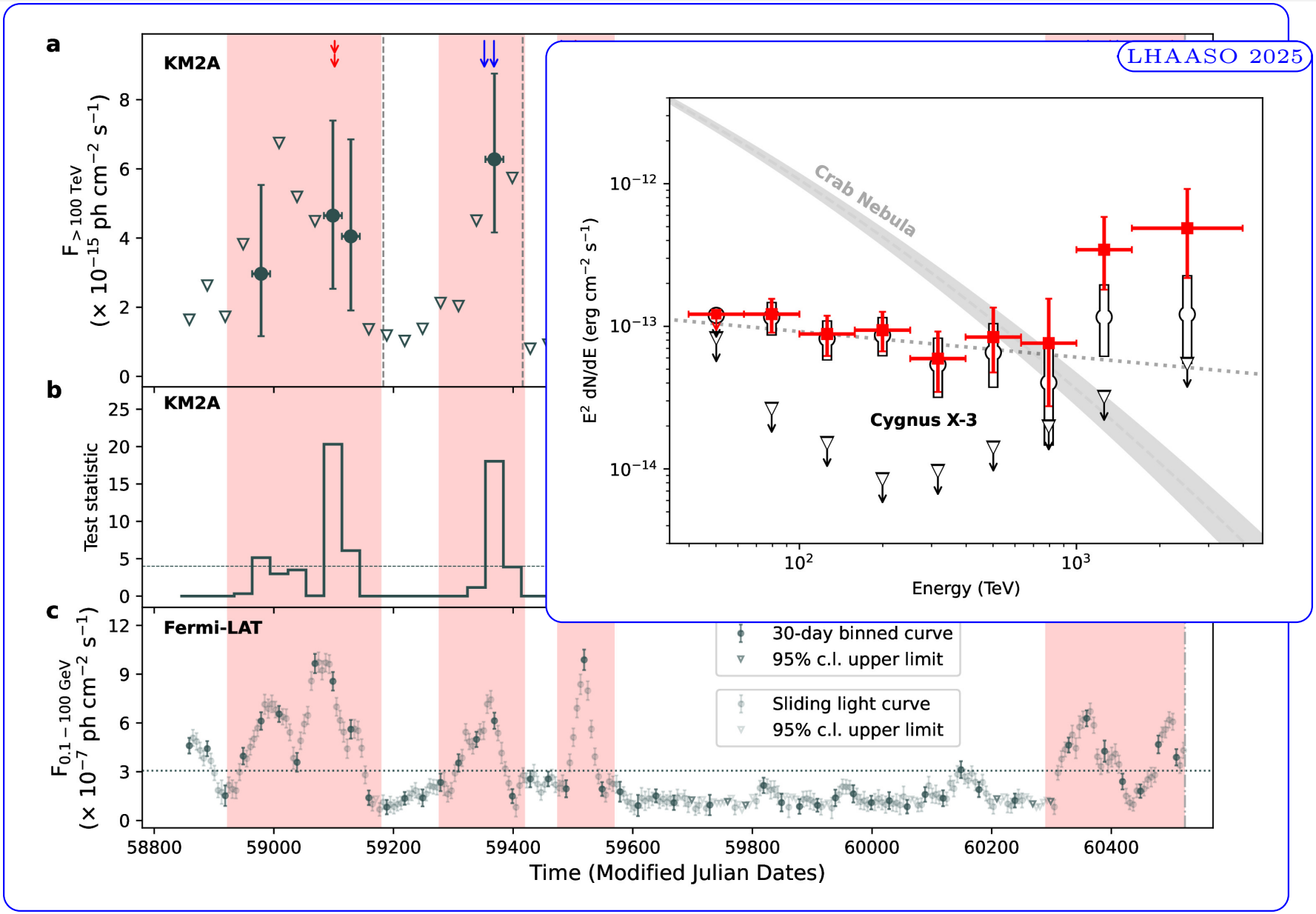

Cyg X-3: Electrons and Protons

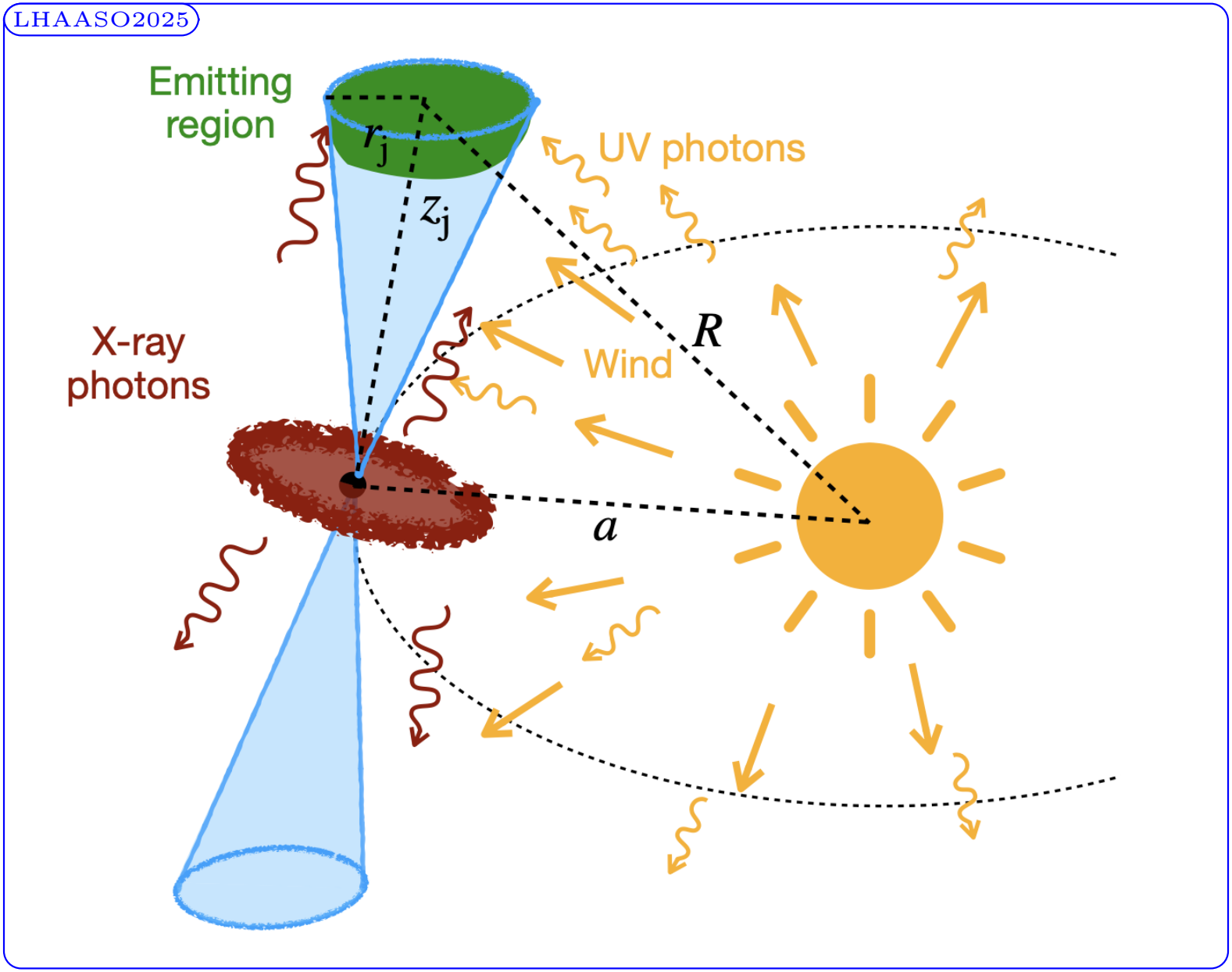

Cyg X-3: Electrons and Protons

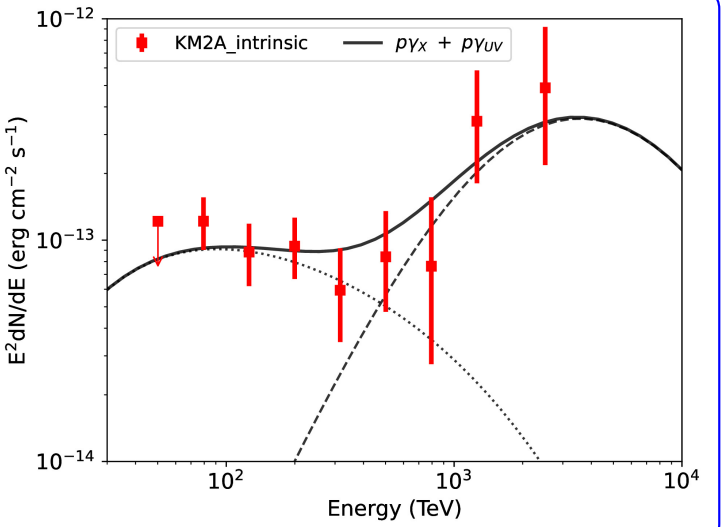

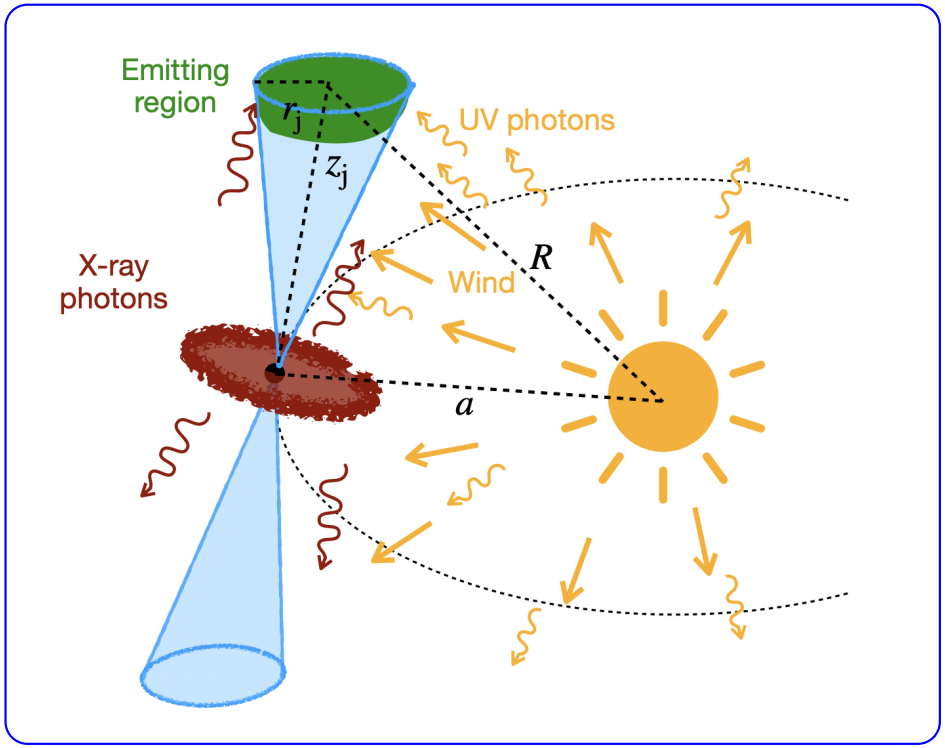

The emission depends on

- Injection spectrum
  - slope
  - maximum energy
  - power
- Geometry of the system
  - location of the emitter
  - bulk Lorentz factor
  - jet orientation

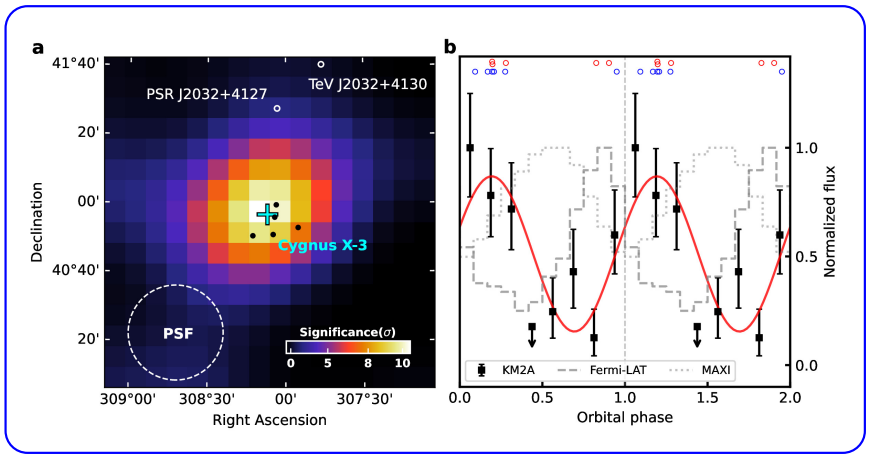

Cyg X-3: Electrons and Protons

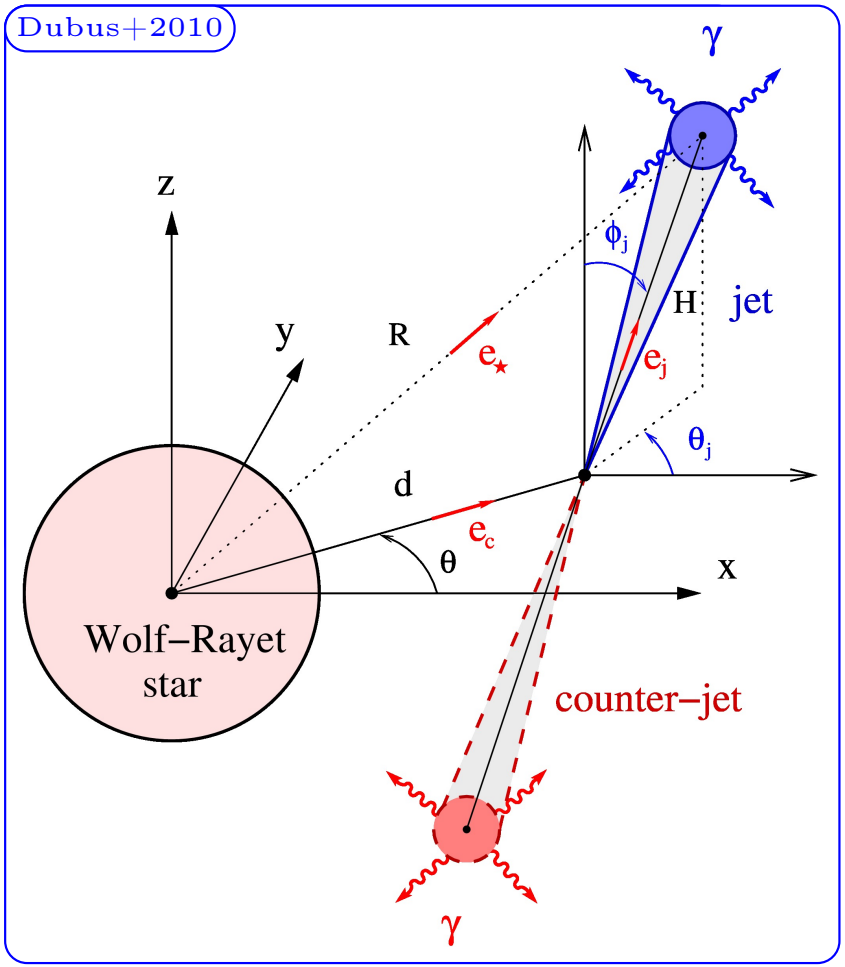

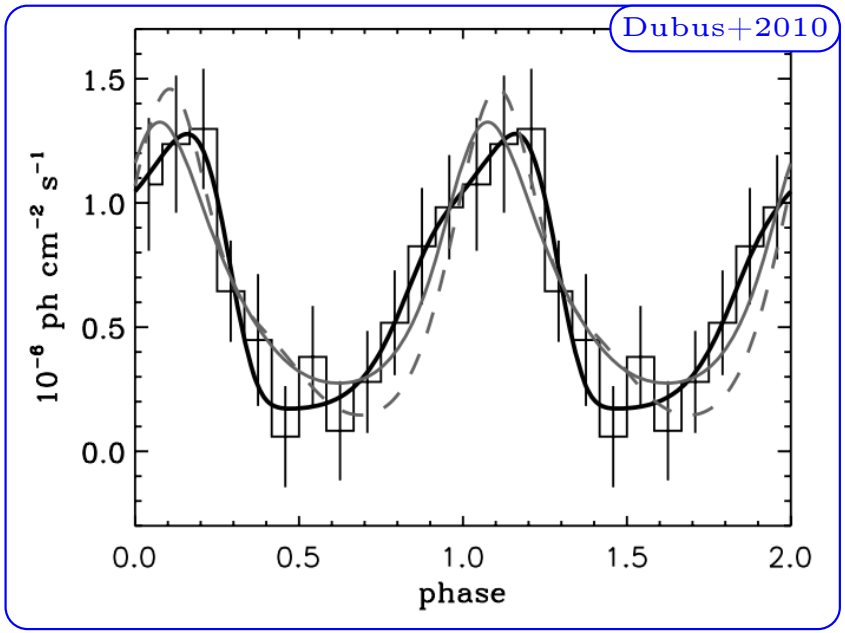

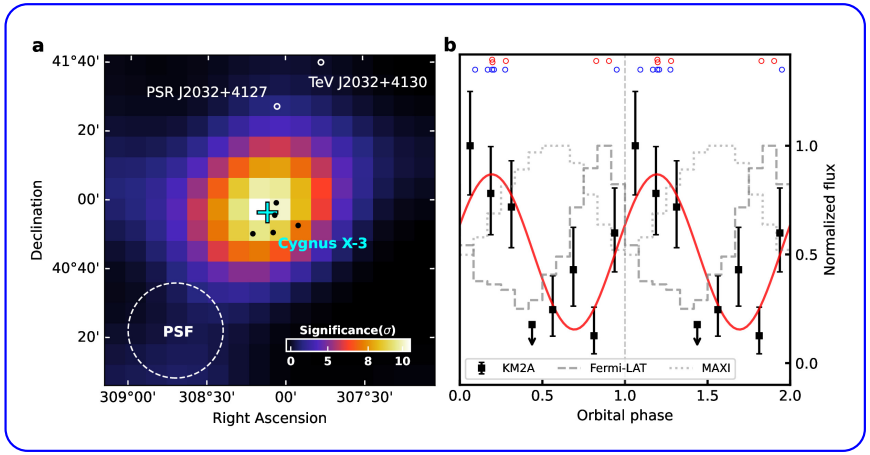

Gamma-rays from Cyg X-3

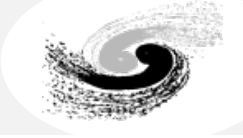

- Relativistic electrons are accelerated in a mildly jet within the binary system [GeV].
- IC emission of these electrons explains the GeV emission (a similar scenario likely takes place in Cyg X-1, Zanin+2016)
- Multi-PeV protons are accelerated within the binary system [UHE].
- The photo-meson process seems to be the most natural scenario (provided that protons reach ~ 10 PeV energy)
- It is not clear if the same process is responsible for the acceleration of protons and electrons (protons are not sensitive to the B-field strength, so hypothetically the proton accelerator can be anywhere within the system)
- Even in a such extreme system as Cyg X-3, protons may not meet enough target to cool in the system (Galactic Super PeVatron?)

Other microquasars (detected with LHAASO)

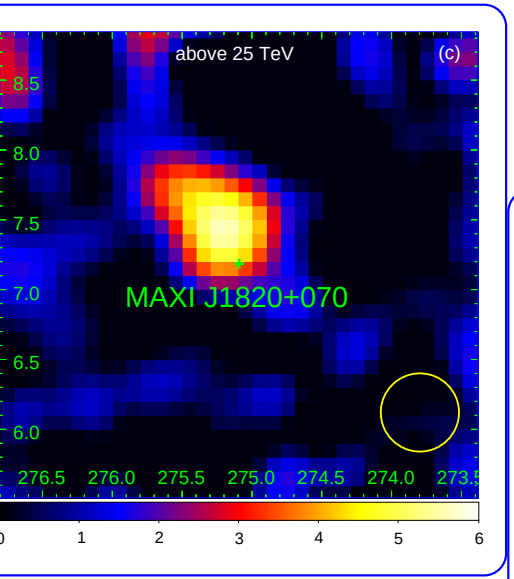

Detections with WCDA will eventually be reported soon

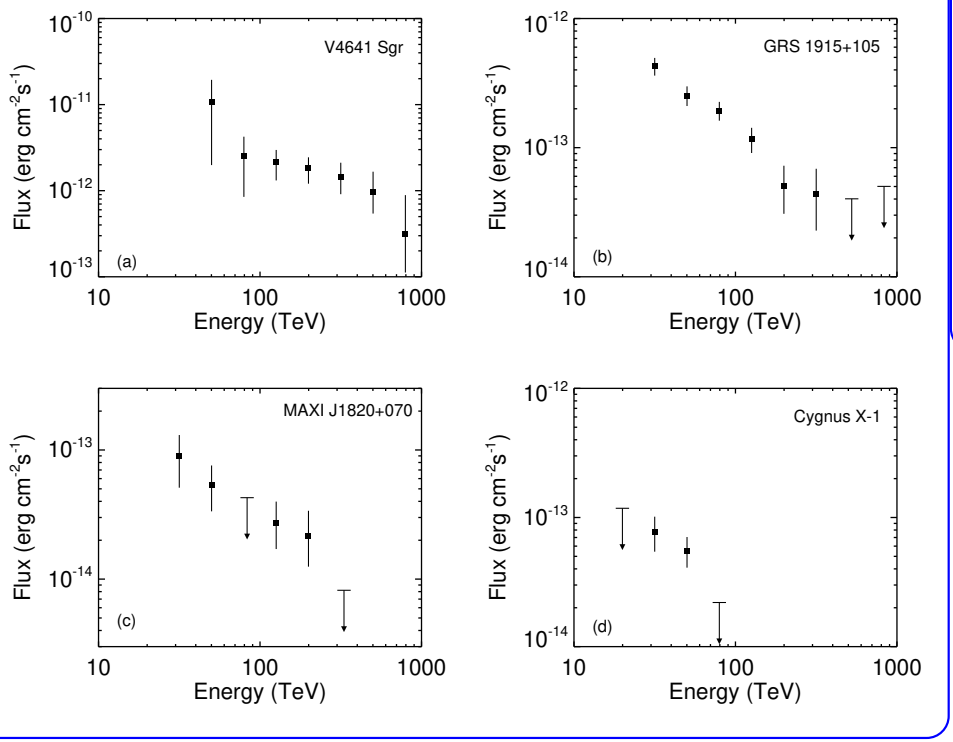

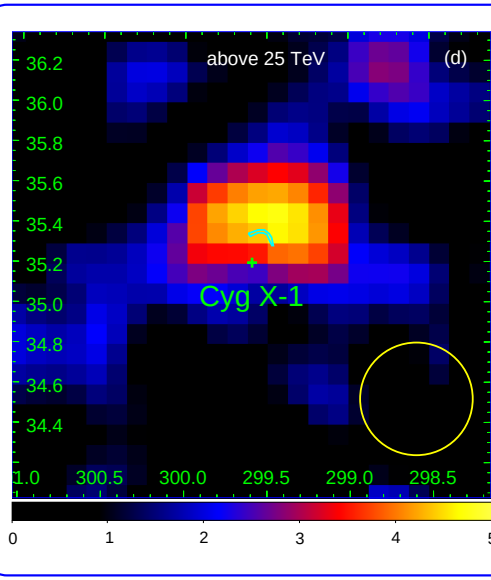

All these sources were detected with KM2A only

Historical claims on detecting Cyg X-3

Orbital phase dependence (Lloyd-Evans+1983)

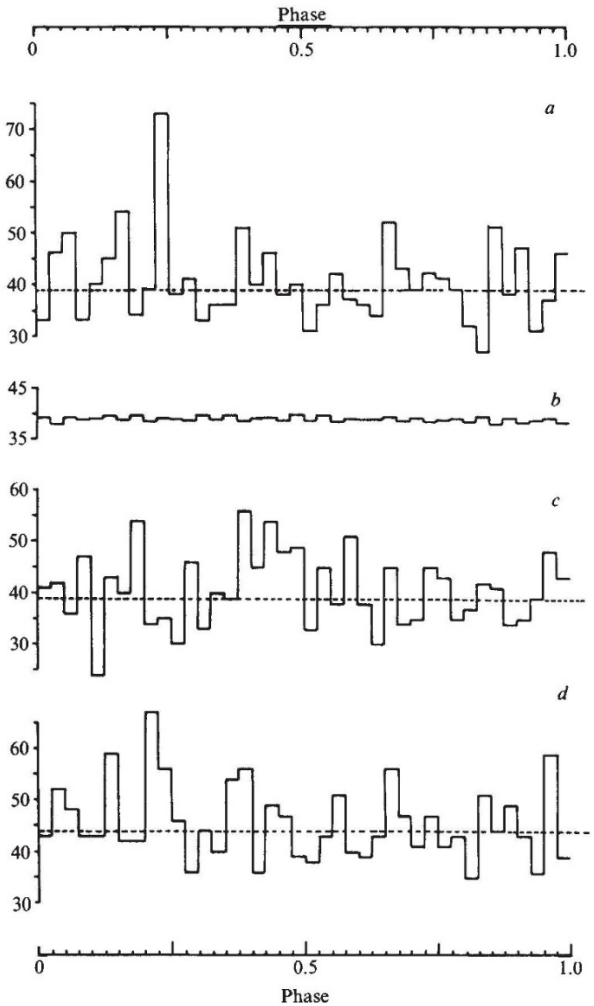

Fig. 1 Phase distributions of events from array B within 9°×6° of Cygnus X-3, folded with a 4.8-h period relative to X-ray minimum. In *a*, *c*, *d* the data are folded using the ephemerides of refs 12, 14, 15 respectively; the dotted lines represent the mean count 'off-source'. The product of the detection efficiency and 'off-source' mean is plotted in *b*, showing the expected contribution to phase nonuniformity from both on-time and atmospheric pressure variations.

VHE emission beyond 10 PeV (Lloyd-Evans+1983)

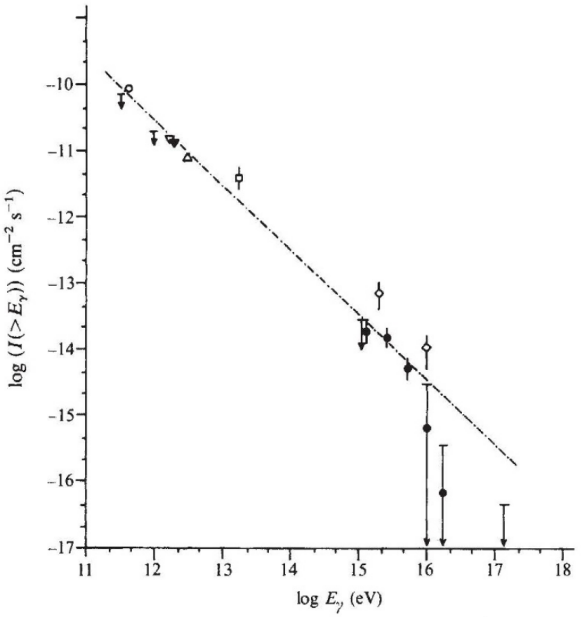

Fig. 3 The time-averaged integral γ-ray flux above 10^{11} eV from Cygnus X-3. Source of measurements: ○, ref. 4; ▽, ref. 2; ▼, ref. 3; △, ref. 5; □, ref. 18; ◇, ref. 10 and ●, this work. The upper limits are obtained from refs 19 and 20 below 10^{12} eV and at 10^{15} eV respectively, and the present work (95% limits) above 10^{16} eV. The dotted line is an estimate of the spectral slope between 5×10^{11} eV and 5×10^{15} eV.

VHE pulsations

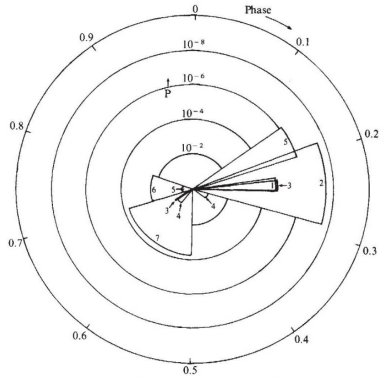

Fig. 2 A summary of the phases (relative to X-ray minimum) for pulsed emission above 500 GeV from Cygnus X-3. The numbered sectors, 1–7, are taken from the present work and refs 10, 10, 18, 2, 3, 4 respectively. The probability of each measurement occurring by chance has been estimated from the cited references (where not explicitly stated) and is plotted radially.

Summary

- At present, two relatively large classes of binary systems—microquasars and binaries with rotation-powered pulsars—are established as VHE gamma-ray sources.
- In systems with pulsars, the gamma-ray emission is most likely produced by ultra-relativistic electrons upscattering soft photons from the optical companion.
- LHAASO has detected TeV emission from (at least) six microquasars out of eight within its field of view, all with emission approaching/above 100 TeV. Despite this consistency, it is not clear if the realized scenarios share much in common across the sources.
- The ability of microquasars to efficiently accelerate particles is consistent with phenomenological expectations based on the electric potential drop across the source (i.e., the Hillas criterion).
- The discovery of energy-dependent morphology in the jets of SS 433 with H.E.S.S. suggests that the TeV emission is generated by leptons.
- DSA seems to be the most viable acceleration mechanism in mildly relativistic jets. In electron-proton plasma it is expected that DSA gives preference to protons, supporting the idea that microquasars could be prominent sources of cosmic rays accelerating hadrons to or even beyond the knee.
- Cyg X-3 is the first clear hadronic PeVatron, and the most extreme accelerator so far found in the Galaxy
- Extreme conditions in Cyg X-3 enable emission via the photo-meson channel, in other systems the hadronic processes might be less efficient